This is to certify that the
thesis entitled

XENOTRANSPLANTATION OF HUMAN PROSTATE CELL LINES: MODELS FOR STUDIES ON CANCER TREATMENT

presented by

AMANDA SUE RIVETTE

has been accepted towards fulfillment
of the requirements for the

Master of Science degree in Zoology

Major Professor's Signature

5/12/05

Date

XENOTRANSPLANTATION OF HUMAN PROSTATE CELL LINES: MODELS FOR STUDIES ON CANCER TREATMENT

By

Amanda Sue Rivette

A THESIS

Submitted to
Michigan State University
in partial fulfillment of the requirements
for the degree of

MASTER OF SCIENCE

Department of Zoology

2005

ABSTRACT

XENOTRANSPLANTATION OF HUMAN PROSTATE CANCER CELL LINES: MODELS FOR STUDIES ON CANCER TREATMENT

By

Amanda Sue Rivette

Prostate cancer is the second leading cause of death from cancer in American men. Using a family of human prostate cancer cell lines developed in our laboratory, that mimic multiple steps in tumor progression, I developed xenograft models using the RWPE2-W99, WPE1-NB26, and CTPE cell lines. When injected sub-cutaneously into immune-deficient mice, RWPE2-W99 forms slow growing, WPE1-NB26 rapidly growing, and CTPE more aggressive, metastatic tumors. I derived two new cell lines, WPE1-NB26-64 and WPE1-NB26-65, from WPE1-NB26 tumors which show increased growth as compared to the parent WPE1-NB26 cells. Cells express cytokeratin 18, androgen receptor and prostate-specific antigen, establishing their prostatic epithelial origin. WPE1-NB26-65 is more invasive than WPE1-NB26 which, in part, may be associated with increased expression of matrix metalloproteinases, MMP-2 and MMP-9, which are barely detectable in WPE1-NB26 cells. Results also show that chemically modified tetracyclines, potential new drugs for cancer treatment, CMTs 2147 and 2215, inhibited cancer cell growth *in vitro* and reduced the size and number of RWPE2-W99 tumors *in vivo*, which mimic the behavior of the majority of human prostate cancers. These results have important applications in studies on tumor progression and for evaluating the efficacy of new drugs for the treatment of prostate cancer.

This thesis is dedicated to Patrick K. Grant, my loving and supportive husband

ACKNOWLEDGEMENTS

I owe a great deal of thanks to those that made possible or assisted me with the work in this thesis. I would like to first thank Dr. Mukta M. Webber, my graduate advisor, for her undying dedication, energetic effort, and constant words of encouragement while helping me complete the requirements for my degree. Dr. Webber, in collaboration with Dr. Richard J. Ablin (University of Arizona) and Dr. William E. Achanzar, (National Cancer Institute at National Institute of Environmental Health Sciences) gave me the opportunity to explore both *in vitro* and *in vivo* cancer research, gain experience working with mice, and publish some of my research results in reputable scientific journals. I thank Dr. Webber, Dr. Ablin, and Dr. Achanzar for these valuable and unique experiences which will undoubtedly have a major impact on my success in the future. I thank Dr. Hynda K. Kleinman, (National Institutes of Health) for her advice on performing xenografts. Committee members, Dr. Daniel E. Williams and Dr. Stephen C. Bromley, provided invaluable support and guidance. Their willingness to get involved with my thesis research is greatly appreciated. Dr. Jean A. Gaymer, another committee member, always offered suggestions when needed and did her best to train me to perform different *in vivo* techniques and answer all of my questions. Animal care training was also provided by Dr. Sally Walshaw and Brenda Paschke, a veterinary technician at the University Laboratory Animal Resources. I would like to thank both Dr. Gaymer and Brenda for their time, patience, and support. The animal tissue samples were processed by the M.S.U. Histopathology lab. I thank Dr. Charles Mackenzie along with members of the lab for their time and effort teaching me about tissue preparation, immunostaining,

and pathology. I would also like to thank Erik J. Tokar and Brooke B. Ancrile for teaching me cell culture. A special thanks to Leanne Pasternak, Mary Tanski, and Elizabeth Grondin who assisted with daily animal care. I also thank Leslie S. Ovitt and Adam K. Keith for their time and assistance with formatting most of the figures and tables in this thesis. Finally and most importantly I would like to thank my husband and family. Thank you Patrick, Mom, Dad, Scott, Carrie, Matt, Melanie, Tony, Andrea, Grandma, Grandpa, and Nan for your unconditional love and support.

TABLE OF CONTENTS

LIST OF TABLES.....xi

LIST OF FIGURES.....xiii

ABBREVIATIONS.....xxv

OBJECTIVES.....xxvii

HYPOTHESES.....xxviii

PART 1
LITERATURE REVIEW.....1
CHAPTER ONE
THE PROSTATE AND NEOPLASTIC CONDITIONS OF THE PROSTATE.....2
Abstract.....3
Keywords.....3
Introduction..... 3
Prostate structure and function.....3
Epithelial marker expression in prostate cell types.....9
Response to androgen and expression of androgen receptor and PSA in prostate cell types.....9
Benign prostatic hyperplasia.....11
Prostate intraepithelial neoplasia (PIN) and prostate cancer.....13
Conclusions.....19
Literature cited.....21

CHAPTER TWO
CHARACTERISTICS OF THREE HUMAN PROSTATE CANCER CELL LINES: PC-3, DU145, AND LNCaP.....24
Abstract.....25
Keywords.....25
Introduction..... 26
Source of cells.....27
Source of PC-3 cells.....27
Source of DU145 cells.....27
Source of LNCaP cells.....28
Cell morphology.....29
Epithelial origin.....29
Response to androgen and the expression of androgen receptor and PSA.....31
Production and response to growth factors.....34
PC-3 cell line.....35

DU145 cell line....36
LNCaP cell line....37
Adhesion properties....39
Proteases....43
Invasion *in vitro*....46
Conclusions....48
Literature cited....50

CHAPTER THREE
RWPE-1 CELL LINE AND ITS DERIVATIVES: RWPE-2, CTPE, AND THE MNU FAMILY OF CELL LINES....56
Abstract....57
Keywords....57
Introduction....58
Source of RWPE-1, RWPE2-W99, MNU, and the CTPE cell line...59
Cell morphology....62
Epithelial origin....62
Response to androgen and the expression of androgen receptor and PSA....63
Production and response to growth factors....66
Adhesion properties....67
Proteases....71
Invasion *in vitro*....72
Conclusions....76
Literature cited....77

CHAPTER FOUR
XENOTRANSPLANTATION OF HUMAN PROSTATE CANCER CELLS....80
Abstract....81
Keywords....81
Introduction....82
Intra-spleen injection....84
Intra-peritoneal injection....86
Intravenous injection....89
Subcutaneous injection....91
Orthotopic injection....95
Surgical orthotopic implantation....98
Models of bone metastasis....100
Conclusions....102
Literature cited....104

CHAPTER FIVE
TETRACYCLINES: APPLICATIONS IN INHIBITION OF TUMOR PROGRESSION AND METASTASIS....107
Abstract....108
Keywords....108

Introduction....109
Chemical modifications of the tetracycline molecule....112
CMT-3 inhibits cell proliferation....114
Possible mechanisms of CMT-3 induced cytotoxicity....117
CMT-3 decreases MMP production....118
CMTs inhibit Matrigel invasion....121
CMT-3 inhibits Dunning tumor growth and metastasis....122
Phase I clinical trial of CMT-3....124
Conclusions....126
Literature cited....127

PART 2
ORIGINAL RESEARCH....130
CHAPTER SIX
EVALUATION OF THE EFFICACY OF CHEMICALLY MODIFIED TETRACYCLINES (CMTs) AS AGENTS FOR THE TREATMENT OF PROSTATE CANCER: A PILOT STUDY USING CMT 2215....131
Abstract....132
Keywords....133
Introduction....133
Materials & Methods....135
In vitro studies....135
Cell culture general....135
Dose response using a microplate assay....135
In vivo studies....136
Mice....136
Animal maintenance....136
Sucrose solution: vehicle for CMT 2215....139
Drug stock solutions....139
Cells for injections....140
Experimental groups....140
Animal weights....142
Tumor size and histology....142
Results....142
In vitro studies....142
Effect of CMT 2215 on anchorage-dependent growth....142
In vivo studies....144
Weight....144
Mice with RWPE2-W99 cell xenografts....144
Mice with CTPE cell xenografts....145
Tumor development....146
RWPE2-W99 cells....146
CTPE cells....147
Histology....147
Histology of RWPE2-W99 tumors in

control mice.....147
Histology of RWPE2-W99 tumors in CMT-treated mice.....148
Histology of the CTPE tumors in control mice.....149
Histology of the CTPE tumors in CMT-treated mice.....151
Histology of CTPE tumor metastasis to the lung.....152
Discussion.....153
Acknowledgements.....155
Literature cited.....156

CHAPTER SEVEN
THE EFFECTS OF CMT 2137 AND 2147 ON TUMOR GROWTH USING THE TUMORIGENIC RWPE2-W99 HUMAN PROSTATE CELL LINE.....157
Abstract.....158
Keywords.....158
Introduction.....159
Materials & Methods.....160
In vitro studies.....160
Cell culture general.....160
Dose response using a microplate assay.....160
In vivo studies.....161
Mice.....161
Animal maintenance.....162
Sucrose solution.....163
Drug stock solution.....163
Cells for injections.....164
Experimental groups.....164
Animal weights.....165
Tumor size and histology.....166
Results.....166
In vitro studies.....166
Effects of CMTs 2137 and 2147 on anchorage-dependent growth.....166
In vivo studies.....167
Animal weight.....167
Tumor volume.....168
Histology.....175
Discussion.....177
Acknowledgements.....179
Literature cited.....180

CHAPTER EIGHT
SELECTION OF CELL LINES WITH ENHANCED INVASIVE PHENOTYPE FROM XENOGRAFTS OF THE HUMAN PROSTATE CANCER CELL LINE WPE1-NB26.....182
Abstract.....183
Keywords.....184
Introduction.....184
Materials & Methods.....188
Materials.....188
Methods.....189
Cells and cell culture.....189
Growth in nude mice by subcutaneous injection.....189
Growth in nude mice by intravenous injection.....190
Selection of WPE1-NB26-64 and WPE1-NB26-65 cell lines.....190
Cell morphology *in vitro*.....191
Immunostaining for cytokeratin expression.....191
Immunostaining for PSA and AR expression.....192
Anchorage-dependent growth in monolayer.....192
Invasion assay.....193
Collection of conditioned medium for MMP activity.....194
SDS-PAGE zymography.....194
Statistical analysis.....195
Results.....196
Histology of xenografts in nude mice.....196
Histology of metastases in nude mice.....198
Cell morphology *in vitro*.....198
Immunostaining for cytokeratin expression.....198
Expression of prostatic epithelial cell markers in cells.....199
Anchorage-dependent growth in monolayer.....200
Comparison of invasive ability.....203
Matrix metalloproteinase (MMP) expression.....203
Discussion.....204
Literature cited.....210

LIST OF TABLES

Table 2.1 Expression of growth factors and their receptors in human prostatic carcinoma cell lines.....38

Table 2.2 Response to exogenous growth factors.....38

Table 2.3 Relative levels of E-cadherin in prostate cells.....42

Table 2.4 Expression of proteases and protease inhibitors in human prostate cancer cell lines.....45

Table 4.1 Incidence of metastasis 6-8 weeks after intra-splenic injection of either PC-3, DU145, or LNCaP cells or their metastatic sublines in athymic mice.....85

Table 4.2 Incidence of metastasis after intra-peritoneal injection of PC-3 cells or metastatic sublines of PC-3 cells in athymic mice.....88

Table 4.3 Metastatic potential of PC-3, DU145, or LNCaP cells in athymic mice following intravenous cell injection.....90

Table 4.4 Incidence of metastasis following subcutaneous injection of PC-3, DU145, or LNCaP cells in athymic mice.....92

Table 4.5 Incidence of metastasis following orthotopic injection of PC-3, DU145, or LNCaP cells in immune-suppressed mice.....97

Table 4.6 Incidence of metastasis to implanted human and host mouse tissue in SCID mice after tail vein injection of PC-3 or LNCaP cells.....101

Table 5.1 Cytotoxicity of DC and CMT-3 in prostate cells.....116

Table 7.1 This table shows the relationship between tumor volume, following injection of RWPE2-W99 cells, and percentage of tumors having the indicated size. Tumor volumes have been divided into four groups. The average tumor volume, range, and percent of tumors having the indicated size in each group are shown for control mice, and mice treated with CMT 2137 or CMT 2147.....170

Table 7.2 This table is a summary of Table 7.1., comparing tumor volumes following injection of RWPE2-W99 cells in control mice and mice treated with CMT2137 or CMT2147. Data are shown as percent of tumors in each group having the indicated tumor volume.....172

Table 7.3 In this table tumor volumes resulting from injection of RWPE2-W99 cells have been divided into nine groups which are arranged from the smallest to the largest. Data are shown as percent of tumors in each group having the indicated tumor volume.....173

LIST OF FIGURES

Images in this thesis are presented in color.

Figure 1.1 The location of the prostate gland with respect to the remainder of the male reproductive and urinary anatomy (Modified from Starr and McMillian, 1997).....4

Figure 1.2 Zonal anatomy of the prostate. There are three glandular zones and the anterior fibromuscular stroma (Ahmed et al., 1997).....5

Figure 1.3 Zonal anatomy of the prostate in anterior-posterior and sagittal planes showing central zone (CZ), peripheral zone (PZ) and transition zone (TZ) (Kirby, 1996).....6

Figure 1.4 The morphology and histology of the central and peripheral zones seen on coronal sections of normal human prostate (Modified from Aumuller,1983).....7

Figure 1.5 Normal prostate gland. Simultaneous demonstration of cell specific markers, X 400. 1: PSA (secretory luminal cell type); 2: high molecular weight cytokeratins (basal cell type); 3: chromogranin A (neuro-endocrine cell type) (Bonkoff and Remberger, 1996).....8

Figure 1.6 Benign prostatic hyperplasia. A. Low power view shows proliferation of glands. B. High-power view shows hyperplastic glands with two layers of cells: an inner columnar and an outer cuboidal or flattened (Cotran et al., 1994).....12

Figure 1.7 Model for PIN-carcinogenesis in the prostate (Kirby et al., 1996).....15

Figure 1.8 Histology of human prostate tissue. Panels A-D depict hematoxylin-eosin stains, while panels E and F show immunohistochemical analyses. A: Low-power view showing the characteristic heterogeneity of prostate tissue, with this region containing a combination of BPH, PIN, and well-differentiated adenocarcinoma. B: High-power view of a region in panel A, showing details of BPH and PIN. The region of BPH has ducts surrounded by basal cells (arrows), which are not found in the region of PIN. The area of PIN shows a transition within the same duct between normal and atypical hyperchromatic cells that contain larger nuclei with prominent nucleoli. C: High-power view showing a nearby area of human prostate with well-differentiated adenocarcinoma that is invading the peri-neural space (N marks the position of the nerve fiber). Note that the carcinoma cells have large nuclei with very prominent nucleoli (arrows). D: View of a different prostate sample with high-grade PIN and a mixture of Gleason grade 4 and 5 carcinoma in the rest of the field. E: Immunohistochemical staining of PIN and carcinoma using anti-cytokeratin 8, which marks all of the epithelial cells. These PIN lesions have a cribiform pattern (arrows), but are still within the confines of a prostatic duct. F: Immunohistochemical staining of a tissue section containing both PIN and carcinoma using anti-cytokeratin 14, which marks the basal cells. Notably, the PIN displays inconsistent staining, whereas the carcinoma has no staining (Abate-Shen and Shen, 2000).....16

Figure 1.9 Gleason grading system. The changes for each grade as assigned by Gleason are shown. A: Gleason grade 1; B: Gleason grade 3; C: Gleason grade 4; D: Gleason grade 5 (Modified from Kirby, 1996).....17

Figure 2.1 Expression of cytokeratin 8 in LNCaP cells is shown by the brown cytoplasmic stain, 400X.....30

Figure 2.2 Indirect avidin-biotin immunoperoxidase staining of LNCaP cells using mAb to PSA. a, cells stained with PSA antibody; b, control. Bar, 20μm. X 532 (Webber et al., 1995).....32

Figure 2.3 Regulation of PSA expression in the LNCaP cell line. Various concentrations of dihydrotestosterone (DHT) were added to the LNCaP cell line. Twenty four h after treatment, total cellular RNA was prepared and 20 μg of total cellular RNA were subjected to Northern analysis. Relative PSA mRNA levels were determined by densitometrical quantification, and the control is defined as 1.0, DHT 0.1 (3.04), DHT 1.0 (3.96), and DHT 10.0 (4.54) (Modified from Hsieh et al., 1993).....33

Figure 2.4 Western blot analysis of E-cadherin in prostate cells. LN=LNCaP cells; nl, normal prostate epithelial cells; PC3=PC-3 cells; DU=DU145 cells. For comparison purposes, LNCaP cells were analyzed at the same time as normal cells (left panel) and in a different analysis with the other two cell lines (right panel). Signals were quantitated by scanning densitometry of X-ray film. Exposure times were 2 min (left panel) and extended to 15 min (right panel) to increase sensitivity; 50 μg of total cellular protein were loaded in each lane, and probed with HECD-1 monoclonal antibody. β-Galactosidase (116 kD) is the molecular weight marker for E-cadherin (124 kD) (Modified from Morton et al., 1993).....41

Figure 2.5 *In vitro* invasion of DU145 and LNCaP cells. Invasive ability of DU145 and LNCaP cell lines was examined by the Boyden chamber *in vitro* invasion assay. 400,000 cells were plated on each "Matrigel"-coated filter and allowed to invade for 24 h. The invasive ability of the highly invasive DU145 cell line was set at 100% invasion (Modified from Bello, 1996).....48

Figure 3.1 Derivation of the MNU-transformed cell lines from RWPE-1, a HPV-18 immortalized human prostatic epithelial cell line. The 2A tumor was derived from treatment with MNU at 50 μg/ml and 3B tumor at 100 μg/ml (Webber et al., 2001).....61

Figure 3.2 Characterization of RWPE-1 cells. Proteins were detected by immunoperoxidase staining. (a) hematoxylin and eosin staining; (b) positive staining for PSA; (c) positive staining for nuclear androgen receptor. Cells for (b) and (c) were pretreated with 5nM mibolerone; (d) a control lacking primary antibody; (e) and (f) positive staining for cytokeratin 8 and 18, respectively. Scale bar is 20 μM. X 625 (Modified from Bello et al., 1997).....64

Figure 3.3 Characterization of RWPE-2 cells. Proteins were detected by immunoperoxidase staining. (a) hematoxylin and eosin staining; (b) positive staining for PSA; (c) positive staining for nuclear androgen receptor. Cells for (b) and (c) were pretreated with 5nM mibolerone; (d) a control lacking primary antibody; (e) and (f) positive staining for cytokeratin 8 and 18, respectively. Scale bar is 20 μM. X 625 (Modified from Bello et al., 1997).....65

Figure 3.4 Characterization of MNU cell lines. Morphology of (hematoxylin and eosin stain): (a) RWPE-1, (b) WPE1-NA22, (c) WPE1-NB14, (d) WPE1-NB11, (e) WPE1-NB26 cells. F-h: PSA and androgen receptor expression in WPE1-NA22 cells treated with mibolerone, as detected by immunostaining; f, positive staining for PSA; g, positive staining for nuclear androgen receptor; and h, a control lacking primary antibody. Bar = 20 μM (Webber et al., 2001).....66

Figure 3.5 Acinar morphogenesis by RWPE-1 and WPE1-NB26 cells in 3-D Matrigel culture. (a) the non-tumorigenic RWPE-1 cells form well organized acini of polarized cells around a central lumen, while WPE1-NB26 cells (b) form a disorganized cell mass, Bar = 25 μm (Modified from Achanzar et al., in press).....69

Figure 3.6 The invasive ability of MNU cell lines compared with that of RWPE-1 and DU-145 cells by a modified Boyden chamber in vitro invasion assay. Cells were plated at 200,000 cells/chamber on a Matrigel-coated filter and allowed to invade for 24 h. +/- SEM. Two tailed t-test is shown as *P = 0.028, **P = 0.007, and ***P = 0.04 (Webber et al., 2001).....73

Figure 3.7 A comparison of the invasive ability of the three tumorigenic cell lines *in vitro* is shown where the invasive ability of WPE1-NB26 cells is taken as 100%. Cells were plated at 200,000 cells/Boyden chamber on Matrigel-coated filters and allowed to invade for 48 h. Results are plotted as ± SD. *P = 0.1095, **P = 0.0008 (Achanzar et al., 2004).....74

Figure 3.8 A schematic diagram showing steps in the multistep process of carcinogenesis and tumor progression in the human prostate and the points possibly represented by RWPE-1, RWPE-2-W99, MNU, and CTPE cell lines in this progression. The sequence of progression from non-malignant RWPE-1 cells to the highly malignant WPE1-NB26 cells: RWPE-1< WPE1-NA22< WPE1-NB14 < RWPE2-W99< WPE1-NB11< CTPE< WPE1-NB26 (Modified from Webber et al., 2001).....75

Figure 5.1 A schematic representation of tetracycline and the chemical modifications of tetracycline that generated the CMT-1, CMT-3, and CMT-8 compounds (Modified from Seftor et al., 1998).....113

Figure 5.2 Effect of doxycycline (DC) and CMT-3 on proliferation of prostate tumor cell lines. Tumor cells were incubated with various concentrations of DC or CMT-3 for 48 hours in complete culture medium. Cell proliferation activity, defined as synthesis of [^{3}H]-thymidine-labeled DNA, was assayed by 2-hour pulse-labeling the cells with [^{3}H]-thymidine as described in the text. Data presented are for three prostate cancer cell lines. Similar results were obtained for other cell lines. Vertical bars represent mean ± SEM from four independent determinations (Lokeshwar, 1999).....115

Figure 5.3 Zymographic detection of gelatinases secreted into the conditioned media from cultures treated with CMT-3 or doxycycline. Culture conditioned media (15 µl/lane, equivalent to 5 x 10^3 cells) from TSU-PR1 (a,b) and MAT LyLu (c,d) cells were separated by SDS-PAGE (8% polyacrylamide) on a gelatin-embedded (1 mg/ml) gel and zymography. The positions of purified MMP-2 and MMP-9 are indicated. Note: the major fraction of MMP-2 from MAT LyLu (bottom) cell conditioned media was active (Mr ~64,000), whereas most TSU-PR1 (top) MMP-2 was in the latent form (Mr 72,000) (Lokeshwar et al., 2002).....119

Figure 5.4 Inhibition of invasive potential of tumor cells by doxycycline (DC) and CMTs. Invasion of tumor cells through the Matrigel-coated filters was assayed following 48 hours of exposure to 5 μg/ml of each drug. Only the drug diluent (0.1% dimethyl sulfoxide) was added to control wells. Percentage of cells that invaded in the control (0.1% DMSO) wells varied from 12.5 ± 6.4% for DU145 cells to 17 ± 4.2 for MAT LyLu cells. 0.1% DMSO had negligible effect on invasion. Results presented are from three independent experiments (Lokeshwar, 1999).....122

Figure 6.1 The facility, experimental design and equipment used for *in vivo* studies. 6.1a. Clinical Center Building; 6.1b. University Laboratory Animal Resources (ULAR) facility; 6.1c. room for housing immune-deficient mice (nude mice); 6.1d. laminar flow mouse cage rack. The cages were arranged in rows for the four groups of mice; row 1 = RWPE2-W99 controls; row 2 = RWPE2-W99 treated; row 3 = CTPE controls; row 4 = CTPE treated. Mice were housed, one mouse per cage, in autoclaved cages, and provided with autoclaved drinking water and irradiated food. 6.1e. laminar flow hood where gavage feeding was performed; 6.1f. Gavage feeding procedure. The control mice were fed 300 μl of a 5% sucrose solution in water by gavage. The treated mice were similarly fed with 0.675 mg or 2.25 mg of CMT 2215/mouse in 300 μl of a 5% sucrose solution starting 3 days prior to cell injection. Gavage feeding was performed daily for a total of 10 weeks.....138

Figure 6.2 The effects of CMT 2215 on anchorage-dependent growth of RWPE2-W99 cells. Cells were plated in 96-well plates at a density of 10,000 cells per well and treated for 5 days. Results are plotted as percent of DMSO-treated control, ±SEM....143

Figure 6.3 Average weight of control and treated mice injected with RWPE2-W99 cells. In the control group, four mice were given vehicle alone (5% sucrose solution in water) by gavage daily for 10 weeks. Four mice in the treated group were given 0.675 mg of CMT 2215/mouse daily by gavage for 10 weeks. The days on which gavage feeding was started, and cells injected, are shown.....144

Figure 6.4 Average weight of control and treated mice injected with CTPE cells. In the control group, three mice were given vehicle alone (5% sucrose solution in water) by gavage daily for 10 weeks. Three mice in the treated group were given 2.25 mg of CMT 2215/mouse daily by gavage for 10 weeks. The days on which gavage feeding was started, and cells injected, are shown.....145

Figure 6.5 a. and b. Nude mice (strain NCRNU-M male, homozygotes, ~8 weeks old from Taconic farms, Germantown, NY) were bilaterally injected subcutaneously with 250 µl of a cell suspension in Matrigel (cells:Matrigel volume 1:1) containing 1 million (a) RWPE2-W99 cells or (b) CTPE cells. Mice were sacrificed 10 weeks later. These mice were fed 300 µl of a 5% sucrose solution by gavage starting 3 days prior to cell injection. Gavage feeding was performed daily for 10 weeks. Arrows point to tumors.....146

Figure 6.6 Histology of the RWPE2-W99 tumors in control mice: Figure 6.6a shows a subcutaneous tumor (arrow). Under the skin, the tumor margin appears to be well defined and separate from the skin. Figure 6.6b shows tumor:adipose tissue interface with clear margins, and the tumor does not show invasion at this site. It is possible that if the animals are maintained for longer than 10 weeks, one may see invasion and metastasis. Figure 6.6c shows tumor histology at a higher magnification. Figure 6.6d shows (arrow) skeletal muscle cells amongst tumor cells. H & E stain.....148

Figure 6.7 Histology of the RWPE2-W99 tumors in CMT-treated mice. Figure 6.7a shows an area of the tumor that does not appear to show any difference from the control tumor. Figure 6.7b shows a representative area with many vacuolated cells. Figure 6.7c shows (arrow) squamous metaplasia. There are also areas that show large lymphocytic infiltration (dark staining nuclei) (Figure 6.7d). Many areas showed what appear to be apoptotic cells (arrows) (Figure 6.7e). Such changes were not seen as frequently in the control tumors. H & E stain.....149

Figure 6.8 Histology of CTPE tumors in control mice. The CTPE tumors are rapidly growing, invasive tumors and invasion was observed at the 10 week experimental period. Figures 6.8a shows a subcutaneous tumor with invasion into the sub-epidermal layer. The tumor has infiltrated into the dermis and does not have clear cut margins as can be seen in Figure 6.8b. Figures 6.8c and 6.8d show that the tumor cells are intermingled with skeletal muscle (M) (Figure 6.8c) and fat cells (FC) (Figure 6.8d). The tumor cell population is very heterogeneous with considerable variation in cell size (Figure 6.8e). H & E stain.....150

Figure 6.9 Histology of CTPE tumors in CMT-treated mice. This figure shows some features observed in CMT-treated CTPE tumors. A tumor with undifferentiated characteristics shown in Figure 6.9a suggests the aggressive nature of CTPE tumors. Invasion into skeletal muscle (M) is seen in Figure 6.9b. Cells which appear to be undergoing apoptosis are shown (arrows) in Figures 6.9c and 6.9d. Such cells were not seen as frequently in the control CTPE tumors. Areas with lymphocytic infiltration were observed in several tumors (Figure 6.9e). H & E stain.....152

Figure 6.10 Histology of the normal lung and of CTPE tumor metastasis to the lung. Figure 6.10a shows a normal area of the lung. One of the control mice (1/3) showed metastasis to the lung. Figures 6.10b and 6.10c are low magnification picture of the lung (L) showing metastatic tumors (T). Figure 6.10d is a higher magnification picture of the lung (L) showing lung tissue:tumor (T) interface. The lung tissue has the alveoli represented by clear spaces against which the tumor tissue has a solid appearance. H & E stain.....153

Figure 7.1 Laminar flow mouse cage rack. The cages were color-coded for the three groups of mice; yellow = controls; blue = 2137; red: 2147. Mice were housed, one mouse per cage, in autoclaved cages, and provided with autoclaved drinking water and irradiated food. The control mice were fed 300 µl of a 5% sucrose solution in water by gavage. The treated mice were similarly fed with 1.2 mg of CMT 2137 or 2147/mouse in 300 µl of a 5% sucrose solution starting 3 days prior to cell injection. Gavage feeding was performed daily for a total of 11 weeks.....162

Figure 7.2 The effects of CMT 2137 or CMT 2147 on anchorage dependent growth of RWPE2-W99 cells. Cells were plated in 96-well plates at a density of 10,000 cells per well and treated for 5 days. Results are plotted as percent of DMSO-treated control, ±SEM.....167

Figure 7.3 Average weight of mice injected with RWPE2-W99 cells. This graph shows weight gain, over time, in the control mice given vehicle alone (5% sucrose solution in water) by gavage daily for 11 weeks, and in the mice gavage-fed with 1.2 mg/mouse of CMT 2137 or CMT 2147 in 5% sucrose solution. Mice were weighed at time zero and then weekly for 11 weeks. Beginning at time zero, mice were gavage-fed for three days prior to the injection of RWPE2-W99 human prostate tumorigenic cell line. The day on which gavage feeding was started (labeled as CMT), and the day when the cells were injected, are shown. RWPE2-W99-C = control; RWPE2-W99-37 = mice on CMT 2137; RWPE2-W99-47 = mice on CMT 2147.....168

Figure 7.4 Relationship between tumor volume, following injection of RWPE2-W99, and percentage of tumors having the indicated tumor size. This is a graphic representation of the data shown in Table 1. Tumor volumes have been divided into four groups. The effects of treatment with CMT 2137 or CMT 2147 are evident in this bar graph. Results indicate that overall, the treatment groups have a larger percentage of small tumors as compared to the control.....171

Figure 7.5 Nude mice (NSWNU-M *nu/nu* strain) were bilaterally injected with 250 µl of a cell suspension in Matrigel (cell: Matrigel volume, 1:1) containing one million RWPE2-W99 cells. Mice were sacrificed 11 weeks later. This figures shows (from left to right) four representative mice with tumors from each of the three groups. A. Control mice (22-C, 25-C, 29-C, and 27-C); B. CMT 2137-treated mice (37-37, 34-37, 35-37, and 32-37); C. CMT 2147-treated mice (48-47, 50-47, 44-47, and 46-47); arrows point to small tumors.....174

Figure 7.6 H & E-stained sections showing tumor histology. Figures 7.6a and 7.6b: Histology of the RWE2-W99 tumors in control mice at low (Figure 7.6a) and high magnification (Figure 7.6b). The tumor appears to be an undifferentiated tumor with clear margins at the interface with connective and adipose tissue. In Figure 7.6b, many mitotic figures can be seen (arrows). Figures 7.6c and 7.6d show a tumor from a mouse treated with 2137. Examination of the tumor at higher magnification (Figure 7.6d) shows little evidence of cells in mitosis, in contrast to the control tumors. Figures 7.6e and 7.6f show a tumor from a mouse treated with 2147. Examination of the tumor at higher magnification (Figure 7.6f) again shows little evidence of cells in mitosis, in contrast to the control tumors. Bar = 10 μm.....176

Figure 8.1 Derivation of MNU-transformed human prostate epithelial cell lines from RWPE-1, a non-tumorigenic human prostatic epithelial cell line, and the subsequent derivation of WPE1-NB26-64 and WPE1-NB26-65 cell lines. The 2A tumor was derived from treatment with MNU at 50 μg/ml and 3B at 100 μg/ml.....186

Figure 8.2 8.2A. Nude mice (NSWNU-M) were bilaterally injected with 250 μl of a cell suspension in Matrigel (cell: Matrigel volume, 1:1) containing two million WPE1-NB26 cells. Mice were sacrificed 14 weeks later. This figure shows two mice with tumors from which the WPE1-NB26-64 and WPE1-NB26-65 cell lines were derived. Bar = 1 cm. 8.2B. Histological sections of the (a) WPE1-NB26-64 and (b) WPE1-NB26-65 tumors. H & E, Bar = 20 microns. 8.2C. Histological sections of mouse lung tissue: (a) Normal area of mouse lung tissue, (b) Necrotic WPE1-NB26 prostate tumor cells in a blood vessel (arrow) of mouse lung at 20 weeks after intravenous cell injection, (c) WPE1-NB26 cells (arrow) surrounded by hyperplastic, fibrous connective tissue in the lung of a mouse at 20 weeks after intravenous cell injection, (d) shows a higher magnification of the metastasis in (c). H & E, Bar = 20 microns. 8.2D. Morphology of (a) WPE1-NB26, (b) WPE1-NB26-64, (c) WPE1-NB26-65 cells. H & E, Bar = 20 microns.....197

Figure 8.3 Characterization of WPE1-NB26, WPE1-NB26-64, and WPE1-NB26-65 cells on the basis of cellular proteins. Proteins were detected by immunoperoxidase staining. (a-c) positive staining for cytokeratin 18, the inset in each is a control lacking primary antibody; (d-f) positive staining for cytokeratin 5/14, the inset in each is a control lacking primary antibody. Bar = 20 microns.....199

Figure 8.4 Immunostaining for androgen receptor (Figure 8.4A) and PSA (Figure 8.4B) demonstrates androgen responsiveness and prostatic epithelial origin of WPE1-NB26, WPE1-NB26-64, and WPE1-NB26-65 cell lines. Cells were treated with 5 nM mibolerone for 6 days. Positive nuclear staining for AR is shown in 8.4A,a,b,c for all three cell lines. Panel a1 shows only weak nuclear staining in untreated control. Panel a2 and other insets are negative controls lacking primary antibody. Positive cytoplasmic staining for PSA is shown in 8.4B,a,b,c for all three cell lines. Panel a1 shows very weak staining in untreated control. Panel a2 and other insets are negative controls lacking primary antibody. Bar = 20 microns.....200

Figure 8.5 8.5A. A comparison of the anchorage-dependent growth of WPE1-NB26, WPE1-NB26-64, and WPE1-NB26-65 cell lines. Cells were plated at densities of 625, 1250, 2500, 5000 and 10,000 cells per well in 96-well plates in complete KSFM. Plates were stained with MTT five days after plating. Absorbance values were measured at 540 nm and plotted ± SEM. Results represent the average of 3 experiments. The growth of both WPE1-NB26-64 and WPE1-NB26-65 cell lines are significantly greater ($p<0.001$) in comparison to the WPE1-NB26 cell line at each cell density using ANOVA. 8.5B. The invasive ability of WPE1-NB26-64 and WPE1-NB26-65 cell lines was compared with that of WPE1-NB26 cells by a modified Boyden chamber *in vitro* invasion assay. Cells were plated at 200,000 cells/ chamber on a Matrigel-coated filter and allowed to invade for 48 h. ± SEM. The difference in the invasive ability of WPE1-NB26-65 as compared to WPE1-NB26 is very significant using ANOVA ($p<0.001$). 8.5C. Zymographic analysis of MMP expression in culture medium of WPE1-NB26, WPE1-NB26-64, and WPE1-NB26-65 cells. Samples of conditioned medium containing 8 μg protein each, were electrophoresed using 10% polyacrylamide gels. Lane 1, WPE1-NB26 cells; Lane 2, WPE1-NB26-64 cells; Lane 3, WPE1-NB26-65 cells. The gel is a representative of 3 independent experiments.....202

Figure 8.6 A schematic diagram showing steps in the multistep process of carcinogenesis and tumor progression in the prostate and the points represented by RWPE-1, the MNU cell lines, and the WPE1-NB26 tumor-derived cell lines, WPE1-NB26-64 and WPE1-NB26-65. The ability of WPE1-NB26 cells to form lung metastases after intravenous injection is also shown.....205

ABBREVIATIONS

AR	Androgen receptor
bFGF	Basic fibroblast growth factor
BPE	Bovine pituitary extract
BPH	Benign prostatic hyperplasia
CCNU	methyl (2-chloroethyl)-3-cyclohexy-1-nitrosourea
CMT	Chemically modified tetracycline
DC	Doxycycline
DHT	Dihydrotestosterone
ECM	Extracellular matrix
EGF	Epidermal growth factor
ELISA	Enzyme-linked immunosorbent assay
FACS	Fluorescence-activated cell sorter
FGF-R	Fibroblast growth factor receptor
HAB	Human adult bone
HAL	Human adult lung
HGPIN	High grade prostatic intraepithelial neoplasia
HPV-18	Human papilloma virus-18
IGF-1	Insulin-like growth factor
IGF-1-R	Insulin-like growth factor receptor
Ki-MuSV	Kirsten murine sarcoma virus
KSFM	Keratinocyte serum-free medium

MMPs	Matrix metalloproteinases
MNU	*N*-methyl-*N*-nitrosourea
MTT	3-[4,5-dimethylthiazol-2-yl]-2, 5-diphenyl tetrazolium bromide
PAI-1	Plasminogen activator inhibitor type-1
PAI-2	Plasminogen activator inhibitor type-2
PIN	Prostatic intraepithelial neoplasia
PSA	Prostate specific antigen
SCID	Severe combined immune deficiency
SOI	Surgical orthotopic implantation
TGF-α	Transforming growth factor-α
TGF-β1	Transforming growth factor-β1
TGF-β1-R	Transforming growth factor-β1 receptor
TIMPs	Tissue inhibitors of matrix metalloproteinases
ULAR	University laboratory animal resources
uPA	Urokinase-type plasminogen activator

OBJECTIVES

1. To develop xenograft models for testing drug efficacy

2. To evaluate the efficacy of chemically modified tetracyclines as agents for the treatment of prostate cancer in cell culture and on xenografts

3. To develop additional xenograft models using a cell line developed in our laboratory

HYPOTHESES

Chemically modified tetracyclines will inhibit:

1. The growth of prostate cancer cells in culture
2. The growth of prostate cancer cells as xenografts in nude mice

PART 1

LITERATURE REVIEW

CHAPTER ONE

THE PROSTATE AND NEOPLASTIC CONDITIONS OF THE PROSTATE

Abstract

The prostate gland is a part of the male reproductive system. Two major prostatic diseases include benign prostatic hyperplasia (BPH) and prostate carcinoma. BPH occurs so frequently in older men it is almost considered a normal aging process. Carcinoma of the prostate is the most frequently diagnosed cancer, excluding skin cancer, and the second leading cause of death in American men. Prostatic intraepithelial neoplasia (PIN) is a common precursor to prostate cancer and it is associated with progressive abnormalities, which are intermediate between normal prostate epithelium and cancer. The importance of recognizing PIN is based on its strong association with prostate carcinoma. Early detection and treatment may prevent progression to invasive and metastatic prostate cancer. Further studies utilizing *in vitro* human prostate cell lines and *in vivo* xenograft models that mimic multiple steps in prostate carcinogenesis, invasion and metastasis will assist in the understanding and treatment of the disease.

Keywords

Androgen receptor, basal cell, benign prostatic hyperplasia, Gleason score, prostate cancer, prostatic intraepithelial neoplasia, prostate specific antigen, secretory luminal cell

Introduction

Prostate Structure and Function:

The prostate is an accessory sex gland in the male reproductive system which also includes the seminal vesicles and the bulbourethreal glands. A diagram of the male reproductive system is shown in Figure 1.1.

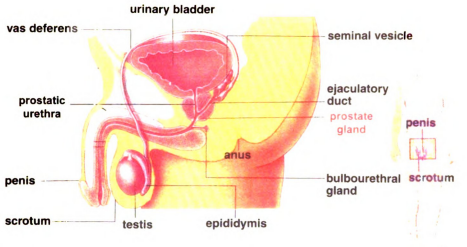

Figure 1.1 The location of the prostate gland with respect to the remainder of the male reproductive and urinary anatomy (Modified from Starr and McMillian, 1997).

The accessory sex glands secrete fluids necessary for sperm movement. The human prostate gland lies posterior to the urinary bladder and surrounds the urethra. The prostatic urethra extends from the urinary bladder to the urethral sphincter and travels directly through the prostate. The prostate secretes 0.5-1ml of fluid directly into the urethra through several small ducts during ejaculation (Dixon et al., 1999). The size of the prostate has been compared to that of a walnut. It is composed of nonglandular stroma and three glandular regions: the peripheral zone, transitional zone and central zone (Figure 1.2 and Figure 1.3).

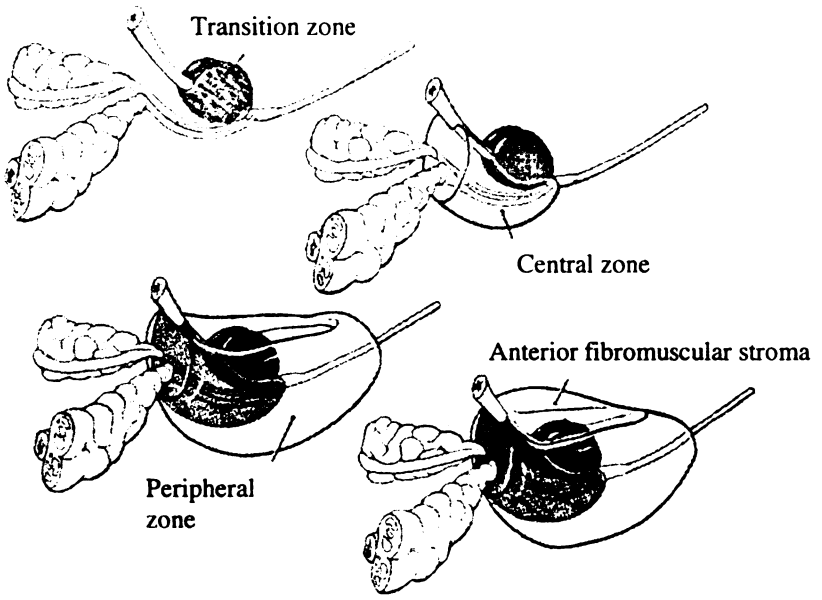

Figure 1.2 Zonal anatomy of the prostate. There are three glandular zones and the anterior fibromuscular stroma (Ahmed et al., 1997).

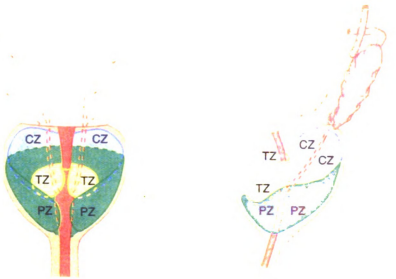

Figure 1.3 Zonal anatomy of the prostate in anterior-posterior and sagittal planes showing central zone (CZ), peripheral zone (PZ) and transition zone (TZ) (Kirby, 1996).

Prostatic stroma is a complex mixture of smooth muscle cells, fibroblasts, blood vessels, nerves and extracellular matrix and it is concentrated at the anterior surface of the prostate. In each zone of the prostate, prostatic acini are embedded in smooth muscle stroma (Kirby, 1996). The glands empty into the urethra independently and are classified as mucosal, submucosal, or main, depending on their location in the gland (Paulson, 2000). The mucosal glands are located in the region immediately surrounding the urethra and are surrounded by the submucosal glands while the main prostatic glands are located in the outermost region of the prostate (Cormack, 2001).

The peripheral zone in the normal prostate is the largest zone and takes up about 65% of the prostatic volume (Kirby, 1996). The peripheral zone extends around the posterolateral peripheral aspects of the gland. The histology of this zone is characterized

by small, simple, acinar spaces lined by tall columnar secretory epithelial cells (Figure 1.4).

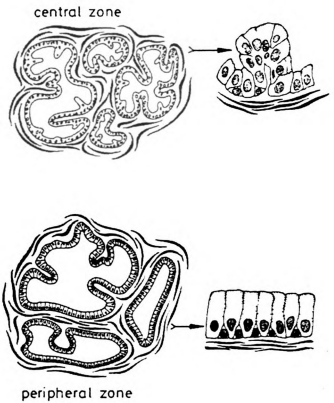

Figure 1.4 The morphology and histology of the central and peripheral zones seen on coronal sections of normal human prostate (Modified from Aumuller,1983).

The second largest zone in the normal prostate is the central zone, which comprises about 25% of the prostatic volume. The central zone surrounds the ejaculatory ducts. Histologically, this zone can be identified by the presence of fairly large acini that are lined by low columnar cuboidal epithelium (Figure 1.4). The smallest zone in the normal prostate is the transition zone, it comprises only 5-10% of the prostatic volume. The transition zone is composed of two bilaterally symmetrical lobules found on the two sides

of the prostatic urethra. In the three zones of normal prostate, prostatic epithelium is composed of two major cell populations; secretory luminal and basal cells.

The basal cells and secretory luminal cells form a pseudo-stratified layer of cells that line the basement membrane in prostate acini (Figure 1.5).

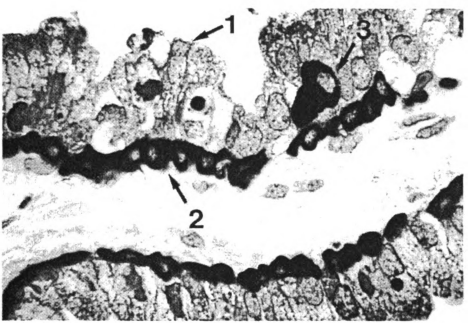

Figure 1.5 Normal prostate gland. Simultaneous demonstration of cell specific markers, X 400. 1: PSA (secretory luminal cell type); 2: high molecular weight cytokeratins (basal cell type); 3: chromogranin A (neuro-endocrine cell type) (Bonkoff and Remberger, 1996).

Interdispersed with the secretory luminal and basal cells are also occasional neuroendocrine cells (Figure 1.5) (Lalani et al., 1997). Basal cells range from small, flattened cells to more cuboidal cells, whereas the morphology of secretory luminal cells is columnar. There are two morphological types of neuroendrocine cells: (1) open, flask-

shaped cells with long slender extensions reaching the lumen, and (2) closed cells without luminal extensions (Abrahamsson et al., 1996). The three cell types found in the prostate differ in their marker expression and in their responses to hormonal regulation.

Epithelial marker expression in prostate cell types:

Basal cells exclusively express high molecular weight cytoskeletal proteins, cytokeratin 5, 14, and 15 (Nagle et al., 1987; De Marzo et al., 1998). While, the luminal cells express cytokeratins 8 and 18 (Brawer et al., 1985). Neuroendocrine cells have been shown to exhibit basal cell specific cytokeratin immunoreactivity and chromagranin A, a pan-endocrine marker (Bonkoff et al., 1994). Other evidence based on studies of androgen receptor and PSA expression in basal, secretory luminal, and neuroendocrine cells has indicated the presence of cell types with intermediate differentiation in normal and hyperplastic tissues (Bonkoff et al., 1994a).

Response to androgen and the expression of androgen receptor and PSA in prostate cell types:

Dihydrotestosterone (DHT) is ultimately responsible for the growth of prostate epithelial cells, it is produced from testosterone by an enzyme called 5-α reductase. The effects of DHT on the development of the normal prostate gland and the growth of prostate tumors are mediated by the androgen receptor (AR). The three cell types differ in their response to hormones and combined with their epithelial marker expression, some intermediate differentiation has been observed between basal, secretory luminal and neuro-endocrine cells.

Basal cells are generally considered to be androgen insensitive and at least a subpopulation may not express the androgen receptor and do not require androgen for survival. However, in some studies basal cells have been shown to express the androgen receptor focally (Bonkoff and Remberger, 1993). In both the developing and adult prostate coexpression of basal cell specific cytokeratins and PSA has also been detected in basal cells (De Marzo et al., 1998). The secretory luminal cells of the prostate express AR and utilize the hormone androgen as a growth, survival, and differentiation factor. Neuro-endocrine cells, similar to most basal cells, lack the AR and are not influenced by circulating androgens (Bonkoff et al., 1993). Yet, neuroendocrine cells have been shown to co-express PSA and chromagranin A (Bonkoff et al., 1994). So it appears that neuroendocrine cells share a common origin with both basal and secretory luminal cell types of the prostate.

The expression of AR and the coexpression of basal and secretory luminal markers in some basal cells may also suggest that these two cell types share a common origin. Coupled with the observation that the proliferative activity in normal prostatic epithelium is localized in the basal cell layer, the presence of pluripotent stem cells in the basal cell layer provides a possible explanation for the development of each of these 3 cell types and intermediate cell types (Bonkoff et al., 1994a and b). Abnormal proliferation of cells in the basal cell compartment of the prostate is commonly associated with a condition called benign prostatic hyperplasia (BPH).

Benign prostatic hyperplasia:

BPH is a common non-malignant condition of the prostate gland in older men. Approximately 50% of men over the age of 50 have symptoms of BPH (Wartinger et al., 1997). BPH results in continuous growth and increases the size of the prostate, but the rate at which the size increases declines over time (Ahmed et al., 1997). BPH has been found to originate from the formation of nodules in the transition zone of the prostate (Rous, 1988). Microscopically the appearance of nodules may be due mainly to glandular proliferation or muscular proliferation of the stroma (Cotran et al., 1994). During the early stages of BPH the nodules are small and, thus, do not disturb the architecture of the prostate, however, as the nodules grow the size of the prostate increases and the architecture is affected. An increase in cell proliferation that results in prostatic growth often causes difficulty and pain during urination due to obstruction of the urethra (Rous, 1988). In patients with BPH, surgery is commonly performed to enlarge the constricted channel or passage through the center of the prostate gland to improve urine flow (Wartinger et al., 1997).

The cause of BPH is unknown but it is likely related to the action of androgens. Dihydrotestosterone (DHT), which is derived from testosterone by the action of 5α-reductase, regulates prostatic growth. With aging in men, DHT accumulates in the prostate where it initiates cell proliferation (Cotran et al., 1994). The role of DHT in BPH is supported by observations in which an inhibitor of 5α -reductase was given to men with this condition. Treatment with 5α -reductase inhibitor reduced the DHT content of the prostate and resulted in a decrease in prostate volume as well as urinary obstruction (McConnell et al., 1992; Rittmaster, 1994). In aging men, estradiol levels

also increase (Cotran et al., 1994). There is evidence to suggest that DHT-mediated prostatic hyperplasia can be influenced by estrogen levels. In castrated animals, prostate hyperplasia can be induced by administration of androgens which can be enhanced by simultaneous administration of 17β-estradiol (Cotran et al., 1994). The hormonal imbalance of androgens and estrogens in older men may lead to a hyperplastic condition of the prostate. Microscopically, in BPH, the epithelium is characteristically arranged into numerous papillary buds and infoldings, which are more prominent than in the normal prostate (Cotran et al., 1994). Hyperplastic glands typically show two layers of cells, an inner columnar and an outer cuboidal or flattened layer (Figure 1.6). Foci of squamous metaplasia and small areas of necrosis are also changes frequently observed in BPH.

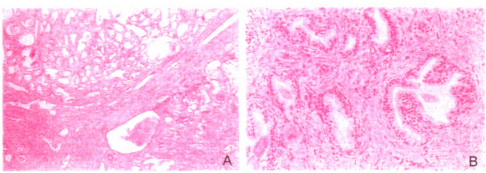

Figure 1.6 Benign prostatic hyperplasia. A. Low power view shows proliferation of glands. B. High-power view shows hyperplastic glands with two layers of cells: an inner columnar and an outer cuboidal or flattened (Modified from Cotran et al., 1994).

Although BPH and early prostate cancer share many of the same signs and symptoms, such as, an increase in the number of cells in the prostate and urinary obstruction, BPH is not considered to be a premalignant lesion, nor a precursor of prostate cancer. While BPH commonly occurs in the transition zone of the prostate, the neoplastic conditions of the prostate gland, prostatic intraepithelial neoplasia (PIN) and prostatic carcinoma, commonly occur in the peripheral zone of the prostate (McNeal et al., 1988; Bostwick, 1994).

Prostate intraepithelial neoplasia (PIN) and prostate cancer:

Prostate intraepithelial neoplasia (PIN) and prostate adenocarcinoma are malignant forms of prostate cancer. Of the 699,560 new cancer cases among American men in 2004, an estimated 230,110 of these will be prostate cancer (American Cancer Society, 2004). Therefore prostate cancers represent 33% of all diagnosed cancer cases, which is more than any other cancer in men except skin cancer. An estimated 29,500 deaths due to prostate cancer will occur in 2004 (American Cancer Society, 2004). Accounting for 10% of all cancer-related deaths, prostate cancer is the second leading cause of cancer death in men, after lung and bronchus cancers (American Cancer Society, 2004).

The majority of prostate adenocarcinomas, more than 70%, arise in the peripheral zone (Kirby, 1996). Although less common, prostate carcinomas may also originate in the central and transitional zones. The central zone, which surrounds the ejaculatory ducts is the source of 10%, while the transition zone is the source of 20% of prostatic cancers (Ahmed et al., 1997). The majority of prostate cancers may arise in the

peripheral zone due to the presence of a high concentration of androgen receptors compared to the central and transition zones of the normal prostate (Kirby, 1996). It is not known whether there are distinct differences between carcinomas that arise in different zones of the prostate.

Clinical studies suggest that PIN predates prostate adenocarcinoma by 10 or more years (Sakr et al., 1993). PIN has been observed in men in their 30s and is thought to be a precursor of prostate adenocarcinomas arising in the peripheral zone (Sharp et al., 2001; Webber et al., 1999). PIN is characterized by a morphology similar to that seen in prostate cancer in which the basal cells of the epithelium are absent (Kirby, 1996). PIN is also characterized by cytologic changes mimicking cancer, including nuclear and nucleolar enlargement (McNeal and Bostwick, 1986). A model of carcinogenesis in the prostate, depicting the development of pre-malignant PIN into prostate adenocarcinoma is shown in Figure 1.7.

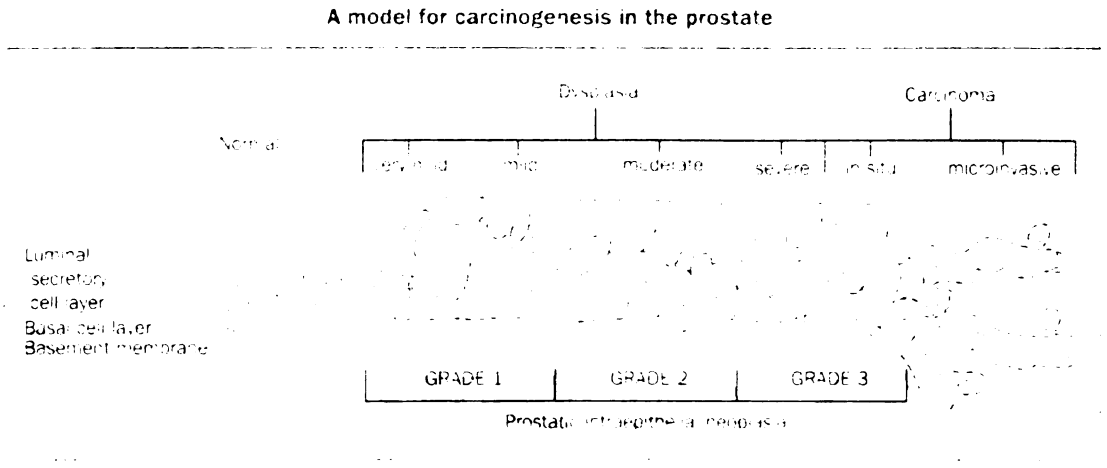

Figure 1.7 Model for PIN-carcinogenesis in the prostate (Kirby et al., 1996).

The diagnosis of PIN as low, moderate or high grade is established by increasing proliferation and cytological changes (Kirby, 1996). Low grade PIN retains an intact basal cell layer, whereas high grade prostate intraepithelial neoplasia (HGPIN) and early invasive cancer are characterized by progressive basal cell layer disruption (Bostwick, 1994). In an autopsy study of 249 cases, HGPIN was observed in 77% of the prostates with cancer, but in only 24% of prostates without cancer (Sakr et al., 1994). This demonstrates the strong association between PIN and prostatic carcinoma.

Most prostate cancer lesions are heterogeneous and multifocal (Abate-Shen and Shen, 2000). For example, benign glands, preneoplastic (PIN) foci, and neoplastic foci of varying severity can all be observed in one region of prostate tissue (Figure 1.8).

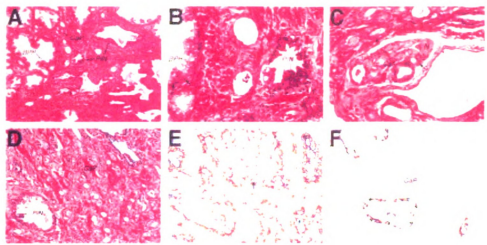

Figure 1.8 Histology of human prostate tissue. Panels A-D depict hematoxylin-eosin stains, while panels E and F show immunohistochemical analyses. A: Low-power view showing the characteristic heterogeneity of prostate tissue, with this region containing a combination of BPH, PIN, and well-differentiated adenocarcinoma. B: High-power view of a region in panel A, showing details of BPH and PIN. The region of BPH has ducts surrounded by basal cells (arrows), which are not found in the region of PIN. The area of PIN shows a transition within the same duct between normal and atypical hyperchromatic cells that contain larger nuclei with prominent nucleoli. C: High-power view showing a nearby area of human prostate with well-differentiated adenocarcinoma that is invading the peri-neural space (N marks the position of the nerve fiber). Note that the carcinoma cells have large nuclei with very prominent nucleoli (arrows). D: View of a different prostate sample with high-grade PIN and a mixture of Gleason grade 4 and 5 carcinoma in the rest of the field. E: Immunohistochemical staining of PIN and carcinoma using anti-cytokeratin 8, which marks all of the epithelial cells. These PIN lesions have a cribiform pattern (arrows), but are still within the confines of a prostatic duct. F: Immunohistochemical staining of a tissue section containing both PIN and carcinoma using anti-cytokeratin 14, which marks the basal cells. Notably, the PIN displays inconsistent staining, whereas the carcinoma has no staining (Abate-Shen and Shen, 2000).

Although cytologically prostate cancer is variable, generally nuclei are large and vacuolated and contain one or more large nucleoli. Microscopically, besides the absence of the basal cell layer, another characteristic of prostate cancer is the observation of glands growing 'back to back' with no intervening stroma (Kirby, 1996). In well-

differentiated tumors, the glandular pattern is apparent, however in some poorly differentiated tumors the glandular pattern is only visible upon careful examination (Cotran et al., 1994). In such cases the tumor cells tend to grow in cords, sheets, or nests with varying amounts of stromal production (Cotran et al., 1994). To assist with the prognosis of prostate cancer and as a way to effectively communicate with other pathologists, the Gleason grading system was developed (Kirby, 1996). Using the Gleason grading system the pattern of the tumor is assigned two grades (ranges from 1-5) which are added together to obtain the Gleason score (ranges from 2-10). The changes for each grade as assigned by Gleason are shown in Figure 1.9.

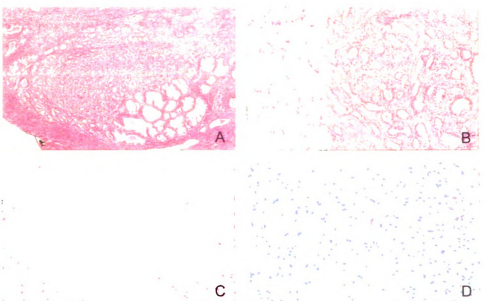

Figure 1.9 Gleason grading system. The changes for each grade as assigned by Gleason are shown. A: Gleason grade 1; B: Gleason grade 3; C: Gleason grade 4; D: Gleason grade 5 (Modified from Kirby, 1996).

Gleason grade 1 tumors are comprised of small, uniform glands exhibiting minimal nuclear changes; the nodules typically possess well-defined borders. Gleason grade 3 is the most common grade of prostate cancer (Kirby, 1996). These tumors show a high degree of variation in architecture, glandular size, shape and regularity; infiltrative borders are generally found. Gleason grade 4 and 5 represent more aggressive tumors with cytologic atypia, extensive infiltrative borders, seminal vesicle extension, and/ or metastatic spread.

It is generally accepted that human prostatic carcinomas are slow growing. Prostate capsular invasion occurs early in invasive prostatic cancer, local and direct spread of cancer is at first mostly posterior. Direct local spread of cancer cells often leads to ureteric obstruction with invasion frequently shown in the fatty tissue between the prostate and rectum, the seminal vesicles, and the bladder (Rose, 1985). Metastatic spread of prostate cancer to the bone is the main cause of morbidity among cancer patients, other common sites of metastases are the lymph nodes and liver (Cotran et al., 1994). The bones commonly involved, in descending order of frequency, are lumbar spine, proximal femur, pelvis, thoracic spine and ribs (Cotran et al., 1994). In contrast to prostate cancer, benign tumors and low grade PIN do not metastasize to other organs.

There are several methods for prostate cancer detection which include: palpation, transurethral resection, transrectal ultra sound, and serum PSA levels. Blood tests to detect PSA and/ or the digital rectal examination are most commonly performed to screen for prostate cancer. Most PSA produced by prostate cells remains within the prostate, while only a small amount gets absorbed into the bloodstream. When a carcinoma develops in the prostate the patient's PSA levels tend to rise. If elevated PSA levels or a

prostatic nodule are detected upon screening then a biopsy is taken to make the diagnosis of cancer. Early prostate cancer has few or no symptoms, but with more advanced disease individuals may experience difficulty or pain during urination which are also symptoms caused by benign conditions (American Cancer Society, 2004). Surgery and radiation may be used to treat early-stage prostate cancer. Supplemental therapies for early-stage disease include: hormonal therapy, chemotherapy, and radiation (or combinations of these treatments) (American Cancer Society, 2004). These therapies may also be used to treat metastatic disease. The extent of prostate cancer can be determined by CT scans, magnetic resonance imaging, or pelvic lymphadenectomy. Instead of immediately treating prostate cancer, an individual that may have a limited life span or a less aggressive stage of the disease, may also elect to just 'watch and wait'.

Many factors seem to play a role in the development of prostate cancer, including environmental influences, race, age, nutrition, cigarette smoking and family history (American Cancer Society, 2004; Plaskon et al., 2003). Although some studies have suggested a genetic linkage in the familial aggregation of prostate cancer, researchers have had difficulty identifying a single susceptibility gene (Simard et al., 2003). Efforts to assist with the treatment of prostate cancer are currently directed towards the development of potential markers of malignant potential for prostate cancer.

Conclusions

The phenotypic and genetic abnormalities which result in the development of BPH and prostatic adenocarcinoma are being intensely investigated. The goal of many investigators is to develop a diagnostic method which can be readily employed to

accurately predict the behavior of an individual cancer. Due to the latent onset of HGPIN and its strong association with prostate cancer, early detection and treatment may prevent progression to invasive and metastatic prostate cancer. Further studies utilizing *in vitro* human prostate cell lines and *in vivo* xenograft models that mimic multiple steps in prostate carcinogenesis, invasion and metastasis will assist in the understanding and treatment of the disease.

Literature cited

Abate-Shen, C. and Shen, M.M.: Molecular genetics of prostate cancer. Genes & Development 14:2410-2434, 2000.

Abrahamsson, P.: Neuroendocrine differentiation and hormone-refractory prostate cancer. Prostate Supplement 6:3-8, 1996.

Ahmed, M.M., Lee, C.T. and Oesterling, J.E.: Current trends in the epidemiology of prostatic diseases: benign hyperplasia and adenocarcinoma. In: Prostate: Basic and Clinical Aspects, R.K. Naz (ed.), Boca Raton, FL, CRC Press, pp.3-25, 1997.

American Cancer Society: Cancer Facts and Figures 2004, Atlanta, GA, pp.16-17, 2004.

Aumuller, G.: Morphologic and endocrine aspects of prostatic function. Prostate 4:195 214, 1983.

Brawer, M.K., Peehl, D.M., Stamey, T.A., and Bostwick, D.G.: Keratin immunoreactivity in the benign and neoplastic human prostate. Cancer Research 45:3663-3667, 1985.

Bonkoff, H. and Remberger, K.: Differentiation pathways and histogenetic aspects of normal and abnormal prostatic growth: A stem cell model. Prostate 28:98-106, 1996.

Bonkoff, H. and Remberger, K.: Widespread distribution of nuclear androgen receptors in the basal cell layer of the normal and hyperplastic human prostate. Virchows Arch [A] 422:35-38, 1993.

Bonkoff, H., Stein, U., and Remberger, K.: Multidirectional differentiation in the normal, hyperplastic, and neoplastic human prostate. Simultaneous demonstration of cell specific epithelial markers. Human Pathology 25:42-46, 1994a.

Bonkoff, H., Stein, U. and Remberger, K.: The proliferative function of basal cells in the normal and hyperplastic human prostate. Prostate 24:114-118, 1994b.

Bonkoff, H., Stein, U., and Remberger, K.: Androgen receptor status in endocrine paracrine cell types of the normal, hyperplastic, and neoplastic human prostate. Virchows Arch [A] 423:291-294, 1993.

Bostwick, D.G.: High grade prostatic intraepithelial neoplasia. Cancer Supplement 75:1823-1836, 1994.

Campbell, N.A., Reece, J.B. and Mitchell, L.G.: Animal reproduction. In: Biology, Fifth Edition, Benjamin Cummings (ed.), Menlo Park, CA, pp.913-935, 1999.

Cormack, D.H.: Essential Histology, Baltimore, Lippincott, Williams and Wilkins, pp. 463, 2001.

Cotran, R.S., Kumar, V. and Robbins, S.L.: Male genital system. In: Robbins Pathologic Basis of Disease, Fifth Edition, F.J. Schoen (ed.), Philidelphia, W.B. Saunders Company, pp. 1023-1031, 1994.

De Marzo, A.M., Nelson, W.G., Meeker, A.K., and Coffey, D.S.: Stem cell features of benign and malignant prostate epithelial cells. Journal of Urology 160:2381 2392, 1998.

Dixon, J.S., Chow, P.H. and Gosling, J.A.: Anatomy and function of the prostate gland. In: Textbook of Prostatitis, J.C. Nickel (ed.), Oxford, UK, Isis Medical Media Ltd., pp.33-46, 1999.

Kirby, R.S., Christmas, T.J., and Brawer, M.: Anatomical and pathological considerations. In: Prostate Cancer, New York, Mosby, pp. 3-21, 1996.

Lalani, E., Laniado, M.E., and Abel, P.D.: Molecular and cellular biology of prostate cancer. Cancer and Metastasis Reviews 16:29-66, 1997.

McConnell, J.D. et al.: Finasteride, an inhibitor of 5α-reductase, suppresses prostatic dihydrotestosterone in men with benign prostatic hyperplasia. Journal of Endocrinological Metabolism 74:505-508, 1992.

McNeal, J.E. and Bostwick, D.G.: Intraductal dysplasia: a premalignant lesion of the prostate. Human Pathology 17:64-71, 1986.

McNeal, J.E., Redwine, E.A., Freiha, F.S. and Stamey, T.A.: Zonal distribution of prostatic adenocarcinoma: Correlation with histologic pattern and direction of spread. American Journal of Surgical Pathology 12:897-906, 1988.

Nagle, R.B., Ahmann, F.R., McDaniel, K.M., Paquin, M.L., Clark, V.A., and Celniker, A.: Cytokeratin characterization of human prostatic carcinoma and its derived cell lines. Cancer Research 47:281-286, 1987.

Paulson, D.F.: Male reproductive system. In: Histology and Cell Biology, Fourth Edition, New York, McGraw-Hill, pp.279-289, 2000.

Plaskon, L.A., Penson, D.F., Vaughan, T.L. and Stanford, J.L.: Cigarette smoking and risk of prostate cancer in middle-aged men. Cancer Epidemiology Biomarkers and Prevention 12:604-609, 2003.

Rittmaster, R.S.: Finasteride. New England Journal of Medicine 330:120-125, 1994.

Rose, E.F.: Neoplasms of the genital conduit system. In: Genitourinary Oncology, D.A. Culp and S.A. Loening (eds.), Philadelphia, Lea & Febiger, pp. 382-464, 1985.

Rous, S.N.: Normal anatomy and normal function. In: The Prostate Book: Sound Advice on Symptoms and Treatment, New York, Norton and Company, pp.19-26, 1988.

Sakr, W.A., Haas, G.P., Cassin, J.J., Pontes, J.E., Crissman, J.D.: The frequency of carcinoma and intraepithelial neoplasia of the prostate in young male patients. Journal of Urology 150:379-385, 1993.

Sharp, R.M., Bello-DeOcampo, D., Quader, S. and Webber, M.M.: *N*-(4-hydroxyphenyl) retinamide (4-HPR) decreases neoplastic properties of human prostate cells: an agent for prevention. Mutation Research 496:163-170, 2001.

Simard, J., Dumont, M., Labuda, D., Sinnett, D., Meloche, C., El-Alfy, M., Berger, L., Lees, E., Labrie, F. and Tavtigian, S.V.: Prostate susceptibility genes: lesions learned and challenges posed. Endocrine-Related Cancer 10:225-259, 2003.

Starr, C. and McMillian, B., (eds): Human Biology, Belmont, CA, Wadsworth, pp. 1-531, 1997.

Wartinger, D.D., Webber, M.M., Chu, W.W., and Bello-Deocampo, D.: Benign tumors of the prostate. In: Prostate Health Watch. Webber, M.M., Wartinger, D.D., Williams, D.E. (eds.), pp. 2-6, 1997.

Webber, M.M., Bello-DeOcampo, D., Quader, S., DeOcampo, N., Metcalfe, W.S. and Sharp, R.M.: Modulation of the malignant phenotype of human prostate cancer cells by *N*-(4-hydroxyphenyl)retinamide (4-HPR). Clinical & Experimental Metastasis 17:255-263, 1999.

CHAPTER TWO

CHARACTERISTICS OF THREE HUMAN PROSTATE CANCER CELL LINES: PC-3, DU145, AND LNCaP

Abstract

The processes of invasion and metastasis in prostate cancer are complex. To increase our understanding of these complex processes, several *in vivo* models, developed from well characterized cell lines, would be useful. Invasive tumor cells show an increase in the expression of growth factors, alter their cell:cell and cell:matrix interactions, and express proteases that degrade the extracellular matrix. Each of these invasive characteristics have been studied in the PC-3, DU145, and LNCaP human prostate cancer cell lines. Based on data collected from *in vitro* studies, all three cell lines are invasive and may serve as suitable models for advanced and metastatic prostate cancer. The LNCaP cell line, however, also carries an androgen receptor mutation. LNCaP cells are therefore useful for studying: i) prostate cancers carrying androgen receptor (AR) mutations and ii) response of prostate cancer cells to androgens, anti-androgens, other hormones, and drugs and agents, whose effects may be mediated by AR in prostate cancers carrying AR mutations. While data collected from a xenograft model, using PC-3 or DU145 cell lines, would be useful and applicable to prostate cancer patients with advanced prostate cancer that does not carry AR mutations.

Keywords

Cell line, DU145, invasion, LNCaP, metastatic, PC-3, prostate cancer

Introduction

Metastatic spread is the main cause of death in prostate cancer patients. It is, therefore, important to develop *in vivo* models for studying prostate cancer metastasis using human cell lines. A few prostate cancer cell lines of human origin are currently available. Some of these cell lines may be suitable for *in vivo* studies, because their invasive behavior has been studied *in vitro*. Cell morphology, differentiation, regulation of growth, and expression of adhesion molecules and proteases all contribute to the invasive behavior of cancer cells. Knowledge of these characteristics of cells and their invasive behavior *in vitro* would enable us to select a suitable model for studying advanced and metastatic prostate cancer. The use of human prostate cancer cell lines in immune-suppressed mice to generate xenografts, permits a direct comparison between the histopathology and molecular biology of the patient-derived specimen and resulting tumors in mice. Since studies using xenografts are an important step before clinical trials of new drugs can be conducted for cancer treatment, the xenograft model should mimic the human disease as closely as possible in order to collect relevant and applicable data.

Xenograft models of human prostate cancer can be used to correlate the invasive behavior of a cell line *in vitro* with its invasive and metastatic behavior *in vivo*. Xenograft models are particularly useful for testing new drugs for chemotherapy. To date most of the studies in the field of human prostate cancer have focused only on three human prostate cancer cell lines, PC-3, DU-145, and LNCaP, because they were developed in the period from 1977 to 1980 and became readily available. Other human prostate cancer cell lines developed more recently are not readily available at the present time. All cell lines should be considered when planning research using xenograft models

to select the most appropriate cells for collecting data prior to human trials. The objective of my own research is to develop xenograft models using newly developed human prostate cancer cell lines. The first step in selecting a cell line for *in vivo* studies is to become familiar with the invasive characteristics of the cell line. In this review the characteristics of the PC-3, DU145, and LNCaP human prostate cancer cell lines and their potential applications, advantages, as well as limitations as xenograft models, are discussed.

Source of cells:

Source of PC-3 cells

PC-3 cells were derived from a 62 year old Caucasian male (Kaighn et al., 1979). His symptoms included urinary retention, weight loss and anemia. Biopsy of the prostate revealed poorly differentiated prostatic adenocarcinoma. Next the patient underwent bilaterial orchiectomy and was treated with diethylstilbestrol, which only transiently improved his condition. Four months later the patient's condition worsened despite cryotherapy and he died. Tumor tissue was taken from a rib of the patient shortly after his death for *in vitro* culture to initiate the PC-3 cell line. Autopsy also revealed abundant tumor in the bone marrow and metastasis in the adrenal. The first report of the PC-3 cell line was published in 1978 (Kaighn et al., 1978).

Source of DU145 cells

In 1975, a 69 year old white male was admitted to Durham Veterans Administration Hospital with widespread metastatic carcinoma of the prostate (Mickey et

al., 1980). He also had a three year history of lymphocytic leukemia. He was treated with diethylstilbestrol, but subsequent evaluation showed further metastatic spread to the central nervous system. He then underwent bilateral orchiectomy, transurethral resection of the prostate and parieto-occipital craniotomy to excise a tumor mass. Tissue removed from the metastatic central nervous system lesion was taken for *in vitro* culture to initiate the DU145 cell line. The brain metastasis was identified as a moderately differentiated adenocarcinoma with foci of poorly differentiated cells. There was brief improvement of central nervous system function but the symptoms recurred and the patient died in 1976 with pneumonia and septicemia. Autopsy results showed tumor metastasis to the right femoral neck, vertebral column, periaortic and celiac nodes, liver, lungs, and brain. The first report of the DU145 cell line was published in 1977 (Mickey et al., 1977).

Source of LNCaP cells

LNCaP cells were derived in 1977 from a patient with metastatic carcinoma in a lymph node. The patient was diagnosed one year earlier with moderately differentiated adenocarcinoma of the prostate and showed minimal response to hormone therapy and no response to chemotherapy (Horoszewicz et al., 1980). Initially the patient was treated with oral estrogen, but six months later disseminated bone metastases were found. Next the patient underwent orchiectomy which only resulted in temporary response. After experiencing pain in his right leg he was admitted to Roswell Park Memorial Institute and was treated with methyl (2-chloroethyl)-3-cyclohexy-1-nitrosourea (CCNU), which is an alkalating agent and Estracyt, a combination of estrogen and mechlorethamine. One month later he was diagnosed with metastatic carcinoma in a lymph node, the material

aspirated for biopsy was used to initiate LNCaP cell culture *in vitro*. Hydronephrosis was also observed at this time due to increased pressure on the ureter by the metastatic lymph node. As a result the patient was treated with *cis*-platinum at which time his disease progressed rapidly. A high dosage of the anti-inflammatory drug, Decadron, temporarily improved his condition but the patient died six months after admission and one and a half years after diagnosis. The first report of the LNCaP cell line was published in 1980 (Horoszewicz et al., 1980).

Prostate cancer arises from epithelial cells lining the glands of the prostate. Therefore, the first step in the process of selecting a cell line to study prostate cancer is to establish that the cells are of epithelial origin. To confirm epithelial origin, one would observe cell morphology and expression of epithelial cell markers.

Cell morphology:

Both PC-3 and DU145 cell lines show typical, polygonal, epithelial morphology. The LNCaP cell line does not have distinct epithelial morphology. The LNCaP cells have a more spindle-shaped and elongated morphology, which is sometimes observed in invasive prostate cancer cells (Webber et al., 2001).

Epithelial origin:

The cytoskeletal proteins, cytokeratins, serve as an important marker for establishing epithelial origin of cells. To insure that the cells have an epithelial origin, immunocytochemistry is commonly performed. Secretory luminal cells of the prostate express cytokeratins 8 and 18 and the basal epithelial cells express cytokeratins 5 and 14.

PC-3, DU145, and LNCaP cells are all positive for cytokeratins 8 and 18, but negative for cytokeratins 5 and 14 by immunohistochemistry (Figure 2.1) (Mitchell et al., 2000). In another study the basal cell marker, cytokeratin 5, was detected in PC-3 and DU145 cell lines (van Bokhoven et al., 2003). The expression of cytokeratin 5 in PC-3 and DU145 cells is consistent with data collected from human prostate samples. In regressed and therapy-resistant prostate cancers, an increase in cytokeratin 5-positive tumor cells was noted when compared with untreated carcinomas (Gil Diez de Medina et al., 1998).

PC-3 and DU145 cell lines are both apparently derived from secretory luminal epithelial cells and may also contain cells that represent either an intermediate phenotype or dedifferentiated luminal cells, while the LNCaP cell line is apparently derived from secretory luminal epithelial cells.

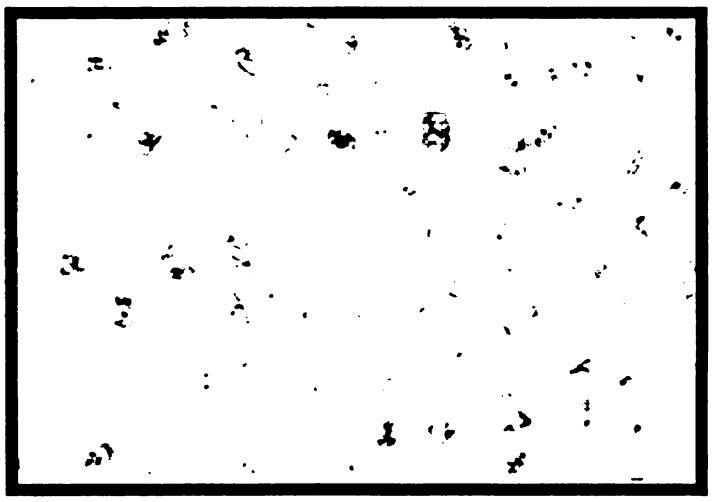

Figure 2.1 Expression of cytokeratin 8 in LNCaP cells is shown by the brown cytoplasmic stain, 400X (Modified from Mitchell et al., 2000).

The next step in characterizing a cell line is to establish that it is indeed of prostatic origin, by determining that cells express some prostate specific marker proteins. One such protein is prostate specific antigen (PSA).

Response to androgen and the expression of androgen receptor and PSA:

PSA is a component of the seminal fluid and serves as a marker for prostatic origin of cells. Normal prostatic epithelial cells are stimulated to grow by androgen and they secrete PSA in response to androgen exposure. Most studies show that PC-3 cells do not express PSA or AR and are androgen insensitive, however, weak staining for PSA has been reported (Kaighn et al., 1979; Garde et al., 1993; Mitchell et al., 2000). Some studies show that the DU145 cell line does not express androgen receptor and is therefore, hormone-insensitive and does not express PSA (Paulson et al., 1977; Garde et al., 1993; Mitchell et al., 2000). However other studies have shown the presence of androgen binding sites in the DU145 cell line using a radioligand binding assay, as well as, immunohistochemistry (Carruba et al., 1994; Brolin et al., 1992).

Regardless of whether or not these cell lines express androgen receptor, PC-3 and DU145 are androgen-insensitive. The ability of PC-3 and DU145 cells to grow in the presence or absence of androgen is consistent with the growth of the tumor cells in both patients. Neither orchiectomy, nor diethylstilbestrol treatment slowed the growth of the prostate cancer in either patient. Since both the DU145 and PC-3 cell lines are hormone insensitive, they show increased expression of several growth factors to assist in their growth and survival.

LNCaP cells respond to androgen and it stimulates their growth, as well as, cytoplasmic PSA expression (Figures 2.2 and 2.3) (Berns et al., 1986; Hsieh et al., 1993; Webber et al., 1995; Mitchell et al., 2000). PSA is also constitutively secreted by LNCaP cells even in the absence of an androgen stimulus. This may be due to a mutation in the androgen receptor.

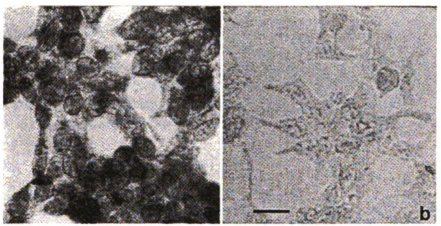

Figure 2.2 Indirect avidin-biotin immunoperoxidase staining of LNCaP cells using mAb to PSA. a, cells stained with PSA antibody; b, control. Bar, 20μm. (Webber et al., 1995).

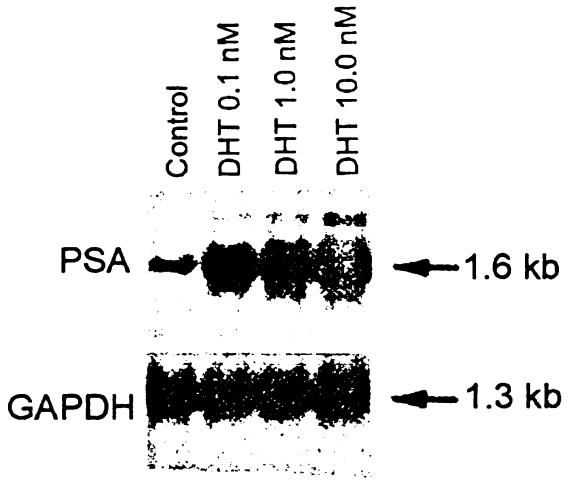

Figure 2.3 Regulation of PSA expression in the LNCaP cell line. Various concentrations of dihydrotestosterone (DHT) were added to the LNCaP cell line. Twenty four h after treatment, total cellular RNA was prepared and 20 μg of total cellular RNA were subjected to Northern analysis. Relative PSA mRNA levels were determined by densitometrical quantification, and the control is defined as 1.0, DHT 0.1 (3.04), DHT 1.0 (3.96), and DHT 10.0 (4.54) (Modified from Hsieh et al., 1993).

The androgen receptor mutation in the LNCaP cells makes the cells responsive not only to androgens but also to anti-androgens, estrogen, and progesterone (Schuurmans et al., 1991; Jiang et al., 2004). The patient that was the source of the LNCaP cell line was treated with estrogen to counter the effects of androgen on prostate cell growth, but six months later bone metastases were found. The altered ligand responsiveness observed may have assisted in the ligand-independent activation of the androgen receptor after estrogen treatment, thus, permitting tumor progression in the patient.

In addition to hormones, growth factors can also assist in androgen-independent cell growth and survival.

Production and response to growth factors:

Growth factors enable cells to maintain local homeostasis and adapt to their biological microenvironment. The secretion of growth factors allows cells to control promotion or inhibition of cellular proliferation and many other functions, such as, cell differentiation and increased or decreased expression of PSA and androgen receptor (Henttu et al., 1993).

A number of growth factors produced by epithelial and stromal cells stimulate prostate cell growth and proliferation. Epidermal growth factor (EGF) and transforming growth factor-α (TGF-α) are stimulatory factors secreted by epithelial cells that share a receptor on epithelial cells. However, TGF-α is only expressed during embryonic development in normal cells. A variety of tumor types have been found to secrete TGF-α, and not the normal EGF (Connolly and Rose, 1990). Stromal derived growth factors that have a stimulatory effect on prostate cells include basic fibroblast growth factor (bFGF), and insulin-like growth factor (IGF). The receptors for these growth factors reside at the cell membrane of both epithelial and stromal cells. Transforming growth factor-β1 (TGF-β1) inhibits epithelial cell growth, however, some prostate cancer cells may lose the ability to be inhibited by TGF-β1 or show a decrease in growth inhibitory response.

Growth factors may be secreted by cells which may affect their own behavior in an autocrine manner, or that of a neighboring target cell in a paracrine manner. One characteristic of progression from a normal to a malignant phenotype is reflected in the increased rate of cell proliferation caused by the autocrine secretion of growth factors (Culig et al., 1994). Increased expression of growth factors may also enhance invasion in

prostate cancer cells (Jarrard et al., 1994). PC-3, DU145, and LNCaP cells secrete and respond to some of their own growth factors, therefore, unlike normal prostate epithelial cells, these cell lines are not as dependent on the local microenvironment for cell growth and survival. The increased expression of these growth factors permits these cells to survive in various microenvironments.

A comparison of growth factor secretion and receptor expression in PC-3, DU145, and LNCaP cell lines is shown in Table 2.1. A comparison of growth factor response in PC-3, DU145, and LNCaP cell lines is shown in Table 2.2.

PC-3 cell line

PC-3 cells exhibit low or undetectable levels of both the receptors and their ligands, for example, epidermal growth factor receptors (EGF-R) and its ligands, EGF and TGF-α (Carruba et al., 1994). Addition of exogenous EGF or exogenous TGF-α to PC-3 cells does not affect cell growth in monolayer cultures (Jarrard et al., 1994; Wilding et al., 1988). PC-3 cells show expression of TGF-β1 and TGF-β1 receptors and addition of TGF-β to PC-3 cells inhibits colony formation in soft agarose (Carruba et al., 1994; Jakowlew et al., 1997).

PC-3 cells also express growth factors that are normally expressed by stromal cells. PC-3 cells produce measurable amounts of bFGF and large amounts of FGF-R mRNA (Nakamoto et al., 1992). Addition of recombinant bFGF to the culture media, does not enhance DNA synthesis in the PC-3 cell line (Nakamoto et al., 1992). Low levels of another stromal-derived growth factor, IGF-1, was observed in conditioned media from PC-3 cells (Kimura et al., 1996). These cells express functional, high affinity

IGF-1 receptors, but do not show a growth stimulatory response to exogenous IGF-1 (Kimura et al., 1996). PC-3 cells may not show a response to exogenous IGF-I because they express almost twice the amount of IGF-II compared to DU145 and LNCaP cells, which may contribute to the autocrine action of IGF-I via the IGF-R (Kimura et al., 1996).

DU145 cell line

Immunofluorescent staining of DU145 cells shows intense staining for TGF-α, but to a lesser extent for EGF (Carruba et al., 1994). Intense staining for EGF-R was also shown in DU145 cells. DU145 cells show very little response to exogenous TGF-α or EGF (Carruba et al., 1994, MacDonald and Habib, 1992). DU145 cells do not show TGF-β1 expression, but they do express TGF-β1 receptors and their growth is inhibited in response to exogenous TGF-β (Carruba et al., 1994; Jakowlew et al., 1997).

DU145 cells, similar to PC-3 cells, express stromal-derived growth factors. DU145 cells produce measurable amounts of bFGF and large amounts of FGF-R (Nakamoto et al., 1992). DU145 cells also show a growth stimulatory response upon addition of recombinant bFGF to the culture medium. These cells express functional, high affinity IGF-1 receptors and produce low levels of IGF-1 (Kimura et al., 1996). Addition of exogenous IGF-1 at low concentrations stimulates the growth of DU145 cells (Lee et al., 2003). In this cell line the overproduced bFGF and IGF-1 activate their respective receptors in an autocrine loop.

LNCaP cell line

LNCaP cells express EGF and TGF-α, as well as their receptors (Carruba et al., 1994). Both exogenous TGF-α and EGF stimulate the growth of LNCaP cells (MacDonald and Habib, 1992; Wilding et al., 1989). LNCaP cells express TGF-β1 receptor and show weak expression of TGF-β (Carruba et al., 1994; Jakowlew et al., 1997). The growth of LNCaP cells is inhibited upon addition of exogenous TGF-β (Jakowlew et al., 1997).

LNCaP cells do not express bFGF, but they do show low levels of FGF mRNA and a growth stimulatory response to recombinant bFGF (Nakamoto et al., 1992). These cells express functional, high affinity IGF-1 receptors and low levels of IGF-1 (Kimura et al., 1996). Addition of exogenous IGF-1 stimulated the growth of LNCaP cells in a dose dependent manner (Lee et al., 2003). In this cell line the overproduced IGF-1 activates the receptor in an autocrine loop.

Table 2.1 Expression of growth factors and their receptors in human prostatic carcinoma cell lines

	LNCaP	DU145	PC-3
Growth factor expression/secretion			
EGF	++	++	+
TGF-α	++	+++	+
bFGF	ND	++	+
IGF-1	+	+	+
TGF-β	(+)	ND	++
Receptor expression			
EGF/TGF-α-R	++	+++	+
FGF-R	+	+++	+++
IGF-1-R	++	++	++
TGF-β-R	++	++	++

(+), weakly positive; +, low measurable levels; +++, high levels; ND, not detectable (Modified from Webber et al., 1997).

Table 2.2 Response to exogenous growth factors

	LNCaP	DU145	PC-3
EGF	+	0	0
TGF-α	+	0	0
bFGF	+	+	0
IGF-1	+	+	0
TGF-β	-	-	-

+, stimulatory effect; -, inhibitory effect; 0, no response (Modified from Webber et al., 1997).

DU145 and PC-3 cells show autocrine regulation of several growth factors, including bFGF and IGF-1, which contributes to the malignant phenotype of these two cell lines. LNCaP cells only show autocrine regulation of IGF-1. This deregulation of growth in favor of proliferation not only aids in the survival of cells in various environments, but it has also been shown to decrease acinar forming ability in 3-D culture (Bello-DeOcampo et al., 2001b). Adhesion proteins, such as, integrins and cadherins are important for acinar morphogenesis and therefore cell organization and cell polarity.

Adhesion properties:

Polarized epithelial cells form the glandular compartment of the prostate and apically secrete their products into a lumen. The maintenance of cell polarity depends on cell:cell and cell:extracellular matrix (ECM) interactions. These interactions are also an important component of cell motility. Integrins provide the link between cells and the ECM whereas cadherins are responsible for cell:cell adhesion. Invasive prostate cancer cells have decreased or abnormal expression of both integrins and cadherins, which assist in their dissemination from the prostate (Bello-DeOcampo et al., 2001b ; Achanazar et al., 2004).

Invasive behavior of prostate cancer cells has been shown to be inversely correlated with the ability to undergo acinar morphogenesis (Bello-DeOcampo et al., 2001b). The non-tumorigenic, RWPE-1 cell line forms acini at a high frequency (100%) in 3-D Matrigel cultures and the cells are not invasive using a Boyden chamber *in vitro* invasion assay. On the other hand, DU145 cells failed to form acini in (three-

dimensional) 3-D Matrigel cultures and were highly invasive in the Boyden chamber *in vitro* invasion assay (Bello-DeOcampo et al., 2001b). Normal acinar morphogenesis in RWPE-1 cells was found to be associated with the expression of both α_6 and β_1 integrins at the basal and baso-lateral surfaces of the cells (Bello-DeOcampo et al., 2001b).

The DU145, PC-3, and LNCaP cell lines were all found to express a relatively similar pattern of α_6 and β_1 integrins, as compared to each other. In prostate carcinoma the pattern of the α_6 and β_1-integrin subunits, which in normal cells, are restricted to the basal and baso-lateral surfaces, are distributed diffusely throughout the cytoplasmic membrane (Knox et al., 1994). Indirect immunofluroescence microscopy shows PC-3, DU145, and LNCaP cells contain α_6 in focal regions on the cell surface (Witkowski et al., 1993). DU145 and LNCaP cells also contain β_1 in focal regions on the cell surface, however PC-3 cells show a diffuse cytoplasmic membrane pattern of β_1. The abnormal expression of α_6 and β_1 integrins is likely to be responsible for the loss of ability to undergo acinar morphogenesis (Bello-DeOcampo et al., 2001b). In addition, this may assist in the invasion of these cells through the basement membrane. Other adhesion proteins, such as, cadherins also play an important role in the progression from a non-invasive to an invasive phenotype.

Cadherins, in addition to integrins, play an important role in maintaining cell:cell adhesion, cell shape, cell polarization and acinar morphogenesis (Bussemakers et al., 1996; Webber et al., 1997, Bello-DeOcampo et al., 2001a, Bello-DeOcampo et al., 2001b). Altered expression of the protein, E-cadherin, has been observed in about 50% of prostate cancer cases (Achanazar et al., 2004; Hayward et al., 1998). In a study of E-cadherin expression in human tumors, expression of E-cadherin in metastatic deposits

was generally reduced or absent, but some metastatic deposits were found to have strong E-cadherin staining (Umbas et al., 1992). The LNCaP cell line was derived from a metastatic deposit but, based on results of Western blot analysis, these cells show strong expression of E-cadherin (Morton et al., 1993). The PC-3 and DU145 cell lines were also derived from a metastatic deposit, but they have less E-cadherin expression than the LNCaP cell line and cultured normal prostate epithelial cells (Figure 2.4 and Table 2.3). These data are consistent with results of immunocytochemistry using these three cell lines. The LNCaP cell line shows strong, positive, homogenous E-cadherin expression in 100% of cells, while E-cadherin staining of PC-3 and DU145 cells show heterogenous expression (Mitchell et al., 2000).

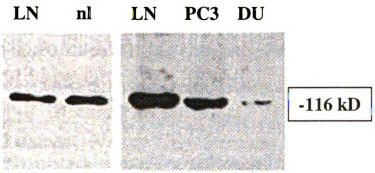

Figure 2.4 Western blot analysis of E-cadherin in prostate cells. LN=LNCaP cells; nl, normal prostate epithelial cells; PC3=PC-3 cells; DU=DU145 cells. For comparison purposes, LNCaP cells were analyzed at the same time as normal cells (left panel) and in a different analysis with the other two cell lines (right panel). Signals were quantitated by scanning densitometry of X-ray film. Exposure times were 2 min (left panel) and extended to 15 min (right panel) to increase sensitivity; 50 μg of total cellular protein were loaded in each lane, and probed with HECD-1 monoclonal antibody. β-Galactosidase (116 kD) is the molecular weight marker for E-cadherin (124 kD) (Modified from Morton et al., 1993).

Table 2.3 Relative levels of E-cadherin in prostate cells*

Cells	E-cadherin
Normal**	1.0
LNCaP	1.1
DU145	0.1
PC-3	0.6

*Levels determined by scanning densitometry of autoradiographs of Western blots.
**All values are relative to levels found in cultured normal prostate epithelial cells and represent the average values from 3 separate experiments (Morton et al., 1993).

Besides E-cadherin, other classical cadherins include, P- and N-cadherin. PC-3 cells, in addition to E-cadherin, express N- and P-cadherin while DU145 cells express increased levels of P-cadherin (Bussemakers et al., 2000; Tran et al., 1999). The increased, abnormal expression of P- or N-cadherin, also referred to as cadherin switching, resulting in the loss of cadherin homeostasis, has been associated with the acquisition of an invasive phenotype (Achanazar et al., 2004). For example, in comparison to the non-tumorigenic human prostate epithelial cell line, RWPE-1, which mimics cadherin expression in normal cells, the related, yet invasive human prostate cancer cell lines, RWPE2-W99, WPE1-NB26 and CTPE, all express varying levels of P- and N-cadherins (Achanazar et al., 2004). RWPE2-W99 and WPE1-NB26 cells express lower than normal levels of P-cadherin, but increased levels of N-cadherin as compared to RWPE-1 cells. While two of the three invasive cell lines show low P-cadherin and increased levels of N-cadherin, CTPE cells show increased levels of

P-cadherin and undetectable levels of N-cadherin. Cadherin switching and heterogeneity of cadherin expression observed in these cell lines mimics cadherin switching and heterogeneous cadherin expression observed in human prostate cancers (Achanazar et al., 2004). A loss or increased expression of one or more cadherins can disrupt homeostasis resulting in a change in cell adhesion, shape, polarization, and motility, and thus, may contribute to an invasive phenotype.

Adhesive functions of cadherins also involve the normal expression of catenins. These proteins form a complex with the cytoplasmic portion of cadherin molecules and couple them to actin cytoskeletons of epithelial cells. Further studies are necessary to confirm the adhesive properties of cadherin expression and its involvement in the invasive behavior in these cell lines.

The invasive potential of these cell lines can also be attributed to the expression of proteases such as matrix metalloproteinases (MMPs).

Proteases:

To metastasize prostate cancer cells must first degrade the ECM. While integrins are responsible for adhering cells to the ECM, proteases are responsible for degradation of the ECM. Type IV gelatinases, MMP-2 and MMP-9, are secreted as zymogens and upon activation they degrade type IV collagen in the basement membrane. The activity of MMPs is modulated by proenzyme activation and expression of their inhibitors, the tissue inhibitors of matrix metalloproteinases (TIMPs). Although both normal and neoplastic cells produce MMPs and other proteases, only malignant cells are invasive. In normal cells homeostasis is maintained between MMPs and their inhibitors. Analysis of

conditioned medium by gelatin zymography and enzyme assays show that both benign and neoplastic prostate tissues secrete latent MMP-9 and latent and active forms of MMP-2 (Lokeshwar et al., 1993). However conditioned medium from malignant prostate explants contained a higher proportion of the active form of MMP-2. Significant amounts of TIMP-1 and TIMP-2 were secreted by adult prostate and benign prostate tissues, but TIMP-1 levels were markedly reduced in conditioned medium from neoplastic tissues and TIMP-2 was absent (Lokeshwar et al., 1993). These data show that increasing levels of active MMP activity and decreasing levels of TIMPs are associated with prostate carcinoma.

Another protease produced by cancer cells is urokinase-type plasminogen activator (uPA), it can activate plasminogen to plasmin which can degrade many ECM proteins and activate collagenases. uPA can also activate collagenases or directly degrade basement membrane components (Reith and Rucklidge, 1992; Webber and Waghray, 1995). Serum levels of u-PA in prostate cancer patients with metastasis are higher than those in healthy controls and in prostate cancer patients without metastasis (Miyake et al., 1999). Thus, the serine protease, u-PA, is considered to play a crucial role in the degradation of the extracellular matrix leading to tumor cell invasion and metastasis (Waghray and Webber, 1995; Webber and Waghray, 1995). Two proteins responsible for the negative regulation of uPA include, plasminogen activator inhibitor type-1 (PAI-1) and plasminogen activator inhibitor type-2 (PAI-2). While little is known about the expression of PAI-2, PAI-1 is undetectable in cells of some aggressive malignancies (Lyon et al., 1995; Soff et al., 1995). A comparison of protease and

protease inhibitor expression in PC-3, DU145, and LNCaP cell lines is shown in Table 2.4.

Table 2.4 Protease and protease inhibitor expression in human prostate cancer cell lines

	LNCaP	DU145	PC-3	Reference(s)
MMP-2	0/+	0	0	Webber, et al., 1996;
MMP-9	0/+	0	0	Dong et al., 2001
TIMP-1	+	++	++	Zhang et al., 2002
TIMP-2	+	++	++	
u-PA	0/+	+++	+++	Waghray and Webber, 1995; Hoosein et al., 1991
PAI-1	0	0	+	Lyon et al., 1995
PAI-2	0	0	+	

0, undetectable; +, trace; ++, low; +++, high expression

Trace levels of MMP-2 and MMP-9 were secreted by LNCaP cells, however gelatinase activity was undetectable in conditioned medium from the DU145 cell line (Webber et al., 1996). Gelatinase activity was also undetectable in the PC-3 cell line (Dong et al., 2001). Although low or no expression of MMPs was observed in LNCaP, DU145 and PC-3 cells, mRNA expression of TIMP-1 is lower in all three cell lines compared to benign prostatic tissue (Zhang et al., 2002). LNCaP cells express lower levels of TIMP-2 mRNA compared to benign prostatic tissue, whereas PC-3 and DU145 cells express higher levels of TIMP-2. LNCaP cells expressed the least amount of

TIMP-1 and TIMP-2 mRNA compared to DU145 and PC-3 cells. Additional testing for active TIMP-1 and TIMP-2 expression should be performed on these three cell lines.

DU145 and PC-3 cells also secrete u-PA, which could contribute to their invasive potential. DU145 cells express five times more extracellular, secreted u-PA activity than the tested normal prostatic epithelial cells (Waghray and Webber, 1995). Three different assays performed on the LNCaP, PC-3, and DU145 cell lines, show very low levels of urokinase secretion by LNCaP cells and higher urokinase levels in PC-3 compared to DU145 cells (Hoosein et al., 1991). The production of plasminogen activator inhibitors was very low or undetectable in these three cell lines. Only a small amount of PAI-1 and PAI-2 protein was detectable in the PC-3 cell line (Lyon et al., 1995). To compare the expression of proteases with the invasive potential of a cell line *in vitro*, a reconstituted basement membrane is used to examine invasive behavior.

Invasion *in vitro:*

The invasive potential of DU145 and PC-3 cells was determined by their ability to invade *in vitro* in a Matrigel invasion assay. Matrigel serves as a reconstituted basement membrane. Invasion by cancer cells through the basement membrane *in vivo* is one of the first steps in the progression to metastasis (Webber et al., 1995). Normal prostate cells are attached to the basement membrane and are not invasive. The invasive ability of DU145 and LNCaP cells was determined using the *in vitro* Boyden chamber assay (Bello, 1996). The invasive ability of PC-3 cells was also determined using the *in vitro* Boyden chamber assay, although the technique varied from the assay with DU145 and LNCaP cells (Fong et al., 1992). The invasion assay performed by (Bello, 1996) used

filters with a smaller pore size, a different chemoattractant and cells were allowed to invade for twenty four hours instead of six hours. (Bello, 1996) also used a different technique to quantify invasive cells, which involved staining the nuclei of cells on the bottom of the filter and extracting dye in addition to counting viable cells in the chamber well.

In comparison to DU145 cells, LNCaP cells showed 19% invasion (Figure 2.5) (Bello, 1996). In comparison to DU145 cells, PC-3 cells were about twice as invasive (Fong et al., 1992). So the PC-3 cell line is the most invasive cell line *in vitro* followed by the DU145 cell line and then the LNCaP cell line. The invasive ability observed *in vitro* in these cell lines is also observed *in vivo*. Nude mice injected subcutaneously with PC-3 cells often develop metastatic tumors or show invasion into surrounding tissues, but metastatic tumors are rare in mice injected subcutaneously with LNCaP cells (Kozlowski et al., 1984; Sato et al., 1997; Rembrink et al., 1997). In a subcutaneous xenograft model of DU145, no macroscopic metastases were visible, however intra-splenic injection of DU145 cells, but not LNCaP cells, did result in the formation of metastasic tumors (Devi et al., 2002; Pettaway et al., 1996; Kozlowski et al., 1984).

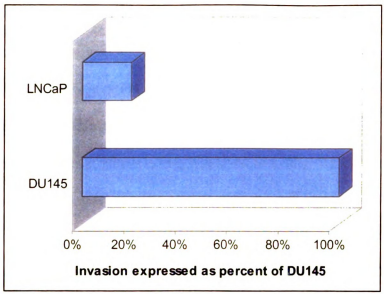

Figure 2.5 *In vitro* invasion of DU145 and LNCaP cells. Invasive ability of DU145 and LNCaP cell lines was examined by the Boyden chamber in vitro invasion assay. 400,000 cells were plated on each "Matrigel"-coated filter and allowed to invade for 24 h. The invasive ability of the highly invasive DU145 cell line was set at 100% invasion (Modified from Bello, 1996).

Conclusions

Derivation of the PC-3, DU145, and LNCaP cell lines from metastatic deposits demonstrates their metastatic potential. Both PC-3 and DU145 cell lines are androgen-insensitive and show autocrine regulation of growth. PC-3 and DU145 cells show varying levels of cadherin expression and PC-3 cells show abnormal $\alpha_6\beta_1$ integrin expression. The PC-3 cell line expresses higher urokinase levels and is about twice as invasive as DU145 cells in the *in vitro* Boyden chamber assay. These cell lines would be useful for studies on androgen insensitive cell growth for developing treatment strategies for prostate cancer patients in which the cancer cells do not respond to hormone therapy.

The LNCaP cell line is androgen-sensitive and also shows autocrine regulation of growth. In comparison to PC-3 and DU145 cells, LNCaP cells show strong expression of E-cadherin and low uPA expression. The LNCaP cell line, *in vitro*, is the least invasive of the three cell lines. Although LNCaP cells are androgen-sensitive, the cells also carry a mutated androgen receptor, which is only observed in a minority of prostate cancer patients. Therefore, the results of some studies with this cell line may not be applicable to all of prostate cancers as many prostate cancer patients do not possess a mutated androgen receptor. The same AR gene mutation described in the LNCaP cell line has been observed in 6 of 24 (25%) prostate tissue specimens derived from patients with advanced prostate cancer (Gaddipati et al., 1994). The LNCaP cell line would be particularly useful for developing treatment strategies for prostate cancer patients in which the cancer cells have a mutated androgen receptor. To better understand prostate cancer and to develop treatments for the majority of prostate cancer patients, a prostate cancer cell line that is androgen-sensitive and has normal androgen receptor expression would be useful. The WPE1-NB26 cell line, developed in our laboratory (Webber et al., 2001) is such a cell line. It is for this reason that I used WPE1-NB26 cells for developing a xenograft model of prostate cancer.

Literature cited

Achanzar, W.E., Lamar, P.C., Tokar, E.J., Rivette, A.S., Bello-DeOcampo, D., Prozialeck, W.C., Webber, M.M., and Walkes, M.P.: Human prostate cell lines mimic heterogeneity of cadherin expression in human prostate cancer. UroOncology 4:15-25, 2004.

Bello, D.: *In vitro* invasion. In: Characterization of immortalized and malignant adult human prostate epithelial cell lines: PWR-1E, RWPE-1, and RWPE-2. Master of Science Thesis, Michigan State University, East Lansing, MI, USA, pp.69-78, 1996.

Bello-DeOcampo, D., Kleinman, H.K., DeOcampo, N.D., and Webber, M.M.: Laminin 1 and $\alpha_6\beta_1$ integrin regulate acinar morphogenesis of normal and malignant human prostate epithelial cells. Prostate 46:142-153, 2001a.

Bello-DeOcampo, D., Kleinman, H.K., and Webber, M.M.: The role of $\alpha 6\beta 1$ integrin and EGF in normal and malignant acinar morphogenesis of human prostatic epithelial cells. Mutation Research 480-481:209-217, 2001b.

Berns, E.M.J.J., de Boer, W., and Mulder, E.: Androgen-dependent growth regulation of and release of specific protein(s) by the androgen receptor containing human prostate tumor cell line LNCaP. Prostate 9:247-259, 1986.

Brolin, J., Skoog, L., and Ekman, P.: Immunohistochemistry and biochemistry in detection of androgen, progesterone, and estrogen receptors in benign and malignant human prostatic tissue. Prostate 20:281-295, 1992.

Bussemakers, M.J.G., and Schalken, J.A.: The role of cell adhesion molecules and proteases in tumor invasion and metastasis. World Journal of Urology 14:151 -156, 1996.

Bussemakers, M.J.G., Van Bokhoven, A., Tomita, K., Jansen, C.F.J., and Schalken, J.A.: Complex cadherin expression in human prostate cancer cells. International Journal of Cancer 85:446-450, 2000.

Carruba, G., Leake, R.E., Rinaldi, F., Chalmers, D., Comito, L., Sorci, C., Pavone Macaluso, M., and Castagnetta, L.A.M.: Steroid-growth factor interaction in human prostate cancer. 1. Short-term effects of transforming growth factors on growth of human prostate cancer cell lines. Steroids 59:412-420, 1994.

Connolly, J.M., and Rose, D.P.: Production of epidermal growth factor and transforming growth factor-α by the androgen-responsive LNCaP human prostate cancer cell line. Prostate 16:209-218, 1990.

Culig, Z., Hobisch, A., Cronauer, M.V., Radmayr, C., Trapman, J., Hittmair, A., Bartsch, B., and Klocker, H.: Androgen receptor activation in prostatic tumor cell lines by insulin-like growth factor-I, keratinocyte growth factor, and epidermal growth factor. Cancer Research 54:5474-5478, 1994.

Devi, G.R., Oldenkamp, J.R., London, C.A., and Iverson, P.L.: Inhibition of human chorionic gonadotropin β-subunit modulates the mitogenic effect of c-*myc* in human prostate cancer cells. Prostate 52:200-210, 2002.

Dong, Z., Nemeth, J., Cher, M.L., Palmer, K.C., Bright, R.C., and Fridman, R.: Differential regulation of matrix metalloproteinase-9, tissue inhibitor of metalloproteinase-1 (TIMP1) and TIMP-2 expression in co-cultures of prostate cancer and stromal cells. International Journal of Cancer 93:507-515, 2001.

Fong, C., Sutkowski, D.M., Kozlowski, J.M., and Lee, C.: Utilization of the boyden chamber to further characterize in vitro migration and invasion of benign and malignant human prostatic epithelial cells. Invasion Metastasis 12:264-274, 1992.

Gaddipati, J.P., McLeod, D.G., Heidenberg, H.B., Sesterhenn, I.A., Finger, M.J., Moul, J.W., and Srivastava, S.: Frequent detection of codon 877 mutation in the androgen receptor gene in advanced prostate cancers. Cancer Research 54:2861 2864, 1994.

Garde, S.V., Sheth, A.P., Porter, A.T., and Pienta, K.J.: A comparative study on expression of prostatic inhibin peptide, prostate acid phosphatase and prostate specific antigen in androgen independent human and rat prostate carcinoma cell lines. Cancer Letters 70:159-166, 1993.

Gil Diez de Medina, S., Salomon, L., Colombel, M., Abbou, C.C., Bellot, J., Thiery, J.P., Radvanyi, F., Van der Kwast, T.H., and Chopin, D.K.: Modulation of cytokeratin subtype, EGF receptor, and androgen receptor expression during progression of prostate cancer. Human Pathology 29:1005-1012, 1998.

Hayward, S.W., Grossfeld, G.D., Tlsty, T.D., and Cunha, G.: Genetic and epigenetic influences in prostate carcinogenesis (Review). International Journal of Oncology 13:35-47, 1998.

Henttu, P., and Vihko, R.: Growth factor regulation of gene expression in the human prostatic carcinoma cell line LNCaP. Cancer Research 53:1051-1058, 1993.

Hoosein, N.M., Boyd, D.D., Hollas, W.J., Mazar, A., Henkin, J., and Chung. L.W.K.: Involvement of urokinase and its receptor in the invasiveness of human prostatic carcinoma cell lines. Cancer Communications 3:255-264, 1991.

Horoszewicz, J.S., Leong, S.S., Chu, T.M., Wajsman, Z.L., Friedman, M., Papsidero, L., Kim, U., Chai, L.S., Kakati, S., Arya, S.K., and Sandberg, A.A.: The LNCaP cell line-A new model for studies on human prostatic carcinoma. In: Progress in Clinical and Biological Research, Models for Prostate Cancer, Murphy, G.P. (ed.), Buffalo, NY, Alan R. Liss Inc., 37:67-84, 1980.

Hsieh, J., Wu, H., Gleave, M.E., von Eschenbach, A.C., and Chung, L.W.K.: Autocrine regulation of prostate-specific antigen gene expression in a human prostatic cancer (LNCaP) subline. Cancer Research 53:2852-2857, 1993.

Jarrard, K.F., Blitz, B.F., Smith, R.C., Patai, B.L., and Rukstalis, D.B.: Effect of epidermal growth factor on prostate cancer cell line PC3 growth and invasion. Prostate 24:46-53, 1994.

Jakowlew, S.B., Moody, T.W., and Mariano, J.M.: Transforming growth factor-beta receptors in human cancer cell lines: analysis of transcript, protein, and proliferation. Anticancer Research 17:1849-1860, 1997.

Jiang, J., Wang, L.F., Fang, Y.H., Jin, F.S., and Jin, W.S.: Proliferative response of human prostate cancer cell to hormone inhibited by androgen receptor antisense RNA. Chinese Medical Journal 117:684-688, 2004.

Kaighn, M.E., Lechner, J.F., Narayan, K.S., and Jones, L.W.: Prostate carcinoma: Tissue culture cell lines. National Cancer Institute Monograph 49:17-21, 1978.

Kaighn, M.E., Narayan, S., Ohnuki, Y., Lechner, J.F., and Jones, L.W.: Establishment and characterization of a human prostatic carcinoma cell line (PC-3). Investigative Urology 17:16-23, 1979.

Kimura, G., Kasuya, J., Giannini, S., Honda, Y., Mohan, S., Kawachi, M.H., Akimoto, M., and Fujita-Yamaguchi, Y.: Insulin-like growth factor (IGF) system components in human prostatic cancer cell-lines: LNCaP, DU145, and PC-3 cells. International Journal of Urology 3:39-46, 1996.

Knox, J.D., Cress, A.E., Clark, V., Manriquez, L., Affinito, K.S., Dalkin, B.L., and Nagle, R.B.: Differential expression of extracellular matrix molecules and the alpha 6-integrins in the normal and neoplastic prostate. American Journal of Pathology 145:167-174, 1994.

Kozlowski, J.M., Fidler, I.J., Campbell, D., Xu, Z., Kaighn, M.E., and Hart, I.R.: Metastatic behavior of human tumor cell lines grown in the nude mouse. Cancer Research 44:3522-3529, 1984.

Lee, H., Pienta, K.J., Kim, W., and Cooper, C.R.: The effect of bone-associated growth factors and cytokines on the growth of prostate cancer cells derived from soft tissue versus bone metastases in vitro. International Journal of Oncology 22:921 -926, 2003.

Lokeshwar, B.L., Selzer, M.G., Block, N.L., and Gunja-Smith, Z.: Secretion of matrix metalloproteinases and their inhibitors (tissue inhibitor of metalloproteinases) by human prostate in explant cultures: reduced tissue inhibitor of metalloproteinase secretion by malignant tissues. Cancer Research 53:4493-4498, 1993.

Lyon, P.B., See, W.A., Xu, Y., and Cohen, M.B.: Diversity and modulation of plasminogen activator activity in human prostate carcinoma cell lines. Prostate 27:179-186, 1995.

MacDonald, A., and Habib, F.K.: Divergent responses to epidermal growth factor in hormone sensitive and insensitive human prostate cancer cell lines. British Journal of Cancer 65:177-182, 1992.

Mickey, D.D., Stone, K.R., Wunderli, H., Mickey, G.H., and Paulson, D.F.: Characterization of a human prostate adenocarcinoma cell line (DU145) as a monolayer culture and as a solid tumor in athymic mice. In: Progress in Clinical and Biological Research, Models for Prostate Cancer, Murphy, G.P. (ed.), Buffalo, NY, Alan R. Liss Inc., 37:67-84, 1980.

Mickey, D.D., Stone, K.R., Wunderli, H., Mickey, G.H., Vollmer, R.T., and Paulson, D.F.: Heterotransplantation of a human prostatic adenocarcinoma cell line in nude mice. Cancer Research 37:4049-4058, 1977.

Mitchell, S., Abel, P., Ware, M., Stamp, G., and Lalani, E.N.: Phenotypic and genotypic characterization of commonly used human prostatic lines. British Journal of Urology International 85:932-944, 2000.

Miyake, H., Hara, I., Yamanaka, K., Arakawa, S., and Kamidono, S.: Elevation of urokinase type plasminogen activator and its receptor densities as new predictors of disease progression and prognosis in men with prostate cancer. International Journal of Oncology 14:535-541, 1999.

Morton, R.A., Ewing, C.M., Nagafuchi, A., Tsukita, Shoichiro, and Isaacs, W.B.: Reduction of e-cadherin levels and deletion of the α-catenin gene in human prostate cancer cells. Cancer Research 53:3585-3590, 1993.

Nakamoto, T., Chang, C., Li, A., and Chodak, G.W.: Basic fibroblast growth factor in human prostate cancer cells. Cancer Research 52:571-577, 1992.

Paulson, D.F., Stone, K.R., Mickey, D.D., Bonar, R.A., and Wunderli, H.: Development and application of basic research techniques in bladder cancer research. Cancer Research 37:2969-2973, 1977.

Pettaway, C.A., Pathak, S., Greene, G., Ramirez, E., Wilson, M.R., Killion, J.J., and Fidler, I.J.: Selection of highly metastatic variants of different human prostatic carcinomas using orthotopic implantation in nude mice. Clinical Cancer Research 2:1627-1636, 1996.

Reith, A., and Rucklidge, G.J.: Invasion of brain tissue by primary glioma: evidence for the involvement of urokinase-type plasminogen activator as an activator of type IV collagenase. Biochemistry and Biophysical Research Communications 186:348-354, 1992.

Rembrink, K., Romijn, J.C., van der Kwast, T.H., Rubben, H., and Schroder, F.H.: Orthotopic implantation of human prostate cancer cell lines: a clinically relevant animal model for metastatic prostate cancer. Prostate 31:168-174, 1997.

Sato, N., Gleave, M.E., Bruchovsky, N., Rennie, P.S., Beraldi, E., and Sullivan, L.D.: A metastatic and androgen-sensitive human prostate cancer model using intraprostatic inoculation of LNCaP cells in SCID mice. Cancer Research 57:1584-1589, 1997.

Schuurmans, A.L.G., Bolt, J., Veldscholte, J., and Mulder, E.: Regulation of growth of LNCaP human prostate tumor cells by growth factors and steroid hormones. Journal of Steroid Biochemical and Molecular Biology 40:193-197, 1991.

Soff, G.A., Sanderowitz, J., Gately, S., Verrusio, E., Weiss, I., Brem, S., and Kwaan, H.C.: Expression of plasminogen activator inhibitor type 1 by human prostate carcinoma cells inhibits primary tumor growth, tumor-associated angiogenesis, and metastasis to lung and liver in an athymic mouse model. Journal of Clinical Investigations 96:2593-2600, 1995.

Tran, N.L., Nagle, R.B., Cress, A.E., and Heimark, R.L.: N-cadherin expression in human prostate carcinoma cell lines. American Journal of Pathology 155:787 -798, 1999.

Umbas, R., Schalken, J.A., Aalders, T.W., Carter, B.S., Karthaus, H.F.M., Schaafsma, H.E., Debruyne, F.M.J., and Isaacs, W.B.: Expression of the cellular adhesion molecule, E-cadherin, is reduced or absent in high grade prostate cancer. Cancer Research 52:5104-5109, 1992.

Waghray, A., and Webber, M.M.: Retinoic acid modulates extracellular urokinase-type plasminogen activator activity in DU-145 human prostatic carcinoma cells. Clinical Cancer Research 1:747-753, 1995.

Webber, M.M., Bello, D., and Quader, S.: Immortalized and tumorigenic adult human prostatic epithelial cell lines: Characteristics and applications part 2. Tumorigenic cell lines. Prostate 30:58-64, 1997.

Webber, M.M., Quader, S.T.A., Kleinman, H.K., Bello-DeOcampo, D., Storto, P.D., Bice, G., DeMednonca-Calaca, W., and Williams, D.E.: Human cell lines as and *in vitro/in vivo* model for prostate carcinogenesis and progression. Prostate 47:1 -13, 2001.

Webber, M.M., and Waghray, A.: Urokinase-mediated extracellular matrix degradation by human prostatic carcinoma cells and its inhibition by retinoic acid. Clinical Cancer Research 1:755-761, 1995.

Webber, M.M., Waghray, A., and Bello, D.: Prostate specific antigen (PSA), a serine protease, facilitates human prostate cancer invasion. Clinical Cancer Research 1:1089-1094, 1995.

Webber, M.M., Waghray, A., Bello, D., and Rhim, J.S.: Mini review: proteases and invasion in human prostate epithelial cell lines: implications in prostate cancer prevention and intervention. Radiation Oncology Investigations 3:358-362, 1996.

Wilding, G., Valverius, E., Knabbe, C., and Gelmann, E.P.: Role of transforming growth factor-α in human prostate cancer cell growth. Prostate 15:1-12, 1989.

Wilding, G., Zugmeier, G., Knabbe, C., Valverius, E., Flanders, K., and Gelmann, E.P.: The role of transforming growth factors α and β in human prostate cancer cell growth. Endocrinology 29:241, 1988.

Witkowski, C.M., Rabinovitz, I., Nagle, R.B., Affinito, K.D., and Cress, A.E.: Characterization of integrin subunits, cellular adhesion and tumorigenicity of four human prostate cell lines. Journal of Cancer Research and Clinical Oncology 119:637-644, 1993.

van Bokhoven, A., Varella-Garcia, M., Korch, C., Johannes, W.U., Smith, E.E., Miller, H.L., Nordeen, S.K., Miller, G.J., and Lucia, M.S.: Molecular characterization of human prostate carcinoma cell lines. Prostate 57:205-225, 2003.

Zhang, J., Jung, K., Lein, M., Kristiansen, G., Rudolph, B., Hauptmann, S., Schnorr, D., Loening, S.A., and Lichtinghagen, R.: Differential expression of matrix metalloproteinases and their tissue inhibitors in human primary cultured prostatic cells and malignant prostate cell lines. Prostate 50:38-45, 2002.

CHAPTER THREE

RWPE-1 CELL LINE AND ITS DERIVATIVES: RWPE2-W99, CTPE, AND THE MNU FAMILY OF CELL LINES

Abstract

Most studies in prostate cancer research have been conducted using cell lines derived from metastatic deposits. To assist in the treatment and prevention of prostate cancer, cell lines that represent earlier stages of prostate cancer are needed. A cell line that mimics normal prostate cell behavior is also necessary for comparison in studies using malignant prostate cell lines. Therefore, several cell lines, all derived from the same parental, RWPE-1 cell line, that represent multiple steps in prostate carcinogenesis and progression, have been generated and extensively characterized. These cell lines all show unique characteristics to study prostate cancer. The parent, RWPE-1 cells, behave much like normal prostate cells while the derived cell lines all show varying degrees of malignant cell behavior. Several characteristics of abnormal cell behavior have been observed during prostate carcinogenesis and tumor progression. Such characteristics include changes in: cell morphology, response to growth factors, as well as, expression of cytoskeletal proteins, adhesion molecules, and proteases. The objective of this chapter is to describe the development and derivation of a family of cell lines, and their characteristics. Further, their applications in studies of prostate cancer prevention and treatment and the development of xenograft models are explored.

Keywords

Cell line, CTPE, prostate cancer, RWPE-1, RWPE2-W99, WPE1-NA22, WPE1-NB11, WPE11-NB14, and WPE1-NB26

Introduction

To assist in the prevention of tumor progression and metastatic spread, which is the main cause of death in prostate cancer patients, human cell lines that represent early events in carcinogenesis and tumor progression would be useful. Cell lines that mimic behavior of normal human prostate cells are also necessary to serve as controls *in vitro* or as standardized models *in vivo* when studying prostate cancer progression. However, normal human epithelial cells require immortalization to provide a practical system for *in vitro* studies (Bello et al., 1997; Webber et al., 1996a). Immortalization is an important step in the process of carcinogenesis. Immortalized cells can be used to study carcinogenesis as well as normal prostatic epithelial cell functions, differentiation, and modulation by growth factors, hormones, and other agents (Webber et al., 1996b). The use of normal, human, immortalized prostate cells along with other human prostate cell lines *in vitro* or *in vivo* allows investigators to obtain comparable data for solving problems in prostate carcinogenesis and metastasis. The three most commonly studied cell lines; PC-3, DU145, and LNCaP, were all derived from metastatic deposits in prostate cancer patients (Kaighn et al., 1979; Mickey et al., 1980; Horoszewicz et al., 1980). They are, therefore, more appropriate for *in vitro* and *in vivo* studies on advanced prostate cancer. In this review characteristics of a normal prostatic epithelial cell line, RWPE-1, and two RWPE-1-derived transformants, RWPE2-W99 and CTPE, as well as, a family of cell lines transformed by *N*-methyl-*N*-nitrosourea (MNU), will be described. Potential applications and advantages of these cells lines as appropriate models of prostate cancer will also be discussed.

Source of RWPE-1, RWPE2-W99, MNU, and the CTPE cell line:

RWPE-1 cells were isolated from the prostate of a 54 year-old Caucasian man undergoing radical prostatectomy (Bello et al., 1997). These cells were immortalized with the human papilloma virus-18 (HPV-18) genome using a plasmid vector and Polybrene-induced DNA transfection followed by shock with dimethyl sulfoxide (Rhim et al., 1994). HPV-18 was used for immortalization because cells are more likely to retain growth and differentiation characteristics of their normal cells of origin and they are non-tumorigenic (Bello et al., 1997; Woodworth et al., 1990; Yankaskas et al., 1993). HPVs are also the most common sexually transmitted disease, and are implicated in the etiology of several cancers (Chen et al., 1993; Webber et al., 1997). The RWPE-1 cell line was further transformed by the Ki-*ras* oncogene to obtain the RWPE-2 cell line (Bello et al., 1997; Webber et al., 1997). To transform RWPE-1 cells, the Kirsten murine sarcoma virus (Ki-MuSV) containing an activated Ki-*ras* oncogene and a helper virus, baboon endogenous virus, were used (Rhim et al., 1994). RWPE2-W99 cells were derived from a colony of RWPE-2 cells growing in agar that was selected for high Ki-*ras* expression. Both, the presence of *ras* mutations and high-risk HPV DNA sequences, have been linked at a relatively high frequency in Japanese men with prostate cancer (Anwar et al., 1992).

A family of cell lines, the MNU cell lines, was also generated from the RWPE-1 cells (Figure 3.1) (Webber et al., 2001). RWPE-1 cells were treated with MNU, a chemical carcinogen, at 50 or 100 μg/ml. Carcinogen-exposed cells were injected subcutaneously in nude mice and tumors were removed 10 weeks after cell injection. Cells from these tumors were grown in culture to give rise to 2A (50 μg/ml MNU) and

3B (100 μg/ml MNU) cells. These cells were again injected subcutaneously into nude mice and tumors were collected and plated in culture to expand the cell population. Cells were then plated in soft agar. Individual colonies were isolated and expanded and gave rise to the MNU cell lines which all share a common lineage; These cell lines include: WPE1-NA22, WPE1-NB14, WPE1-NB11, and WPE1-NB26 (Figure 3.1).

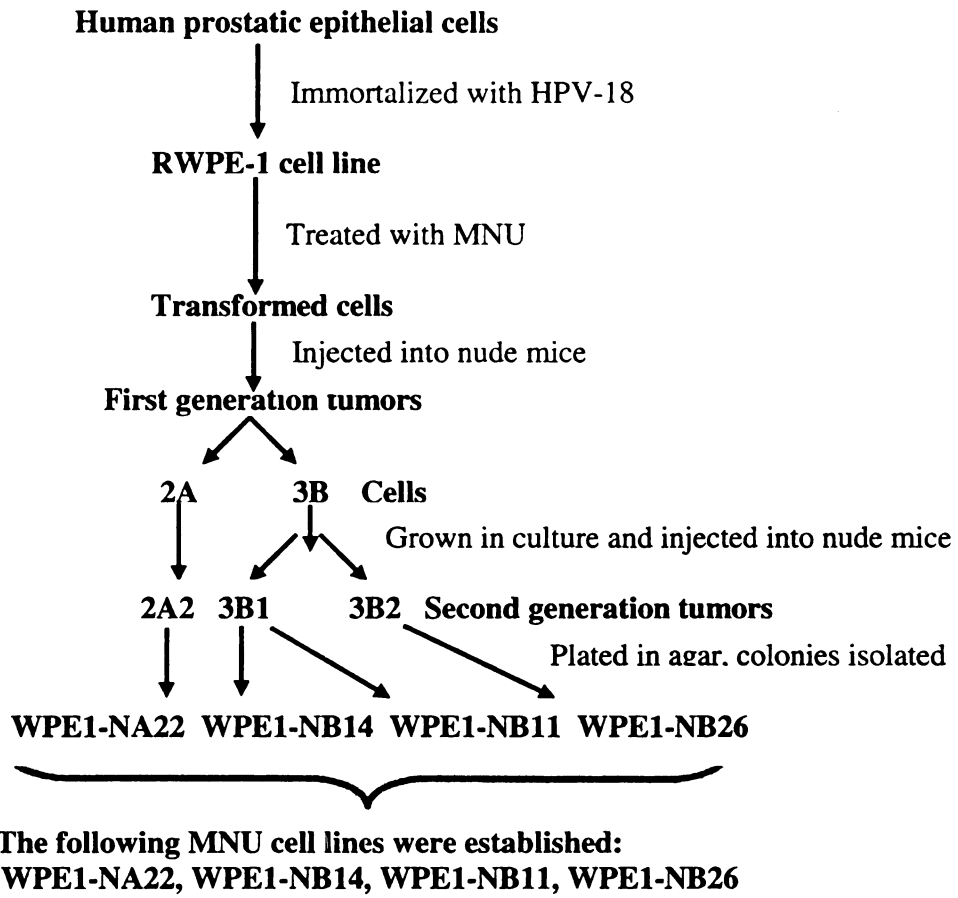

Figure 3.1 Derivation of the MNU-transformed cell lines from RWPE-1, a HPV-18 immortalized human prostatic epithelial cell line. The 2A tumor was derived from treatment with MNU at 50 μg/ml and 3B tumor at 100 μg/ml (Webber et al., 2001).

RWPE-1 cells were also transformed by *in vitro* cadmium exposure for 8 weeks to obtain the CTPE cell line (Achanazar et al., 2001). Cadmium, a known human carcinogen, has been implicated in prostate cancer etiology and cancer progression (Waalkes et al., 1997). Cadmium is also an effective carcinogen in rats, and the rat prostate was found to be a target for cadmium carcinogenesis. This suggests that

occupational or environmental cadmium exposure is a risk factor for the development of prostate malignancies. So, CTPE, RWPE2-W99, and the MNU family of cell lines, each have many applications in the study of prostate cancer, such as, identifying molecular changes associated with cadmium, Ki-*ras* or MNU. To confirm epithelial origin of these cell lines, cell morphology and the expression of cytokeratins were examined.

Cell morphology:

RWPE-1 and RWPE2-W99 cells have a typical, polygonal, epithelial morphology (Figures 3.2a and 3.3a) (Bello et al., 1997). The morphology of the MNU cell line, WPE1-NA22, closely resembles that of RWPE-1 cells (Figure 3.4a and b) (Webber et al., 2001). However, the cell morphology of another MNU cell line, WPE1-NB26, was more elongated compared to RWPE-1 cells (Figure 3.4e). The morphology of the other two MNU cell lines, WPE1-NB14 and WPE1-NB11, was in between polygonal and elongated (Figure 3.4c and d).

Epithelial origin:

Cytokeratins are cytoskeletal proteins that are important markers expressed by epithelial cells. Secretory luminal epithelial cells of the prostate express cytokeratins 8 and 18, while basal epithelial cells of the prostate express cytokeratins 5 and 14. Both RWPE-1 and RWPE-2 cells express cytokeratins 8 and 18 (Figures 3.2e and f and 3.3e and f), which establishes their epithelial origin (Bello et al., 1997). All of the MNU cell lines show expression of cytokeratins 8 and 18 confirming their epithelial origin (Webber

et al., 2001). CTPE cells also express cytokeratin 18 (Webber, M.M., personal communication).

Several additional markers, such as, the expression of androgen receptor (AR) and prostate specific antigen (PSA) are also necessary to confirm prostatic epithelial origin of the cell lines.

Response to androgen and the expression of androgen receptor and PSA:

Prostatic epithelial cells express androgen receptor and in response to androgen exposure, they express PSA. Both RWPE-1 and RWPE-2 cell lines show a growth response to a synthetic androgen, mibolerone, and express PSA and AR, as assessed by immunocytochemistry (Figures 3.2 and 3.3, b-d) (Bello et al., 1997). CTPE cells also express PSA in response to androgen exposure (Webber, M.M., personal communication). The cell lines of the MNU family show a growth stimulatory response to mibolerone and express PSA and AR, however, the expression pattern of AR varies amongst the cell lines (Figure 3.4f-h) (Webber et al., 2001). WPE1-NB11 and WPE1-NB26 cells were found to show homogeneous, strong nuclear staining while the WPE1-NA22 and WPE1-NB14 cells were found to show heterogeneous nuclear staining. The ability of RWPE-1, RWPE2-W99, CTPE and the MNU family of cell lines to respond to androgens, confirms their prostatic origin. Cell response to growth factors is an important aspect of cell behavior.

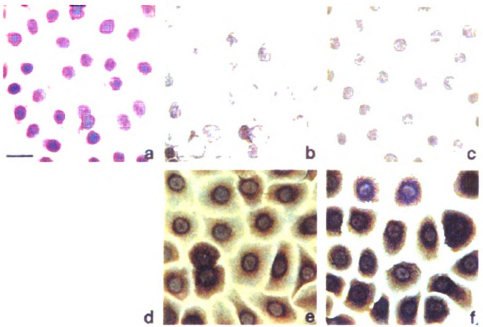

Figure 3.2 Characterization of RWPE-1 cells. Proteins were detected by immunoperoxidase staining. (a) hematoxylin and eosin staining; (b) positive staining for PSA; (c) positive staining for nuclear androgen receptor. Cells for (b) and (c) were pretreated with 5nM mibolerone; (d) a control lacking primary antibody; (e) and (f) positive staining for cytokeratin 8 and 18, respectively. Scale bar is 20 μM. X 625 (Modified from Bello et al., 1997).

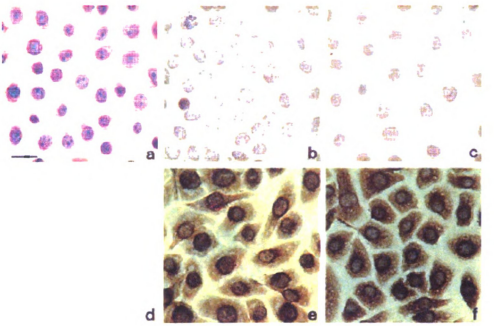

Figure 3.3 Characterization of RWPE-2 cells. Proteins were detected by immunoperoxidase staining. (a) hematoxylin and eosin staining; (b) positive staining for PSA; (c) positive staining for nuclear androgen receptor. Cells for (b) and (c) were pretreated with 5nM mibolerone; (d) a control lacking primary antibody; (e) and (f) positive staining for cytokeratin 8 and 18, respectively. Scale bar is 20 μM. X 625 (Modified from Bello et al., 1997).

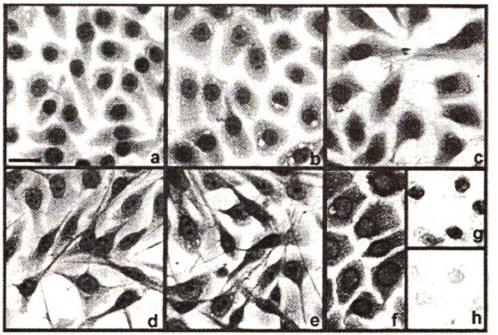

Figure 3.4 Characterization of MNU cell lines. Morphology of (hematoxylin and eosin stain): (a) RWPE-1, (b) WPE1-NA22, (c) WPE1-NB14, (d) WPE1-NB11, (e) WPE1-NB26 cells. F-h: PSA and androgen receptor expression in WPE1-NA22 cells treated with mibolerone, as detected by immunostaining; f, positive staining for PSA; g, positive staining for nuclear androgen receptor; and h, a control lacking primary antibody. Bar = 20 μM (Webber et al., 2001).

Production and response to growth factors:

Malignant cells tend to secrete and respond to their own growth factors in an autocrine manner, to assist in their growth and survival in various microenvironments. For this reason, when malignant cells are treated with exogenous growth factors *in vitro*, they may not show a marked response. Epidermal growth factor (EGF) stimulates epithelial cell growth while transforming growth factor-β (TGF-β) inhibits epithelial cell growth, however, some prostate cancer cells may lose the ability to be inhibited by TGF-β or show a decrease in growth inhibitory response.

RWPE-1 cells show a response, similar to normal cells, to EGF and TGF-β (Bello et al., 1997). The MNU family of cell lines show a growth stimulatory response to exogenous EGF and an inhibitory response to TGF-β, however, the response varied amongst the four cell lines (Webber et al., 2001). The WPE1-NA22 and WPE1-NB14 cells were more responsive to the growth stimulatory effects of EGF than the WPE1-NB11 and WPE1-NB26 cells. WPE1-NB26 cells were also the least responsive to the inhibitory effects of TGF-β, with WPE1-NB11 being the most responsive to TGF-β. Cell response to growth factors has not yet been published for the CTPE cell line. These data suggest that the RWPE-1 cell line responds to growth factors similar to normal cells, with the other cell lines being less responsive, and showing varying degrees of responsiveness. The WPE1-NB26 cell line shows the least amount of responsiveness to exogenous growth factors, and thus, is considered to represent the most malignant cell line of the MNU family in terms of growth factor response. Deregulation of growth in favor of proliferation has been correlated with loss of cell organization (Bello-DeOcampo et al., 2001b). Loss of cell organization has also been correlated with abnormal integrin and cadherin expression.

Adhesion properties:

In glandular tissues, such as the prostate, cell:matrix and cell:cell adhesions mediated by integrins and cadherins respectively, result in cell polarization and organization into acini. Invasive behavior of prostate cancer cells has been shown to be inversely correlated with the ability to undergo acinar morphogenesis (Bello-DeOcampo et al., 2001b). RWPE-1 cells, like normal cells, organize into acini with distinct lumens

lined by a single layer of cells in 3-D Matrigel culture (Figure 3.5a) (Bello-DeOcampo et al., 2001b). However, the tumorigenic, RWPE-2 cells remain as single cells or form small aggregates (Webber et al., 1997). The ability of the RWPE-1 cell line to polarize and form acini is consistent with their normal growth regulation and strong, basal expression of the $\alpha_6\beta_1$ integrin (Bello-DeOcampo et al., 2001b).

In 3-D Matrigel culture, the malignant, WPE1-NB26 cells form solid masses of disorganized cells (Figure 3.5b) (Bello-DeOcampo et al., 2001b). In the WPE1-NB26 cell line, β_1 integrin expression is strong and positive, yet, diffuse. Another explanation for the loss of cell organization is the lack of α_6 integrin staining observed in cell masses of WPE1-NB26 (Bello-DeOcampo et al., 2001b). These results demonstrate that while α_6 integrin expression decreases or is lost in WPE1-NB26 cells, β_1 expression is altered so that its expression is no longer confined basally, but is diffusely expressed throughout the cell surface. The abnormal expression of $\alpha_6\beta_1$, correlates with the loss of ability of the RWPE-2 and WPE1-NB26 cell lines to undergo cell organization and acinar formation. CTPE cells in 3-D Matrigel culture show some polarization compared to RWPE2-W99 and WPE1-NB26 cells, which do not show any signs of cell organization in 3-D culture, but the expression of $\alpha_6\beta_1$ is not known in the CTPE cell line (Achanazar et al., 2004).

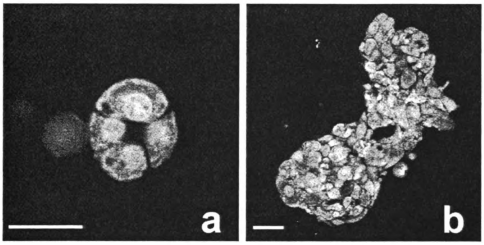

Figure 3.5 Acinar morphogenesis by RWPE-1 and WPE1-NB26 cells in 3-D Matrigel culture. (a) the non-tumorigenic RWPE-1 cells form well organized acini of polarized cells around a central lumen, while WPE1-NB26 cells; (b) form a disorganized cell mass, Bar = 25 μm (Modified from Achanzar et al., 2004).

Cadherins, in addition to integrins, play an important role in maintaining cell:cell adhesion, cell shape, cell polarization and acinar morphogenesis (Bussemakers et al., 1996; Webber et al., 1997, Bello-DeOcampo et al., 2001a, Bello-DeOcampo et al., 2001b). Altered expression of the protein, E-cadherin, has been observed in about 50% of prostate cancer cases (Achanazar et al., 2004; Hayward et al., 1998). Non-tumorigenic, RWPE-1 cells, and the more malignant, WPE1-NB26 cells, exhibit strong and uniform plasma membrane localization of E-cadherin using immuno-fluorescence, but the staining was weak in RWPE2-W99 cells and heterogeneous in CTPE cells (Achanzar et al., 2004). These results show that only two of the three malignant human prostate cell lines tested, RWPE2-W99 and CTPE, express decreased, variable levels E-cadherin and its expression is abnormally localized.

Besides E-cadherin, other classical cadherins include, P- and N-cadherin. The increased, abnormal expression of P- or N-cadherin, also referred to as cadherin switching, resulting in the loss of cadherin homeostasis, has been associated with the acquisition of an invasive phenotype (Achanazar et al., 2004). In comparison to RWPE-1 cells, which mimic cadherin expression observed in normal human prostate epithelial cells, the malignant RWPE2-W99, WPE1-NB26 and CTPE cells, all express varying levels of P- and N-cadherins (Achanazar et al., 2004). RWPE2-W99 and WPE1-NB26 cells express lower than normal levels of P-cadherin, but increased levels of N-cadherin as compared to RWPE-1 cells. The levels of N-cadherin in the RWPE2-W99 and WPE1-NB26 cell lines are 2.8 and 8-fold higher than the level observed in RWPE-1 cells respectively. While two of the three malignant cell lines show low P-cadherin and increased levels of N-cadherin, CTPE cells show increased levels of P-cadherin and undetectable levels of N-cadherin. The level of P-cadherin in the CTPE cell line is 2-fold higher that the level observed in the RWPE-1 cell line.

Cadherin switching and heterogeneity of cadherin expression observed in these cell lines mimics cadherin switching and heterogeneous cadherin expression observed in human prostate cancers (Achanazar et al., 2004). These results are also consistent with cadherin expression observed in other human prostate cancer cell lines such as PC-3 and DU145 (Bussemakers et al., 2000; Tran et al., 1999). A loss or increased expression of one or more cadherins can disrupt homeostasis resulting in a change in cell adhesion, shape, polarization, and motility, and thus, may contribute to an invasive phenotype.

Invasive prostate cancer cells have decreased or abnormal expression of both integrins and cadherins, which assist in their dissemination from the prostate (Bello-DeOcampo et al., 2001b; Achanazar et al., 2004). Abnormal expression of adhesion molecules such as, integrins and cadherins, facilitate cell invasion by allowing cells to detach and move into the surrounding tissues. To degrade the extracellular matrix and invade surrounding tissues, cancer cells secrete proteolytic enzymes.

Proteases:

Although both normal and neoplastic cells produce matrix metalloproteinases (MMPs) and other proteolytic enzymes, only malignant cells are invasive. Normal cells may express proteases during such processes as tissue remodeling, but this expression is transient. Many human prostate cancers show elevated secretion of proteolytic enzymes, MMP-2 and MMP-9, which can degrade the extracellular matrix and thus assist in the spread of tumor cells (Lokeshwar et al., 1993; Festuccia et al., 1996). Another protease, urokinase-type plasminogen activator (u-PA), is also secreted by normal cells but higher levels of expression are associated with metastatic prostate cancer (Waghray and Webber, 1995). u-PA can degrade the extracellular matrix directly, but it can also activate MMP-2 and MMP-9, that are involved in the degradation of type IV collegen in the basement membrane (Webber and Waghray, 1995).

RWPE-1 and RWPE2-W99 both secrete detectable levels of MMP-2 and MMP-9 (Webber et al., 1996b). However, RWPE-2 cells secrete higher levels of both MMP-2 and MMP-9 than RWPE-1 cells. RWPE-2 cells also produce considerably higher levels

of u-PA compared to RWPE-1 cells and normal prostatic epithelium (Webber et al., 1996b).

CTPE cells secrete higher levels of active MMP-2 and MMP-9 compared to the RWPE-1 cell line (Achanzar et al., 2001). The levels of protease expression are not known for the family of MNU cell lines, however their invasive behavior *in vitro* has been characterized. The invasive potential of a cell line can also be examined *in vitro* using the Boyden chamber invasion assay.

Invasion *in vitro:*

The invasive ability of a cell line can be examined *in vitro* using a reconstituted basement membrane and a Boyden chamber. In this assay, Matrigel serves as a reconstituted basement membrane and is composed of several matrix proteins. The Boyden chamber assay is a useful *in vitro* test, since invasion by cancer cells through the basement membrane *in vivo* is one of the first steps in the progression to metastasis. The invasive ability of the MNU cell lines was determined using the Boyden chamber invasion assay and was compared with invasion by DU145 cells. The invasive ability of a cell line derived from a metastatic deposit, DU-145, was set at 100%. In comparison to this cell line, the RWPE-1 and MNU cell lines showed different invasive abilities (Figure 3.6) (Webber et al., 2001).

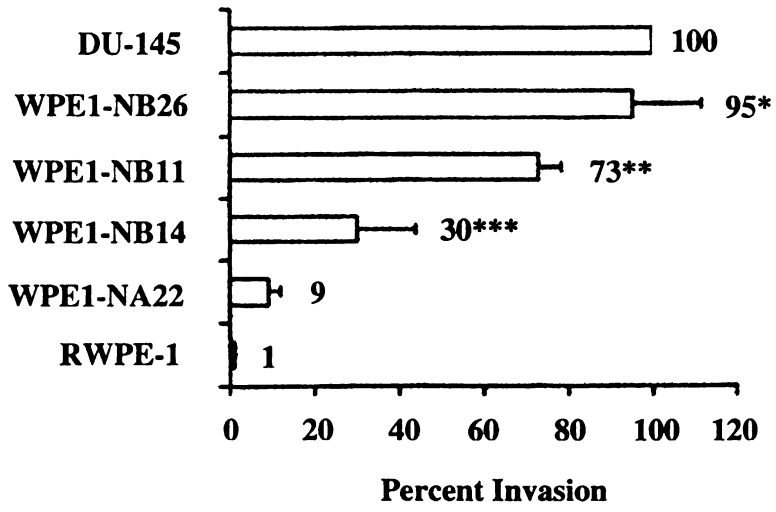

Figure 3.6 The invasive ability of MNU cell lines compared with that of RWPE-1 and DU-145 cells by a modified Boyden chamber in vitro invasion assay. Cells were plated at 200,000 cells/chamber on a Matrigel-coated filter and allowed to invade for 24 h. +/- SEM. Two tailed t-test is shown as *P = 0.028, **P = 0.007, and ***P = 0.04 (Webber et al., 2001).

The WPE1-NA22 cells showed low invasion (9%), which was not significantly higher than that of the non-tumorigenic, non-invasive, RWPE-1 cells (1%), in comparison to the highly metastatic DU-145 cell line. WPE1-NB14 and WPE1-NB11 cells showed 30% and 73% invasion respectively, and WPE1-NB26 showed the highest invasion (95%). In another *in vitro* Boyden chamber assay, the invasive potential of WPE1-NB26 was set at 100% (Achanzar et al., 2004). In comparison to the WPE1-NB26 cells, CTPE cells show 78% invasion and RWPE2-W99 cells show 55% invasion (Figure 3.7).

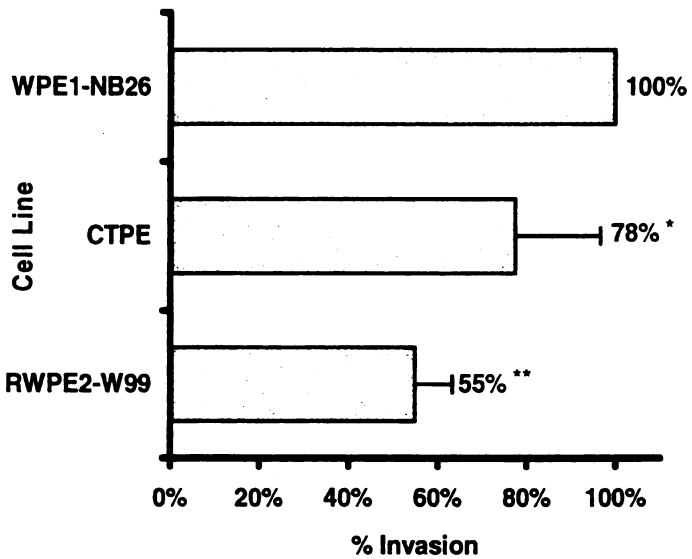

Figure 3.7 A comparison of the invasive ability of the three tumorigenic cell lines *in vitro* is shown where the invasive ability of WPE1-NB26 cells is taken as 100%. Cells were plated at 200,000 cells/Boyden chamber on Matrigel-coated filters and allowed to invade for 48 h. Results are plotted as ± SD. $*p = 0.1095$, $**p = 0.0008$ (Achanzar et al., 2004).

RWPE-1 cells are non-tumorigenic when injected subcutaneously in nude mice while RWPE2-W99 cells form slow growing tumors (Achanzar et al., 2004). After subcutaneous injection into nude mice, the WPE1-NA22 cells form the slowest growing tumors amongst the MNU family of cell lines (Webber et al., 2001). Both WPE1-NB14 and WPE1-NB11 cells form tumors of intermediate size, and WPE1-NB26 cells form the largest tumors that are invasive. CTPE cells form large rapidly growing tumors that are highly invasive when injected subcutaneously in nude mice (Achanzar et al., 2004).

On the basis of their characteristics, the cell lines in this paper have been ranked in the following order of increasing malignancy: RWPE-1 cell line at the non-malignant end of the process of carcinogenesis, WPE1-NA22 showing the lowest invasive ability, followed by WPE1-NB14, RWPE2-W99, and WPE1-NB11 showing intermediate, but progressively increasing invasive abilities, and CTPE and WPE1-NB26 cell lines showing the greatest invasive ability (Figure 3.8).

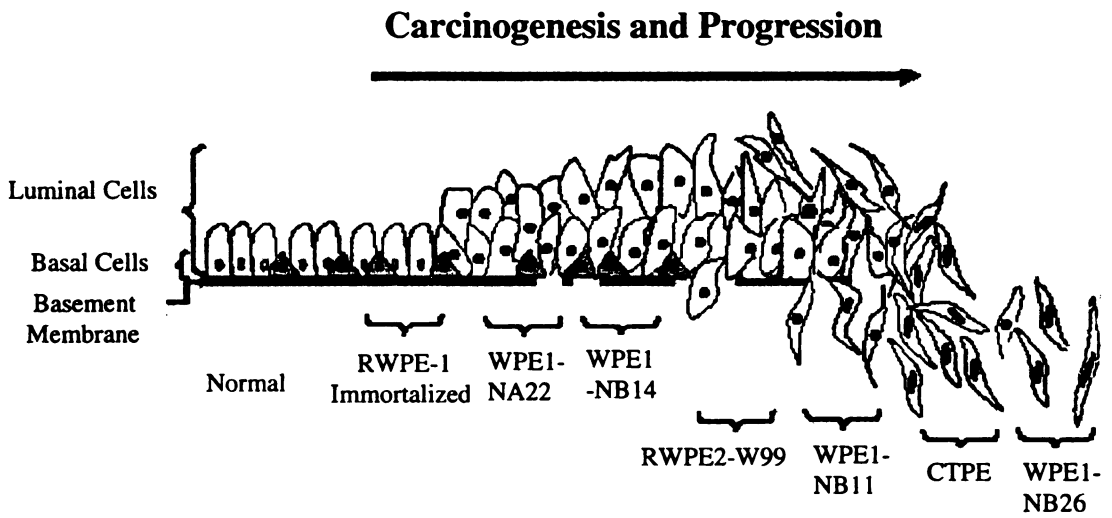

Figure 3.8 A schematic diagram showing steps in the multistep process of carcinogenesis and tumor progression in the human prostate and the points possibly represented by RWPE-1, RWPE-2-W99, MNU, and CTPE cell lines in this progression. The sequence of progression from non-malignant RWPE-1 cells to the highly malignant WPE1-NB26 cells: RWPE-1< WPE1-NA22< WPE1-NB14< RWPE2-W99< WPE1-NB11< CTPE< WPE1-NB26 (Modified from Webber et al., 2001).

Conclusions

Each of the human prostate cell lines discussed have some unique characteristics for studying prostate carcinogenesis and cancer progression. The RWPE-1 cell line has characteristics of normal prostate tissue even though the cells have been immortalized. RWPE-1 cells show epithelial morphology, respond to growth factors, polarize and form acini *in vitro* and are non-tumorigenic *in vivo*. RWPE-1 cells may, therefore, be useful as a comparison in studies with other prostate cell lines, especially its related cell lines. The behavior of RWPE2-W99 and MNU cell lines, as far as their tumorigenicity and invasive ability *in vivo* is concerned, is consistent with their malignant characteristics *in vitro*. The RWPE-2 and MNU cell lines show varying degrees of malignant characteristics which permits studies on prostate carcinogenesis, prostate cancer progression, and testing agents for chemoprevention and treatment of early stage prostate cancer. The CTPE cell line, another derivative of the parent RWPE-1 cell line, serves as a useful model of cadmium-induced prostate cancer in men. The fact that all of these cell lines are derived from the same parental, RWPE-1 cells, allows one to examine molecular events associated with prostate carcinogenesis and tumor progression. The prostate cell lines used in my study include: RWPE2-W99, WPE1-NB26, and CTPE.

Literature cited

Achanzar, W.E., Lamar, P., Tokar, E.J., Rivette, A.S., Bello-DeOcampo, D., Prozialeck, W.C., Webber, M.M., and Waalkes, M. P.: Human prostate cell lines mimic heterogeneity of cadherin expression in human prostate cancer. UroOncology 4:15-25, 2004.

Achanzar, W.E., Kiwan, B.A., Liu, J., Wuader, S.T., Webber, M.M., and Waalkes, M.P.: Cadmium-induced malignant transformation of human prostate epithelial cells. Cancer Research 61:455-458, 2001.

Anwar, K., Nakakuki, K., Shiraishi, T., Naiki, H., Yatani, R., and Inuzuka, M.: Presence of *ras* oncogene mutations and human papillomavirus DNA in human prostate carcinomas. Cancer Research 52:5991-5996, 1992.

Bello, D., Webber, M.M., Kleinman, H., Wartinger, D.D., and Rhim, J.S.: Androgen responsive adult human prostatic epithelial cell lines immortalized by human papillomavirus 18. Carcinogenesis 18:1215-1223, 1997.

Bello-DeOcampo, D., Kleinman, H.K., DeOcampo, N.D., and Webber, M.M.: Laminin 1 and $\alpha_6\beta_1$ integrin regulate acinar morphogenesis of normal and malignant human prostate epithelial cells. Prostate 46:142-153, 2001a.

Bello-DeOcampo, D., Kleinman, H.K., and Webber, M.M.: The role of $\alpha_6\beta_1$ integrin and EGF in normal and malignant acinar morphogenesis of human prostatic epithelial cells. Mutation Research 480-481:209-217, 2001b.

Bussemakers, M.J.G., Van Bokhoven, A., Tomita, K., Jansen, C.F.J., and Schalken, J.A.: Complex cadherin expression in human prostate cancer cells. International Journal of Cancer 85:446-450, 2000.

Chen, T., Pecoraro, G., and Defendi, V.: Genetic analysis of in vitro progression of human papillomavirus-transfected human cervical cells. Cancer Research 53:1167-1171, 1993.

DeMarzo, A.M., Nelson, W.G., Meeker, A.K., and Coffey, D.S.: Stem cell features of benign and malignant prostate epithelial cells. Journal of Urology 160:2381 2392, 1998.

Festuccia, C., Bologna, M., Vicentini, C., Tacconelli, A., Miano, R., Violini, S., and Mackay, A.R.: Increased matrix metalloproteinase-9 secretion in short-term tissue cultures of prostatic tumor cells. International Journal of Cancer 69:386 393, 1996.

Horoszewicz, J.S., Leong, S.S., Chu, T.M., Wajsman, Z.L., Friedman, M., Papsidero, L., Kim, U., Chai, L.S., Kakati, S., Arya, S.K., and Sandberg, A.A.: The LNCaP cell line-A new model for studies on human prostatic carcinoma. In: Progress in Clinical and Biological Research, Models for Prostate Cancer, Murphy, G.P. (ed.), Buffalo, NY, Alan R. Liss Inc., 37:67-84, 1980.

Kaighn, M.E., Narayan, S., Ohnuki, Y., Lechner, J.F., and Jones, L.W.: Establishment and characterization of a human prostatic carcinoma cell line (PC-3). Investigative Urology 17:16-23, 1979.

Lokeshwar, B.L., Selzer, M.G., Block, N.L., and Gunja-Smith, Z.: Secretion of matrix metalloproteinases and their inhibitors (tissue inhibitor of metalloproteinases) by human prostate in explant cultures: reduced tissue inhibitor of metalloproteinase secretion by malignant tissues. Cancer Research 53:4493-4498, 1993.

Mickey, D.D., Stone, K.R., Wunderli, H., Mickey, G.H., and Paulson, D.F.: Characterization of a human prostate adenocarcinoma cell line (DU145) as a monolayer culture and as a solid tumor in athymic mice. In: Progress in Clinical and Biological Research, Models for Prostate Cancer, Murphy, G.P. (ed.), Buffalo, NY, Alan R. Liss Inc., 37:67-84, 1980.

Rhim, J.S., Webber, M.M., Bello, D., Lee, M.S., Arnstein, P., Chen, L., and Jay, G.: Stepwise immortalization and transformation of adult human prostate epithelial cells by a combination of HPV-18 and v-Ki-ras. Proceedings of the National Academy of Sciences U.S.A. 91:11874-11878, 1994.

Tran, N.L., Nagle, R.B., Cress, A.E., and Heimark, R.L.: N-cadherin expression in human prostate carcinoma cell lines. American Journal of Pathology 155:787 -798, 1999.

Waalkes, M.P., Rehm, S., Coogan, T.P., and Ward, J.M.: Role of cadmium in the etiology of cancer of the prostate. In: J.A. Thomas and H.D. Colby (eds.), Endocrine Toxicology, Ed. 2, pp. 227-243. Washington, DC: Taylor & Francis, 1997.

Waghray, A., and Webber, M.M.: Retinoic acid modulates extracellular urokinase-type plasminogen activator activity in DU-145 human prostatic carcinoma cells. Clinical Cancer Research 1:747-753, 1995.

Webber, M.M., Quader, S.T.A., Kleinman, H.K., Bello-DeOcampo, D., Storto, P.S., Bice, G., DeMendonca-Calaca, W., and Williams, D.: Human cell lines as an in vitro/in vivo model for prostate carcinogenesis and progression. Prostate 47:1-13, 2001.

Webber, M.M., Bello, D., Kleinman, H.K., and Hoffman, M.P.: Acinar differentiation by non-malignant immortalized human prostatic epithelial cells and its loss by malignant cells. Carcinogenesis 18:1225-1231, 1997.

Webber, M.M., Bello, D., Kleinman, H.K., Wartinger, D.D., Williams, D.E., and Rhim, J.S.: Prostate specific antigen and androgen receptor induction and characterization of an immortalized adult human prostatic epithelial cell line. Carcinogenesis 17:1641-1646, 1996a.

Webber, M.M., Bello, D., and Quader, S.: Immortalized and tumorigenic adult human prostatic epithelial cell lines: characteristics and applications part 1. Cell markers and immortalized nontumorigenic cell lines. Prostate 29:386-394, 1996b.

Webber, M.M., and Waghray, A.: Urokinase-mediated extracellular matrix degradation by human prostatic carcinoma cells and its inhibition by retinoic acid. Clinical Cancer Research 1:755-761, 1995.

Woodworth, C.D., Waggoner, S., Barnes, W., Stoler, M.H., and DiPaolo, J.A.: Human cervical and foreskin epithelial cells immortalized by human papillomavirus DNAs exhibit dysplastic differentiation in vivo. Cancer Research 50:3709-3715, 1990.

Yankaskas, J.R., Haizlip, J.E., Conrad, M., Koval, D., Lazarowski, E., Paradiso, A.M., Rinehart, C.A. Jr, Sarkadi, B., Schlegel, R., and Boucher, R.C.: Papilloma virus immortalized tracheal epithelial cells retain a well-differentiated phenotype. American Journal of Physiology 264:C1219-C1230, 1993.

CHAPTER FOUR

XENOTRANSPLANTATION OF HUMAN PROSTATE CANCER CELLS

Abstract

The metastatic process is not only determined by the characteristics of the tumor, but also by its surrounding microenvironment. The implantation site of tumors cells has been shown to influence both the rate of tumorigenesis, as well as the rate and pattern of metastasis in immune-suppressed mice. This illustrates the importance of tumor-stromal cell interaction and emphasizes the critical role of epigenetic factors in influencing prostate cancer growth. Although intrinsic tumor cell factors are important in determining the incidence of metastatic spread, it is also evident that simple manipulation of the route of tumor cell injection can allow maximum expression of the metastatic phenotype. The orthotopic site, the prostate, appears to result in metastasis to several organs following cell injection or tissue implantation while other sites may lack or only show metastasis to few organs. The metastatic phenotype of the cell lines discussed in this chapter are different and they are not affected in the same way by alteration of injection site in immune-suppressed mice. Therefore one should evaluate each xenograft before designing a study, to select an appropriate model for prostate cancer.

Keywords

Cell lines, DU145, injection, prostate cancer, LNCaP, metastasis, PC-3, subline, technique, xenograft

Introduction

In vivo models are important for studying the behavior, growth and gene expression of tumor tissue in a more natural environment that cannot be easily mimicked *in vitro*. Metastatic spread to other tissues, angiogenesis, and interaction with stromal cells are lacking *in vitro*. In addition, most animals rarely develop spontaneous prostate cancer metastasis. For example, in non-human primates prostatic carcinoma is almost non-existent (Waters et al., 1998; Hughes and Lang, 1978). Although canine models show a rate and pattern of prostate cancer progression and metastasis similar to humans, the lack of control over the population of dogs that will develop prostate cancer and subsequent bone metastasis makes the use of this model difficult (Navone et al., 1999; Waters et al., 1998). Rodent models have been developed for a variety of cancers and tumors may be induced or implanted in them that grow rapidly and often metastasize, but the cells are nevertheless of rodent origin. With the use of immune-suppressed mice as a model of prostate cancer, it is possible to study human prostate cells, such as, patient derived specimens or established prostate cell lines, in an *in vivo* environment.

When cells or tissues are transplanted from one species to another it is called a xenograft. Human tumor xenotransplantation began after the discovery of a mutant mouse with low immunity. The nude mouse, a hairless mutant, has a normal complement of bone marrow-dependent B-cells, but lacks a thymus, which is essential for the production of T-cells and, therefore, has a deficient cell-mediated immune response (Rygaard and Povlsen, 1982). Another immune-suppressed mouse model for xenotransplantation, consists of mice with severe combined immune deficiency (SCID) (Bosma et al., 1983). The SCID mutation selectively impairs the differentiation of

lymphopoietic stem cells and as a result they are deficient in immunologic functions mediated by B- and T-cells. Therefore, SCID mice are even more immune-deficient than nude mice allowing a higher percentage of tumor engraftment, enhanced tumor growth rate, and less tumor regression of human tumors (Kim, 1996; Sato et al., 1997). However their enhanced immune-deficiency, as compared to nude mice, also makes SCID mice more susceptible to infection.

In 1977 the first transplantable human prostate xenograft, PC-82, was established (van Weerden and Romijn, 2000). Small fragments of human prostate cancer tissue were transplanted subcutaneously in athymic, nude mice. Many prostate cancer xenografts have been established since then. Using xenograft models of prostate cancer it is possible to determine the influence of the microenvironment on gene expression, growth, and behavior of tumor cells within the prostate gland and other organ sites. Hormonal status may also be altered in prostate cancer xenografts to study the importance of androgen-independence in tumor progression and metastasis. Xenograft models are particularly useful for testing new drugs for chemotherapy. Since studies using xenografts are an important step before clinical trials of new drugs can be conducted for cancer treatment, the xenograft model should mimic the human disease as closely as possible in order to collect relevant and applicable data.

Xenograft models of prostate cancer that represent various aspects of human prostate cancer exist, however most lack metastasis to bone (van Weerden and Romijn, 2000). A xenograft model of prostate cancer that metastasizes to bone would be useful because metastatic spread to the bone is the main cause of morbidity among prostate cancer patients. Another obstacle with xenograft models is the sustained growth of

human prostate cells in immune-suppressed mice. Therefore, several approaches have been attempted to overcome such obstacles. These approaches include different implantation sites, implantation of a high number of cells, implantation of cultured pieces of tissue rather than a cell suspension, and the use of *in vivo*-selected cell lines or sublines. These approaches will further be discussed with the aim of identifying appropriate xenograft models of human prostate cancer and metastasis. This information will be useful when selecting a xenograft model for prostate cancer studies, as key features and their utility in understanding the mechanisms of prostate carcinogenesis and metastasis will be provided for several xenograft models.

Intra-spleen injection:

Most investigators use the technique of intrasplenic cell injection to examine the metastatic potential of a cell line. The spleen filters foreign particles from the bloodstream and also eliminates damaged blood cells. Blood leaving the spleen empties into the splenic vein which then empties into the hepatic portal vein before it enters the liver (Paulsen, 2000). Transplantation of human prostate cancer cells to the intrasplenic site in a nude mouse requires anesthesia and surgery. After anesthetizing the mouse an incision is made in the left flank through the skin and peritoneum to expose the spleen for cell injection. The incidence of metastasis after the intra-splenic injection of either PC-3, DU145, LNCaP cells or their metastatic sublines is shown in Table 4.1.

Table 4.1 Incidence of metastasis 6-8 weeks after intra-splenic injection of either PC-3, DU145, or LNCaP cells or their metastatic sublines in athymic mice.

	Lung	Liver	Abdomen*	Reference
DU145	30%	0	0	Kozlowski et al., 1984
PC-3	80%	100%	85%	Kozlowski et al., 1984
PC-3	14%	14%	57%	Sherwood et al., 1990
431-P	20%	60%	50%	Shevrin et al., 1989
LNCaP	NR	0	NR	Pettaway et al., 1996
LNCaP-LN3	NR	40%	NR	Pettaway et al., 1996

*Includes tumor ascites
NR, Not reported

Intra-splenic injection of PC-3 cells ($5X10^5$) resulted in 16/20 mice developing lung metastases, 20/20 mice developing liver metastases and 13/20 mice were found to have tumor ascites (Kozlowski et al., 1984). After intra-splenic injection of DU145 cells ($5X10^5$) only 3/10 mice developed pulmonary metastases while metastases to the liver were not observed (Kozlowski et al., 1984). In another study using the same technique, injection of PC-3 cells ($1X10^6$) in athymic mice was found to show metastasis in the liver 1/7, lung 1/7, and diaphragm 4/7 (Sherwood et al., 1990). Although a higher cell number was used compared to Kozlowski et al. 1984, the incidence of metastases observed did

not increase. These results demonstrate the inconsistency of this injection technique. Instead of increasing the cell number some investigators develop sublines to obtain a higher incidence of metastasis after cell injection. For example, intra-splenic injection of a PC-3 subline, 431-P ($1X10^6$), which was obtained from the 16^{th} passage of PC-3 cells injected subcutaneously in athymic mice, resulted in liver metastases in 6/10 mice, intra-abdominal tumor growth in 5/10 mice, and lung lesions in 2/10 mice (Shevrin et al., 1989).

A subline of LNCaP cells also shows greater metastatic potential than the parental LNCaP cell line. Intra-splenic injection of LNCaP ($2X10^6$) did not result in any visible tumors in the spleen, pancreas, or liver (Pettaway et al., 1996). However, liver metastases were observed in 4/10 mice after intrasplenic injection of the LNCaP metastatic subline, LNCaP-LN3. LNCaP-LN3 was derived from a tumor from a lymph node after cell injection of LNCaP cells in the prostate.

The intra-peritoneal cavity is another site used by investigators to examine the metastasic behavior of a cell line.

Intra-peritoneal injection:

Metastases resulting from the intra-peritoneal route of tumor cell injection have been attributed to improved tumor vascularity due to the absence of the restrictive fibrous sheath around the primary tumor (Morrissey et al., 1980; Takahashi et al., 1978). Another advantage of this site is that anesthesia is not necessary for cell injection in athymic mice.

Athymic mice given an intraperitoneal injection of PC-3 cells ($1X10^6$) showed metastases to the lung (1/7) and liver (4/7) three weeks after cell injection (Ware et al., 1985). In comparison to the parental PC-3 cell line, it's two sublines, 1-LN and clone 4, were both found to show a higher incidence of metastases in athymic mice given an intraperitoneal cell injection (Table 4.2). The 1-LN cell line was recovered from a lymph node metastasis in a PC-3 tumor bearing mouse and clone 4 is a clonal derivative of 1-LN. In addition, both 1-LN and clone 4 cells formed solid tumor masses that adhered to the lining of the peritoneal cavity in all mice, ascitic fluid was found in 3/7 1-LN injected mice. Another subline of PC-3 cells, 431-P, also resulted in a high incidence of abdominal tumor growth after intra-peritoneal cell injection (Shevrin et al., 1989). Intra-abdominal tumor growth and malignant ascites developed in 17/22 mice and lung metastases were observed in 6/22 mice (Table 4.2).

Table 4.2 Incidence of metastasis after intra-peritoneal injection of PC-3 cells or metastatic sublines of PC-3 cells in athymic mice.

	Lung	Liver	Abdomen	Reference
PC-3	14%	57%	0	Ware et al., 1985
1-LN	71%	71%	100%	Ware et al., 1985
clone 4	80%	80%	100%	Ware et al., 1985
431-P	29%	0%	77%*	Shevrin et al., 1989

*Includes tumor growth and ascitic fluid

The lack of tumor cell spread after intra-peritoneal cell injection may be due to the mice developing a high number of abdominal metastases. This is supported by the results of implantation experiments with sublines with preferential metastatic abilities. Organ-targeted sublines showed an increase in non-specific metastasis after intra-peritoneal injection in SCID mice (Wang and Stearns, 1991).

The intra-venous cell injection technique, in contrast to the intrasplenic and intra-peritoneal injection techniques, places cells directly in circulation via the tail vein, so the growth of metastatic tumors may be more dependent on cell behavior rather than the selected microenvironment.

Intra-venous injection:

Before reaching the general circulation, cells injected via the tail vein must first pass through the lung, therefore, the lungs are the most common site of metastatic tumor growth following intravenous cell injection. Human prostate cancer cells transfected with a marker gene and injected intravenously in athymic, nude mice, show a high number of micrometastases in the lungs compared to liver, bone, kidney, and brain tissues one hour after cell injection (Holleran et al., 2002).

Cells injected via the tail vein behave differently than when they are placed at another site such as in the spleen or the intraperitoneal cavity. For example, the incidence of lung metastases decreases and the incidence of metastatic tumor growth in other organs are more common following intrasplenic or intraperitoneal cell injection in comparison to intravenous cell injection (Ware et al., 1985; Shevrin et al., 1989). Following intravenous cell injection in athymic mice, both PC-3 and DU145 cells colonize the lungs, however, LNCaP cells do not metastasize (Kozlowski et al., 1984; Ware et al., 1985; Pettaway et al., 1996) (Table 4.3).

Table 4.3 Metastatic potential of PC-3, DU145, or LNCaP cells in athymic mice following intravenous cell injection.

		Reference(s)
PC-3	++	Kozlowski et al., 1984; Ware et al., 1985
DU145	+	Kozlowski et al., 1984
LNCaP	0	Pettaway et al., 1996

0, non-metastatic; +, 1-20% metastatic; ++, 20-50% metastatic

Sublines of LNCaP cells, generated from repeated *in vivo* selection of LNCaP cells, are also non-metastatic following intravenous cell injection in athymic mice, while sublines of PC-3 cells show a higher incidence of lung metastasis in comparison to the parental PC-3 cells (Pettaway et al., 1996).

Sublines of PC-3 cells have also been generated that preferentially metastasize at ~80% efficiency to the lumbar vertebrae, the mandibular region of the right cheek, the rib cartilage, and the right front knee bone in SCID mice (Wang and Stearns, 1991). These sublines of PC-3 cells, which preferentially metastasize, were continuously grown and selected both *in vitro* and following intravenous cell injection in SCID mice. Metastases to bone have been observed following intravenous injection of a PC-3 subline, 431-P, but this required occlusion of the inferior vena cava during cell injection (Shevrin et al., 1988). Although sublines may show a high incidence of metastasis, experiments with PC-3 and DU145 cells, which have not undergone any selection processes, have resulted in a relatively low incidence of lung metastasis.

In separate groups of mice given injections of either DU145 of PC-3 ($1X10^6$) cells via the lateral tail vein, only 1 out of fifteen (6.6%) mice showed microscopic metastases in the lungs (Kozlowski et al., 1984). In another study, tail vein injection of PC-3 cells ($1X10^6$) resulted in a higher incidence of lung metastases, 47% (Ware et al., 1985). The difference in the incidence of lung metastases observed in the two studies using PC-3 cells could be due to a technical error such as misinjection. In a recent study application of colloidal gold labeled with an isotope followed by quantification in tissue samples by neutron activation was shown to be a valid method for quantifying the tail vein injection technique (Groman and Reinhardt, 2004). To avoid or reduce technical errors during intravenous cell injection one could use the colloidal gold method or consider other techniques for cell injection. The least difficult technique for cell injection, the subcutaneous method, results in very little experimental error since the site is readily accessible for cell injection as well as observation and measurement of the subsequent tumor.

Subcutaneous injection:

The subcutaneous cell injection technique does not require surgery or anesthesia although some investigators use anesthesia to ensure the accuracy of cell injection. The subcutaneous cell injection technique also allows one, not only to observe tumor growth, but also to measure the resulting tumor. Therefore, the subcutaneous xenograft model may be useful for studies which involve hormonal manipulation or screening of potential treatments that inhibit or slow tumor growth for additional testing in clinical trials. The

presence or lack of metastasis following subcutaneous cell injection of PC-3, DU145, or LNCaP cells is shown in Table 4.4.

Table 4.4 Incidence of metastasis following subcutaneous injection of PC-3, DU145, or LNCaP cells in athymic mice.

	Lung	Lymph node	Reference
PC-3	20%	60%	Rembrink et al., 1997
DU145	0%	0%	Devi et al., 2002; Mickey et al., 1977
LNCaP	0%	0%	Rembrink et al., 1997; Stephenson et al., 1992

After subcutaneous cell injection of PC-3 or DU145 (~$2X10^5$) cells, 8/9 (89%) and 4/6 (67%) of the mice respectively developed tumors (Trikha et al., 1998). Although PC-3 cells had a higher take rate compared to DU145 cells, no metastases were observed in any of the mice after 8-14 weeks. In addition, subcutaneous injection of a higher number of DU145 cells does not result in metastasis (Devi et al., 2002; Mickey et al., 1977). DU145 cells placed at the subcutaneous site also do not show accelerated tumor growth compared to animals without hormone treatment, which corresponds to their hormone-insensitive behavior *in vitro* (Mickey et al., 1977). In contrast to DU145 cells, subcutaneous injection of a higher number of PC-3 cells ($1X10^6$), results in lung and lymph node metastases in 1/5 and 3/5 mice respectively, six weeks after cell injection (Rembrink et al., 1997).

LNCaP cells do not show signs of metastasis, regardless of the cell number, after subcutaneous cell injection (Rembrink et al., 1997; Stephenson et al., 1992). In these two studies, testing the *in vivo* growth of LNCaP cells following subcutaneous cell injection, the tumor take rate was less than 10%. However, the tumor take rate was 68% when LNCaP cells were mixed with Matrigel for subcutaneous cell injection (Lim et al., 1993). Furthermore the growth of LNCaP cells can be manipulated by castration of LNCaP-bearing athymic nude mice (Lim et al., 1993). Castration leads to involution of the tumor and stabilization of serum PSA level. This xenograft model using LNCaP cells may be useful as a model of hormone-sensitive human prostate cancer. But the results collected from studies using the hormone-sensitive model may only be applicable to human prostate cancers in which the cells express an androgen receptor mutation, as observed in LNCaP cells.

Sublines of human prostate cancer cells such as PC-3 and LNCaP, are eight times more metastatic and twice as tumorigenic, respectively, in comparison to the parental cell lines following subcutaneous cell injection (Kozlowski et al., 1984; Pettaway et al., 1996). Among the three most commonly tested cell lines, PC-3, DU145, and LNCaP, only the PC-3 cell line metastasizes after subcutaneous cell injection. Therefore, as a subcutaneous xenograft model, the PC-3 cell line may be useful for evaluating treatments that may prevent or slow metastasis from the primary tumor, whereas LNCaP and DU145 cells may be more useful for evaluating treatments that may slow or inhibit primary tumor growth. For ideal studies on primary tumor growth, a family of cell lines exists that represents a progression of tumor growth when injected subcutaneously in nude mice from small, slow-growing tumors to large, fast-growing tumors that are invasive.

Included in this family of cell lines is the parental, non-tumorigenic, RWPE-1 cell line which serves as a control *in vitro* or as a standardized model *in vivo* when studying prostate cancer progression. RWPE-1 cells were isolated from the normal prostate of a 54 year-old Caucasian man undergoing radical prostatectomy because of cystectomy for bladder cancer and immortalized with the human papilloma virus-18 (HPV-18) (Bello et al., 1997; Rhim et al., 1994). Several tumorigenic cell lines, the MNU cell lines, were derived from RWPE-1 by transformation with *N*-methyl-*N*-nitrosourea (MNU) (Webber et al., 2001). These cell lines include: WPE1-NA22, WPE1-NB14, WPE1-NB11, and WPE1-NB26. RWPE-1 cells were also transformed by Ki-*ras* or cadmium exposure to obtain the RWPE-2 and CTPE cell lines, respectively (Bello et al., 1997; Achanazar et al., 2001).

Cells were tested for tumorigenicity by subcutaneously injecting $5X10^5$ cells with Matrigel in athymic, nude mice. As indicated in previous experiments, the RWPE-1 cell line does not form tumors in nude mice, and when injected with Matrigel, the cells organized similarly to normal glands *in vivo*. All of the MNU cell lines were capable of forming tumors when injected into nude mice. The WPE1-NA22 cells were found to form the slowest growing tumors, followed by WPE1-NB14 and WPE1-NB11 cells, which formed tumors of intermediate size, while WPE1-NB26 cells formed the largest tumors (Webber et al, 1997). The MNU cell lines are unique because they show progression of characteristics from non-tumorigenic, to low, and then to a high level of malignancy and mimic different stages of carcinogenesis and progression as they occur in the human prostate.

The related, RWPE-2 cells form small, slow-growing tumors in mice following subcutaneous cell injection and provide a model for prostate cancers in which the cells show increased expression of Ki-*ras* (Bello et al., 1997). CTPE cells not only produce tumors, but these cells are invasive when inoculated ($1X10^6$) subcutaneously into nude mice (Achanazar et al., 2001). Tumors arose in 18/20 mice within six weeks after inoculation with CTPE cells and 80% of these tumors invaded into the subdermal muscle, fat, or connective tissue. These results indicate the highly aggressive nature of the CTPE cells and should lead to a better understanding of the mechanisms involved metastasis, as well as, in cadmium-induced prostatic malignancies. The six cell lines; WPE1-NA22, WPE1-NB14, WPE1-NB11, WPE1-NB26, RWPE-2, and CTPE, all share a common lineage and represent a unique and relevant model which mimics stages in prostatic intra-epithelial neoplasia and progression to invasive cancer and can be used to study carcinogenesis, progression, intervention, and chemoprevention (Webber et al., 2001). The subcutaneous site is easily accessible for cell injection and most human prostate cancer cell lines form tumors, but for prostate cancer cells it does not correspond with their anatomic origin or orthotopic site, the prostate.

Orthotopic Injection:

In 1992, the technique of orthotopic transplantation was reintroduced as a means of inducing spontaneous metastasis originating from the prostate (Fu et al., 1992; Stephenson et al., 1992; van Weerden et al., 2000). Several investigators have observed a higher incidence of metastasis following orthotopic cell injection compared to subcutaneous cell injection of PC-3, DU145, and LNCaP cells in immune-suppressed

mice (Waters et al., 1995; Pettaway et al., 1996; Sato et al., 1997; Rembrink et al., 1997; Trikha et al., 1998). Cell injection at the orthotopic site in immune-suppressed mice requires anesthesia, surgery, and technical experience. Some drugs used by investigators for anesthetizing mice prior to orthotopic cell injection include; methoxyflurane, nembutal, and tribromoethanol. After anesthetizing the mouse, an incision is made in the abdominal wall to expose the prostate for cell injection. Cells suspended in Hank's balanced salt solution, serum free medium (SFM), or Ham's medium have been administered with a 28 or 30 gauge needle in 20-40 μl into the prostate in immune-suppressed mice. Successful cell injection is usually confirmed by the absence of leakage from the prostate or visualizing the expansion of the prostate or both. After cell injection the prostate gland is placed back inside the abdominal wall and the incision is either closed with nylon or silk sutures or wound clips.

The incidence of metastasis following orthotopic cell injection of PC-3, DU145, or LNCaP cells is shown in Table 4.5.

Table 4.5 Incidence of metastasis following orthotopic injection of PC-3, DU145, or LNCaP cells in immune-suppressed mice.

	Time[+]	Lung	Lymph node	Other	Reference(s)
PC-3					
~200,000	8-14	NR	0%	0%	Trikha et al.,1998
5×10^5	9	10%	100%	18%[a]	Waters et al.,1995
1×10^6	7	100%	100%	NR	Rembrink et al.,1997
DU145					
~200,000	7	NR	50%	100%[b]	Trikha et al., 1998
LNCaP					
1×10^6	13	0%	57%	NR	Rembrink et al.,1997
2×10^6	14	NR	28%	NR	Pettaway et al.,1996

+, weeks
a, kidney metastasis
b, peritoneal metastasis
NR, not reported

In SCID mice given orthotopic injections of either PC-3 or DU145 (~200,000) cells, metastasis was only observed in mice given DU145 cells (Trikha et al., 1998). Seven weeks following orthotopic cell injection of DU145 cells, all four mice inoculated were dead, whereas some mice given orthotopic injections of PC-3 cells survived twice as long. Upon examination, all mice inoculated with DU145 cells were positive for peritoneal invasion and two of the mice also showed lymph node metastasis (Trikha et al., 1998). In another study using the orthotopic cell injection technique, but a higher number of PC-3 cells (5×10^5), 10/10 mice and 1/10 mice showed lymph node and lung metastasis, respectively, and in 2 athymic mice, metastatic tumors were also observed in the kidney after 8-9 weeks (Waters et al., 1995). The difference in the metastatic potential of PC-3 cells compared to DU145 cells following orthotopic cell injection may

be due to experimental error or DU145 cells may be more metastatic because orthotopic injection of less cells resulted in metastasis. Regardless, both PC-3 and DU145 cells metastasize following orthotopic cell injection in immune-suppressed mice.

LNCaP cells are also metastatic following orthotopic cell injection, however, the mice are maintained for more than 90 days, which is approxiamately twice as long as mice given PC-3 or DU145 cells (Rembrink et al., 1997; Pettaway et al., 1996). Not only are the mice less likely to survive longer than about 9 weeks, but a lower cell number results in a higher incidence of metastasis in mice given orthotopic cell injections of PC-3 or DU145 cells compared to LNCaP cells (Table 4.5). Therefore, LNCaP cells are considered the least invasive compared to PC-3 and DU145 cells following orthotopic cell injection. While orthotopic cell injection results in a higher incidence of metastasis compared to subcutaneous cell injection, another technique, surgical orthotopic implantation (SOI), results in a higher incidence of metastasis compared to orthotopic cell injection (Fu et al., 1992; Wang et al., 1999).

Surgical Orthotopic Implantation (SOI):

Surgical orthotopic implantation is a technique which involves the implantation of tissue pieces in the prostate. This technique does require anesthesia and surgery, similar to the orthotopic cell injection technique; however, the use of tissue pieces instead of a cell suspension allows one to avoid spillage outside of the prostate during cell injection and, therefore, limit artificial metastasis (An et al., 1998). One of the most common anesthetics for SOI is isoflurane inhalation. Following anesthesia, an incision is made in the abdominal wall to expose the prostate. An incision is then made in the prostate

capsule for implantation of tumor tissue. Tissue pieces are collected from tumors that grow following subcutaneous cell injection in immune-suppressed mice. After the tumor tissue has been implanted in the prostate, the prostate capsule is closed with sutures and subsequently the abdominal wall. One side effect associated with SOI is urinary obstruction due to large local tumor growth (Fu et al., 1992; An et al., 1998; Wang et al., 1999). Hydronephrosis or swelling of the kidneys as a result of urinary obstruction, has also been observed (Fu et al., 1992; An et al., 1998; Wang et al., 1999).

After orthotopic implantation of tissue pieces of PC-3, each about 1 mm^3 in size, local growth and metastasis to the bladder and kidney, as well as, distant metastases to the lymph nodes were observed. In mice implanted with DU145, tumor tissue was only found to invade the lamina propria of the urinary bladder. Although distant metastases were not observed in mice implanted with DU145, hydronephrosis due to urinary blockage was observed by both locally growing tumors of PC-3 and DU145 (Fu et al., 1992).

As observed following SOI of PC-3, LNCaP tumors were often found to show invasion to the seminal vesicles, the bladder, and the lower abdominal wall (An et al., 1998; Wang et al., 1999). Distended urinary bladder and hydronephrosis were also frequently seen (An et al., 1998; Wang et al., 1999). Microscopic examination of tissue sections from mice implanted with PC-3 or LNCaP, demonstrated that both groups of mice were found to have similar incidences of lung and lymph node metastases (An et al., 1998; Wang et al., 1999). The results of these studies show that using the SOI technique one can obtain a high incidence of local tumor growth in the prostate, as well as, distant metastases. However, even though PC-3, DU145, and LNCaP all appear to be highly

tumorigenic and invasive following SOI, metastatic spread to bone was not observed. Models of prostate cancer with metastasis to bone would be useful for prostate cancer studies since metastatic deposits develop in bone before metastases to soft viscera become apparent (Bubendorf et al., 2000).

Models of Bone Metastasis:

More than 80% of prostate cancer patients develop bone metastases, and are generally associated with poor prognosis (Linehan et al., 1992). Since xenograft models of prostate cancer rarely show metastasis to bone, PC-3 or LNCaP cells were injected directly into the femur medullas of nude mice to compare their intraosseal growth (Soos et al., 1997). PC-3 and LNCaP tumors both colonized the bone marrow within a week. PC-3 tumors eventually broke through the bone cortex, invaded the surrounding tissues, and metastasized to the regional lymph nodes, however, LNCaP remained localized within the bone and appeared to regress and die after displacing the normal bone marrow cells. The different growth requirements of these two cell lines may explain the regression of LNCaP cells and the survival of PC-3 cells in mouse bone. As a more useful and ideal model of human prostate cancer metastasis to bone, investigators transplant human tissue, bone or lung, into immune-suppressed mice prior to human prostate cancer cell injection. This permits one to study the interaction between tumor cells and a human organ environment.

Human adult bone (HAB), human adult lung (HAL), or mouse bone was transplanted subcutaneously in nude mice prior to intravenous cell injection of PC-3 or LNCaP (Yonou et al., 2001). Eight weeks after intravenous cell injection several organs

were evaluated for metastases. The incidence of metastasis to implanted human and host mouse tissue is shown in Table 4.6.

Table 4.6 Incidence of metastasis to implanted human and host mouse tissue in SCID mice after tail vein injection of PC-3 or LNCaP cells.

	Human Bone[a]	Human Lung[a]	Mouse Bone[a]	Mouse Bone	Mouse Lung
PC-3	13/20	0/20	1/20	3/20	5/20
LNCaP	7/20	0/20	0/15	0/20	2/20

(Yonou et al. Cancer Research 61:2177-2182, 2001.)
a, transplanted human, adult tissue or host mouse tissue

In this model of bone metastasis, very few tumors developed when murine fetal bone was used suggesting that homing of human prostate cancer cells to bone is human-specific. PC-3 and LNCaP cells preferentially metastasized to HAB over HAL, which reflects the clinical features of prostate cancer (Yonou et al., 2001). PC-3 and LNCaP cells were derived from metastatic deposits, so to assist in understanding the mechanism of prostate cancer metastasis under conditions similar to those in the human body, additional models using clinical specimens or cell lines isolated from primary tumors may be more useful.

Conclusions

Each xenograft method has unique properties which provide opportunities to identify the multiple molecular pathways in prostate cancer and metastasis. Intrasplenic cell injection of prostate cancer cells usually results in metastasis to the liver and abdominal cavity. Following intraperitoneal cell injection, mice develop a high incidence of abdominal metastases. Intravenous cell injection, without manipulation of the vena cava, is capable of resulting in a high incidence of lung metastasis and with manipulation of the vena cava, it is also possible to achieve metastasis to bone using this technique. The subcutaneous cell injection technique seems most promising for studies testing drugs that may slow or inhibit primary tumor growth. Distant metastasis can be observed using orthotopic cell injection or tissue implantation, however metastasis to bone has not been observed. For such studies, the femur of immune-suppressed mice may be used as the site of cell injection or the xenograft model with human bone may be useful.

The panel of xenografts available make excellent models for molecular and genetic analysis, gene discovery, and for testing new therapies. Hypotheses generated by experimentation with xenografts can be correlated with clinical data and also tested in transgenic and knockout models to increase our ability to prevent and control prostate cancer. Similar to the relevance of a broad panel of xenograft models, it is essential to establish various metastatic sublines, which follow the preferential spread to bone as observed in the patient. Metastatic model systems will enable us to study the requirements for tumor cells to metastasize and grow in several organs including bone and hopefully lead to therapies targeting this process. The combination of multiple

resources and models should lead to advances in our ability to prevent and treat prostate cancer.

Literature cited

Achanzar, W.E., Diwan, B.A., Liu, J., Quader, S.T., Webber, M.M., and Waalkes, M.P.: Cadmium-induced malignant transformation of human prostate epithelial cells. Cancer Research 61:455-458, 2001.

An, Z., Wang, X., Geller, J., Moossa, A.R., and Hoffman, R.M.: Surgical orthotopic implantation allows high lung and lymph node metastatic expression of human prostate carcinoma cell line PC-3 in nude mice. Prostate 34:169-174, 1998.

Bello, D., Webber, M.M., Kleinman, H., Wartinger, D.D., and Rhim, J.S.: Androgen responsive adult human prostatic epithelial cell lines immortalized by human papillomavirus 18. Carcinogenesis 18:1215-1223, 1997.

Bosma, G.C., Custer, R.P. and Bosma, M.J.: A severe combined immunodeficiency mutation in the mouse. Nature 301:527-530, 1983.

Bubendorf, L., Schopfer, A., Wagner, U., Sauter, G., Moch, H., Willi, N, Gasser, T.C., and Mihatsch, M.J.: Metastatic patterns of prostate cancer: an autopsy study of 1,589 patients. Human Pathology 31:578-583, 2000.

Devi, G.R., Oldenkamp, J.R., London, C.A., and Iversen, P.L.: Inhibition of human chorionic gonadotropin β-subunit modulates the mitogenic effect of c-myc in human prostate cancer cells. Prostate 53:200-210, 2002.

Fu, X., Herrera, H., and Hoffman, R.M.: Orthotopic growth and metastasis of human prostate carcinoma in nude mice after transplantation of histologically intact tissue. (Letter to the editor) International Journal of Cancer 52:987-990, 1992.

Groman, E.V. and Reinhardt, C.P.: Method to quantify tail vein injection technique in small animals. Contemporary Topics 43:35-38, 2004.

Holleran, J.L., Miller, C.J., Edgehouse, N.L., Pretlow, T.P., and Culp, L.A.: Differential experimental micrometastasis to lung, liver, and bone with lacZ-tagged CWR22R prostate carcinoma cells. Clinical & Experimental Metastasis 19:17-24, 2002.

Hughes, H.C. and Lang, C.M.: Basic principles in selecting animal species for research projects. Clinical Toxicology 13:611-621, 1978.

Kozlowski, J.M., Fidler, I.J., Campbell, D., Xu, Z., Kaighn, E.M., and Hart, I.R.: Metastatic behavior of human tumor cell lines grown in the nude mouse. Cancer Research 44:3522-3529, 1984.

Lim, D.J., Liu, X., Sutkowski, D.M., Braun, E.J., Lee, C., and Kozlowski, J.M.: Growth of an androgen-sensitive prostate cancer cell line, LNCaP, in nude mice. Prostate 22:109-118, 1993.

Linehan, W.M., Long, J.P., Steeg, P.S., and Gnarra, J.R.: Metastatic models and molecular genetics of prostate cancer. Journal of the National Cancer Institute 84:914-915, 1992.

Navone, N.M., Logothetis, C.J., von Eschenback, A.C., and Troncoso, P.: Model systems of prostate cancer: uses and limitations. Cancer and Metastasis Reviews 17:361-371, 1999.

Paulsen, D.F.: Lymphoid system. In: Histology & cell biology: examination & board review, fourth edition. New York, McGraw-Hill, pp.163-180, 2000.

Pettaway, C.A., Pathak, S., Greene, G., Ramirez, E., Wilson, M.R., Killion, J.J., and Fidler, I.J.: Selection of highly metastatic variants of different human prostatic carcinomas using orthotopic implantation in nude mice. Clinical Cancer Research 2:1627-1636, 1996.

Rembrink, K., Romijn, J.C., van der Kwast, T.H., Rubben, H., and Schroder, F.H.: Orthotopic implantation of human prostate cancer cell lines: a clinically relevant animal model for metastatic prostate cancer. Prostate 31:168-174, 1997.

Rhim, J.S., Webber, M.M., Bello, D., Lee, M.S., Arnstein, P., Chen, L., and Jay, G.: Stepwise immortalization and transformation of adult human prostate epithelial cells by a combination of HPV-18 and v-Ki-ras. Proceedings of the National Academy of Sciences U.S.A. 91:11874-11878, 1994.

Rygarrd, J. and Povlsen, C.O.: Athymic (nude) mice. In: The mouse in biomedical research, volume IV. Foster, H.L., Small, D.J. and Fox, J.G. (eds), New York, Academic Press, pp. 51-67, 1982.

Sato, N., Gleave, M.E., Bruchovsky, N., Rennie, P.S., Beraldi, E., and Sullivan, L.D.: A metastatic and androgen-sensitive human prostate cancer model using intraprostatic inoculation of LNCaP cells in SCID mice. Cancer Research 57:1584-1589, 1997.

Sherwood, E.R., Ford, T.R., Lee, C., and Kozlowski, J.M.: Therapeutic efficacy of recombinant tumor necrosis factor α in an experimental model of human prostatic carcinoma. Journal of Biological Response Modifiers 9:44-52, 1990.

Shevrin, D.H., Gorny, K.I., and Kukreja, S.C.: Patterns of metastasis by the human prostate cancer cell line PC-3 in athymic nude mice. Prostate 15:187-194, 1989.

Shevrin, D.H., Kukreja, S.C., Ghosh, L., and Lad, T.E.: Development of skeletal metastasis by human prostate cancer in athymic nude mice. Clinical & Experimental Metastasis 6:401-409, 1988.

Stephenson, R.A., Dinney, C.P.N., Gohji, K., Ordonez, N.G., Killion, J.J., and Fidler, I.J.: Metastatic model for human prostate cancer using orthotopic implantation in nude mice. Journal of the National Cancer Institute 84:951-957, 1992.

Soos, G., Jones, R.F., Haas, G.P., and Wang, C.Y.: Comparative intraosseal growth of human prostate cancer cell lines LNCaP and PC-3 in the nude mouse. Anticancer Research 17:4253-4258, 1997.

Trikha, M., Raso, E., Cai, Y., Fazakas, Z., Paku, S., Porter, A.T., Timar, J., and Honn, K.V.: Role of αIIbβ3 integrin in prostate cancer metastasis. Prostate 35:185-192, 1998.

van Weerden, W.M. and Romijn, J.C.: Use of nude mouse xenograft models in prostate cancer research. Prostate 43:263-271, 2000.

Wang, X., An, Z., Geller, J., and Hoffman, R.M.: High-malignancy orthotopic nude mouse model of human prostate cancer LNCaP. Prostate 39:182-186, 1999.

Wang, M. and Stearns, M.E.: Isolation and characterization of PC-3 human prostatic tumor sublines which preferentially metastasize to select organs in S.C.I.D. mice. Differentiation 48:115-125, 1991.

Ware, J.L., Lieberman, A.P., Webb, K.S., and Vollmer, R.T.: Factors influencing phenotypic diversity of human prostate carcinoma cells metastasizing in athymic nude mice. Exploratory Cell Biology 53:163-169, 1985.

Waters, D.J., Sakr, W.A., Hayden, D.W., Lang, C.M., McKinney, L., Murphy, G.P., Radinsky, R., Ramoner, R., Richardson, R.C., and Tindall, D.J.: Workgroup 4: spontaneous prostate carcinoma in dogs and nonhuman primates. Prostate 36:64 67, 1998.

Webber, M.M., Quader, S.T.A., Kleinman, H.K., Bello-DeOcampo, D., Storto, P.D., Bice, G., DeMednonca-Calaca, W., and Williams, D.E.: Human cell lines as and *in vitro/in vivo* model for prostate carcinogenesis and progression. Prostate 47:1 13, 2001.

Yonou, H., Yokose, T., Kamijo, T., Kanomata, N., Hasebe, T., Nagai, K., Hatano, T., Ogawa, Y., and Ochiai, A.: Establishment of a novel species- and tissue-specific metastasis model of human prostate cancer in humanized non-obese diabetic/severe combined immunodeficient mice engrafted with human adult lung and bone. Cancer Research 61:2177-2182, 2001.

CHAPTER 5

TETRACYCLINES: APPLICATIONS IN INHIBITION OF TUMOR PROGRESSION AND METASTASIS

Abstract

Tetracycline analogs or chemically modified tetracyclines (CMTs) are potential compounds for preventing prostate cancer progression and metastasis. They have been shown to inhibit cell proliferation and invasion through Matrigel, in the *in vitro* invasion assay, of several prostate cancer cell lines, as well as cause a decrease in matrix metalloproteinase (MMP) production and activity *in vitro*. MMPs are important enzymes involved in prostate cancer progression and metastasis. A possible cytotoxic mechanism of CMTs may include the induction of programmed cell death, but the most important feature of CMTs for cancer treatment is their ability to inhibit MMPs. *In vivo*, CMTs inhibit tumor incidence, tumor growth, and metastasis to the lungs in Copenhagen rats given subcutaneous injection of MAT LyLu, Dunning rat prostate cancer cells. In rats given an intravenous cell injection of MAT LyLu tumor cells and treated daily by gavage with CMT-3, both an increase in survival and a decrease in metastasis were observed. In a phase I clinical trial of CMT-3, patients with advanced refractory metastatic cancers were given a daily dose of CMT-3. Disease stabilization continued for more than 61 days in patients with certain malignancies, including sarcomas and a metastatic Sertoli-Leydig cell tumor of the ovary. These results suggests that additional screening of CMT compounds could lead to the identification of compounds which show greater efficacy in the treatment of prostate cancer.

Keywords

Chemically modified tetracyclines, invasion, matrix metalloproteinases, metastasis, tetracylines

Introduction

Metastatic spread of cancer, a major obstacle in curing cancer, remains to be overcome. Therefore, an increased understanding of the steps that take place during metastasis as well as the design and use of therapeutic strategies to inhibit these steps are needed. Once class of molecules that may play a role in the process of metastasis are, matrix metalloproteinases (MMPs). Therefore, control of MMP activity has generated considerable interest as a possible target to inhibit tumor progression, invasion, and metastasis (Chambers and Matrisian, 1997; Wojtowicz-Praga et al., 1997). One group of compounds, tetracycline antibiotics, which have long been recognized as useful adjuncts in the treatment of periodontal diseases, have been shown to inhibit MMP activity, and therefore, may be useful for inhibiting tumor progression (Golub et al., 1991).

Steps in the process of metastasis, where MMPs are thought to be involved, include the following: escape of cells from the primary tumor, intravasation (entry of cells into the blood or lymphatic circulation), survival and transport in the circulation, arrest in distant organs, extravasation (escape of cells from the circulation), and growth of cells to form secondary tumors in the new organ environment (Chambers and Matrisian, 1997; Fidler, 1991; Liotta et al., 1993). Tumor cells then interact with the stromal components of the new organ, which results in either the elimination of tumor cells or their colonization due to stimulation of cell proliferation and angiogenesis (Lokeshwar et al., 1999).

MMPs can be broadly subdivided into three classes based on their substrate specificity: collagenases, stromelysins, and gelatinases (Wojtowicz-Praga et al., 1997). MMPs are secreted as zymogens and upon activation degrade basement membrane

components and facilitate tissue destruction. Their activity is modulated by proenzyme activation and expression of their inhibitors, tissue inhibitors of matrix metalloproteinases (TIMPs). Activation of MMPs requires the proteolytic removal of the pro-domain located at its amino terminus end. This cleavage breaks the cysteine/zinc ion interaction and instead allows water molecules to interact with zinc, which is necessary for activation (Chu, 1998). MMPs may be activated by other proteolytic enzymes, such as uPA and other MMPs (Fridman et al., 1995; Webber and Waghray, 1995).

Although both normal and neoplastic cells produce MMPs and other proteinases, only malignant cells are invasive (Lokeshwar et al., 1993). Localized degradation of ECM occurs where the expression of active proteolytic enzymes is higher than their natural inhibitors, TIMPs. An imbalance of secretion between MMPs and TIMPs in prostatic carcinoma has been observed (Lokeshwar et al., 1993). TIMPs were not detected in conditioned medium from primary prostate carcinoma and activated gelatinases were not detected in the conditioned medium from normal adult prostate explants.

An increased expression of the gelatinases, MMP-2 and MMP-9, whose substrate is type IV collagen, have been shown to be associated with malignant progression of prostate cancer (Liotta et al., 1977; Liotta et al., 1980; Webber et al., 1996). Studies of human prostate tumor tissue have shown that levels of both MMP-2 and MMP-9 are low in normal prostate and organ-confined tumors with Gleason sum of 5 or lower, whereas they were highly expressed in tumors with Gleason sum of 8-10 (Wood et al., 1997). Of significant interest is the increased expression of activated MMP-2 in prostate cancer progression (Lokeshwar et al., 1993; Stearns and Stearns, 1996).

Anti-MMP or anti-collagenase activity of tetracyclines makes these molecules useful for the treatment of cancer but also other diseases where tissue destruction takes place, such as, rheumatoid arthritis, skin lesions, corneal ulcers, and periodontitis (Golub et al., 1991). Most prostate cancer patients initially undergo some type of androgen ablation treatment to slow tumor growth. However, deprivation of androgens to prostate almost always leads to the onset of a more aggressive, metastatic, hormone-refractory incurable phase of the disease (Newling, 1996). To treat the metastatic phase of the disease, drugs that inhibit the metastatic process and do not discriminate between androgen-sensitive and androgen-insensitive prostate tumor cells are needed (Lokeshwar et al., 1999). Inhibitors of MMP activity, such as tetracycline analogs, are drugs with such a potential.

Following administration, tetracyclines distribute widely throughout the body and into tissues and secretions, including the prostate and urine, however their half life is in the range of 6-12 hours (Kapusnik-Uner et al., 1995). Besides the need for continuous administration, other limitations of tetracyclines include, antibiotic resistance and toxicity as a result of long term exposure. Therefore, the tetracycline molecule has been chemically modified in multiple ways, generating a new family of compounds called CMTs (chemically modified tetracyclines). The derivation of some of the CMT drugs, as well as, results of some studies testing the effects of CMTs on prostate cancer will be further discussed.

Chemical modifications of the tetracycline molecule:

One of the first modifications to the tetracycline molecule involved removal of the dimethylamino group from the carbon-4 position of the "A" ring, resulting in the CMT called 4-de-dimethylaminotetracycline (CMT-1) (Figure 5.1). This modification eliminated the drug's antimicrobial activity but did not reduce the ability of the drug to block the activity of collagenases (Golub et al. 1991).

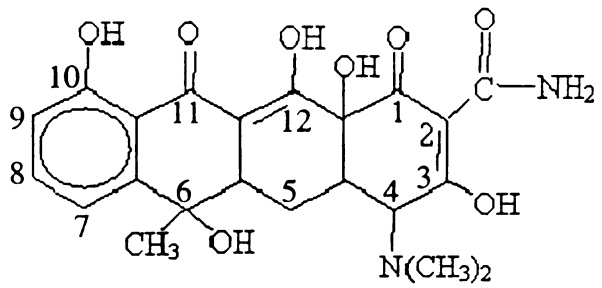

Tetracycline

Molecule	Group(s) Removed from Tetracyline	Position(s)
CMT-1	$-N(CH_3)_2$	(4)
CMT-3	$-N(CH_3)_2$; CH3(OH)	(4; 6)
CMT-8	$-N(CH_3)_2$; OH	(4; 6)

Figure 5.1 A schematic representation of tetracycline and the chemical modifications of tetracycline that generated the CMT-1, CMT-3, and CMT-8 compounds (Modified from Seftor et al., 1998).

Also shown in Figure 5.1, are the chemical structures of subsequent CMTs along with tetracycline. Each of the CMTs were shown to inhibit collagenase activity *in vitro*, however, when the carbonyl oxygen at carbon 11 and the hydroxyl group at carbon 12 were removed from tetracycline to produce CMT-5 (pyrazole derivative), the collagenase-inhibitory activity of the molecule was lost (Golub et al., 1991). Thus, the two side chains at carbon 11 and carbon 12, are considered to be involved with anticollagenase activity.

CMT-3 inhibits cell proliferation:

The effect of CMTs on *in vitro* cell proliferation of prostate cancer cells varied greatly (Lokeshwar et al., 2002). In the three cell lines tested, LNCaP, TSU-PR1, and MAT LyLu, all CMTs, except CMT-7, were significantly cytotoxic. CMT-3 was the most cytotoxic tetracycline analogue tested. Therefore, most prostate cancer studies only test the effects of CMT-3. In another study, following a 48 hour incubation period with a range of concentrations of doxycycline or CMT-3, inhibition of cell proliferation of PC-3, DU145, and MAT LyLu cells was dose dependent (Figure 5.2) (Lokeshwar, 1999). CMT-3 was significantly more potent than doxycycline; a 5-fold lower concentration of CMT-3 compared to doxycycline was needed to decrease cell proliferation by 50%.

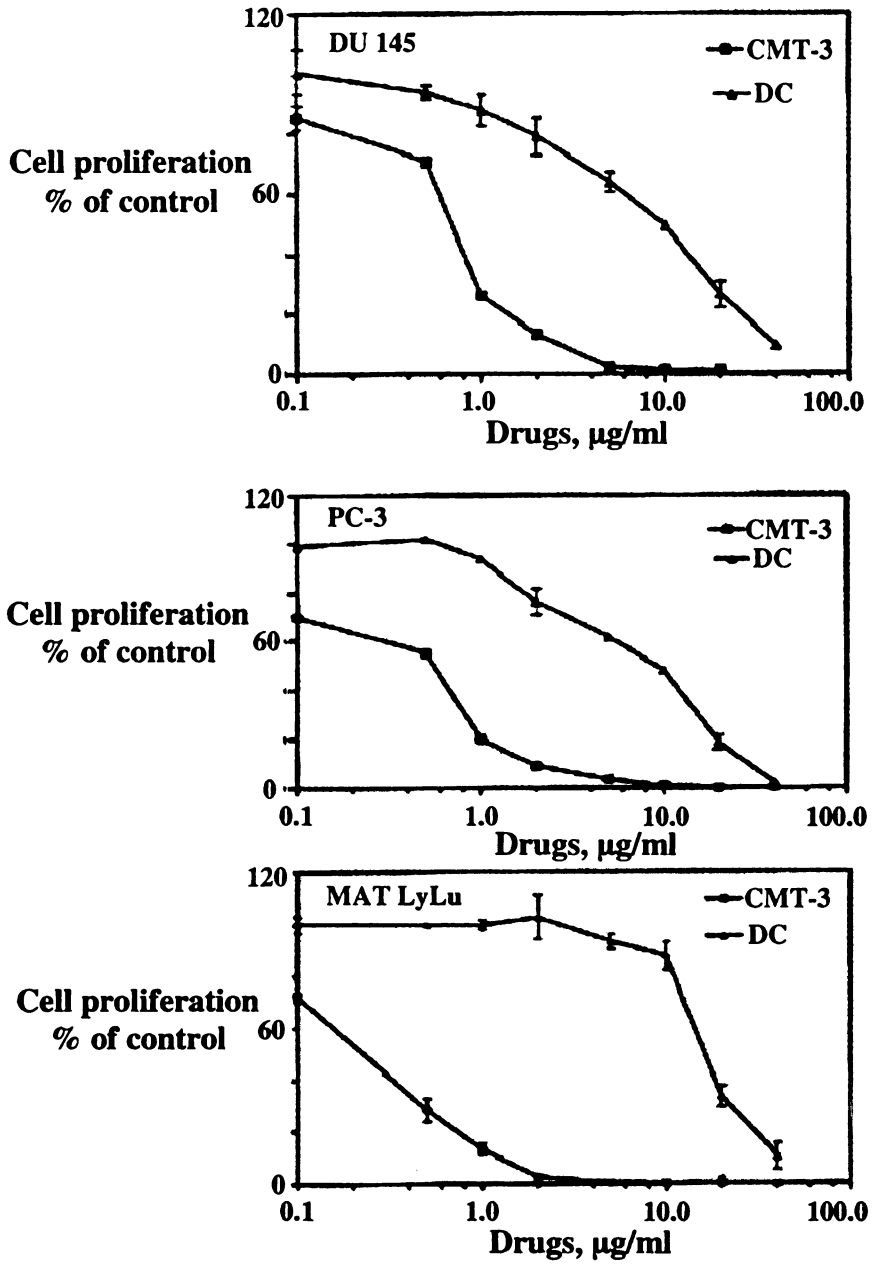

Figure 5.2. Effect of doxycycline (DC) and CMT-3 on proliferation of prostate tumor cell lines. Tumor cells were incubated with various concentrations of DC or CMT-3 for 48 hours in complete culture medium. Cell proliferation activity, defined as synthesis of [^{3}H]-thymidine-labeled DNA, was assayed by 2-hour pulse-labeling the cells with [^{3}H]-thymidine as described in the text. Data presented are for three prostate cancer cell lines. Similar results were obtained for other cell lines. Vertical bars represent mean ± SEM from four independent determinations (Lokeshwar, 1999).

In several prostate cancer cell lines, CMT-3 was found to be 8-fold more effective than doxycycline at inhibiting cell survival *in vitro* (Table 5.1). CMT-3 was also 10-fold more effective at inhibiting clonogenic survival of two human prostate cancer cell lines (Lokeshwar, 1999). The possible mechanisms of CMT-3 induced toxicity will be further discussed.

Table 5.1 Cytotoxicity of DC and CMT-3 in Prostate Cells

Cell line[1]	GI_{50}[2]	
	DC	CMT-3
ALVA 101 (4)	16.67 ± 1.3[b]	3.1 ± 0.34
BPH-1 (3)	9.68 ± 2.45	4.78 ± 1.68
CaP 139 (1)	18.7 ± 3.7	9.3 ± 2.11
DU 145 (8)	19.8 ± 4.25	2.3 ± 0.53
LNCaP (5)	6.3 ± 1.35	2.29 ± 0.96
MAT Lylu (7)	9.09 ± 2.95	2.36 ± 0.86
PC-3 (5)	16.55 ± 1.06	4.8 ± 0.96
TSU PR-1 (5)	18.64 ± 5.1	6.7 ± 1.2

[1] Numbers of replicate experiments are given in parentheses.
[2] Growth inhibition was calculated from linear regression of the dose-response curves generated for each experiment using log (dose) *vs.* cell proliferation (% of control). Correlation coefficient (r) was always ≥0.95 (negative). Results are presented as mean ± SEM μg/ml (1 μg/ml = 2.2 μm) of at least 3 GI_{50} values calculated from each experiment. (Lokeshwar et al., 2002).

Possible mechanisms of CMT-3 induced cytotoxicity:

Many anti-tumor drugs which inhibit cell proliferation also induce apoptosis or programmed cell death (Lokeshwar, 1999). This has been shown with CMT-3. Culture media from cells incubated with various concentrations of CMT-3 were assayed for soluble nucleosomes resulting from apoptosis (Lokeshwar et al., 1998). CMT-3 was found to induce apoptosis in >80% of the cells in all seven prostate cancer cell lines tested and induction of apoptosis was both dose and time dependent (Lokeshwar et al., 1998; Lokeshwar, 1999). Only at 5-10 fold higher concentration was doxycycline able to induce similar levels of apoptosis as CMT-3 treated cells. In another study the minimum incubation time required for CMT-3 to induce apoptosis was similar to the time range of maximum expression in cellular [OH^-] and detectable depolarization of the mitochondria (Lokeshwar et al., 2002). These results suggest that CMT-3-induced apoptosis is associated with production of free radicals and depolarization of the mitochondria. In fact mitochondrial depolarization is frequently observed in cells undergoing apoptosis (Lemasters et al., 1998).

In addition to the induction of apoptosis, cell cycle progression was blocked in prostate cancer cell cultures treated with CMT-3 (Lokeshwar et al., 2002). A significant increase in the accumulation of cells at the G_0/G_1 phase was observed; from ~50% in the control cell population to up to 85% in cells treated with CMT-3. Similarly, a decrease in the S-phase fractions was observed in PC-3, DU145 and LNCaP, which is indicative of the inhibition of cell cycle regulators (Lokeshwar et al., 2002). The molecular mechanisms of the cytotoxic effects of CMT-3 are still under study. Another proposed

mechanism to explain the ability of CMT-3 to inhibit cell growth, invasion and metastasis may be due to inhibition of MMPs.

CMT-3 decreases MMP production:

MMPs are important enzymes involved in prostate cancer progression and metastasis. It has been previously suggested that tetracycline's inhibitory effect on MMPs may involve the drug's well-known ability to bind metal ions like zinc, which are required by the MMPs to maintain their proper conformation and hydrolytic activity (Golub et al., 1983 and 1991). In support of this, addition of excess zinc has been shown to overcome the inhibition of gelatinases and collagenase by doxycycline (Lee et al., 1992; Yu et al., 1992). The amount of MMP synthesized and secreted by prostate cancer cells is lower in monolayer cultures treated with CMT-3 as compared to untreated cells (Lokeshwar et al., 2002).

MMP activity in serum-free conditioned medium from drug-treated rodent and human prostate cancer cells, MAT LyLu and TSU-PR1 respectively, were analyzed by zymography (Lokeshwar et al., 2002). TSU-PR1 cultures predominantly secreted latent forms of MMP-2 and MMP-9 while MAT LyLu cells secreted activated MMP-2 (62kDa) but little MMP-9 (Figure 5.3).

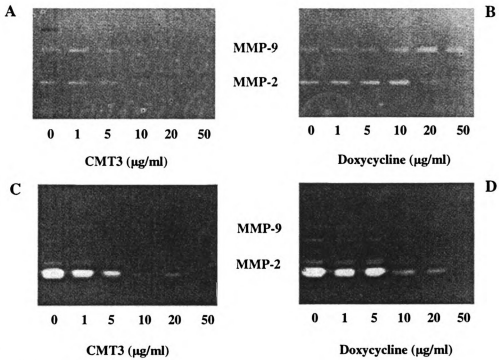

Figure 5.3 Zymographic detection of gelatinases secreted into the conditioned media from cultures treated with CMT-3 or doxycycline. Culture conditioned media (15 μl/lane, equivalent to 5 x 10^3 cells) from TSU-PR1 (a,b) and MAT LyLu (c,d) cells were separated by SDS-PAGE (8% polyacrylamide) on a gelatin-embedded (1 mg/ml) gel and zymography. The positions of purified MMP-2 and MMP-9 are indicated. Note: the major fraction of MMP-2 from MAT LyLu (bottom) cell conditioned media was active (Mr ~64,000), whereas most TSU-PR1 (top) MMP-2 was in the latent form (Mr 72,000) (Lokeshwar et al., 2002).

Incubation of TSU-PR1 and MAT LyLu cell lines with CMT-3 decreased the secretion of MMPs in both cell lines in a dose-dependent manner (Lokeshwar et al., 2002). Similar to other results, CMT-3 was more effective than doxycycline; cells treated with CMT-3 secreted significantly less MMP than the cells treated with doxycycline. In this experiment treatment of prostate cancer cells with CMT-3 resulted in a decrease in the amount of both MMP-2 and MMP-9.

To establish further that the observed decreases in MMP levels in conditioned medium were indeed due to the drug-induced inhibition of MMP production/secretion, protein levels of MMPs in CaP 139 cells were measured by an enzyme-linked immunosorbent assay (ELISA) that uses a monoclonal anti-MMP-2 antibody (Lokeshwar et al., 2002). CaP 139 cells were derived from a primary human prostate tumor. A dose-dependent decrease in the levels of secreted MMP-2 was observed by the CaP 139 cells treated with CMT-3 or doxycycline. In CaP 139 cells MMP-2 levels decreased by 51% and 74% at 20 μg/ml doxycycline and 10 μg/ml CMT-3, respectively.

ELISA kits were also used to measure the protein levels of the natural inhibitors of MMPs, TIMPs, in Ca 139 cells treated with CMT-3 (Lokeshwar et al., 2002). The decreases in TIMP-1 and TIMP-2 levels were 33% and 10.27%, respectively at 10 μg/ml CMT-3. These data show that both TIMP-1 and TIMP-2 levels were much less inhibited by CMT-3 than MMP-2. This suggests that CMT-3 reduces invasive activity of tumor cells, not only by inhibiting MMP synthesis and secretion, but also by not affecting TIMP levels significantly. The lack of total inhibition of MMP activity in tumor cells by CMT-3 could be due to the production of other proteinases, which are capable of activating MMPs, but are not inactivated by CMTs (Lokeshwar et al., 2002). One such proteinase is urokinase-type plasminogen activator (uPA) (Webber and Waghray, 1995). It has been reported that CMTs do not inhibit uPA secretion or activity (Chang et al., 1996).

CMTs inhibit Matrigel invasion:

The invasive activity of two human prostate cancer cell lines, PC-3 and DU145, and one rodent prostate cancer cell line, MAT LyLu, were assayed following 48 hours of exposure to 5 μg/ml of each CMT (CMT-1, 2, 3, 4, 6, 7 and 8) or doxycycline. The percentage of cells that invaded through Matrigel-coated filters in the control wells were used to determine percent inhibition of Matrigel invasion in treated wells for each cell line tested. As shown in Figure 5.4, CMT-3 was the most potent inhibitor of invasive activity of PC-3, DU145 and MAT LyLu cells while CMT-6 was the least potent inhibitor (Lokeshwar, 1999).

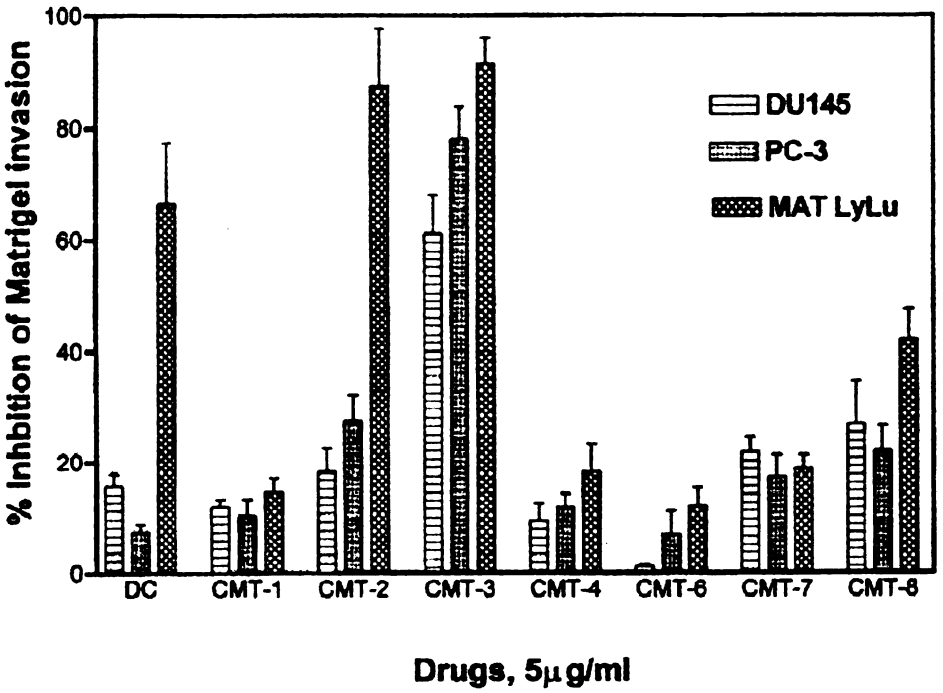

Figure 5.4 Inhibition of invasive potential of tumor cells by doxycycline (DC) and CMTs. Invasion of tumor cells through the Matrigel-coated filters was assayed following 48 hours of exposure to 5 μg/ml of each drug. Only the drug diluent (0.1% dimethyl sulfoxide) was added to control wells. Percentage of cells that invaded in the control (0.1% DMSO) wells varied from 12.5 ± 6.4% for DU145 cells to 17 ± 4.2 for MAT LyLu cells. 0.1% DMSO had negligible effect on invasion. Results presented are from three independent experiments. (Lokeshwar, 1999).

Doxycycline and CMT-2 were minimally effective as inhibitors of invasion of the Dunning rat MAT LyLu prostate cancer cells. These results show that CMT-3 is not only the most cytotoxic CMT but it is also the most effective inhibitor of Matrigel invasion by prostate cancer cells.

CMT-3 inhibits Dunning tumor growth and metastasis:

The androgen-insensitive Dunning rat MAT LyLu cell line was chosen for *in vivo* studies in Copenhagen rats. These cells are highly tumorigenic upon subcutaneous

injection of as low as $5X10^4$ cells and metastasize to the lymph nodes and lungs only 12 days post cell injection (Isaacs et al., 1986). In rats bearing subcutaneous tumors and given treatment (40 mg/kg) for 21 days with a daily oral gavage of CMT-3 or doxycycline, tumor incidence and tumor growth rate were only significantly reduced in the CMT-3 gavage-fed group (Lokeshwar, 1999). A regression or disappearance of palpable tumor was observed in CMT-3 treated groups, but not in the control or doxycycline treated groups. Spontaneous metastasis to the lungs was reduced significantly in groups treated with doxycycline or CMT-3, the number of metastatic foci were reduced to 49.7% and 41.2% of control, respectively. These results could only be obtained if the tumor cell inoculum was lowered from $1X10^6$ cells/site to $1X10^5$ cells/site. When rats were given subcutaneous injections of $1X10^6$ cells/site, tumor incidence and tumor growth were not affected by oral administration of CMT-3 or doxycycline. In this experiment, rats began treatment with the test agent (CMT-3 or doxycycline) on the same day as cell injection.

In another study, pre-dosing tumor-bearing rats with CMT-3 at 40 mg/kg with daily gavage for 7 days and using the tumor cell inoculum of $2X10^5$ cells/site resulted in a remarkable reduction in tumor incidence and significant tumor remission (Lokeshwar et al., 2002). More than 90% of the rats in control and doxycycline-treated groups developed tumors in 3 independent experiments. In contrast, the incidence of rats developing tumors in CMT-3-treated groups was significantly lower ($55 \pm 9\%$) than that for control or doxycycline-treated groups. In two separate experiments tumor regression was observed in 20% and 30% of CMT-3-treated groups. This enhanced efficacy of

CMT-3 upon pre-dosing suggests that CMT-3 treatment will be effective if administered prior to the appearance of clinical signs.

In rats given an intravenous cell injection of MAT LyLu tumor cells ($5X10^4$), daily treatment by gavage with CMT-3 resulted in both an increase in survival and a decrease in skeletal and soft tissue metastasis (Lokeshwar, 1999; Selzer et al., 1999). Treatment with CMT-3 also resulted in a delayed onset or a total lack of paraplegia following intravenous cell injection compared to control animals. As observed in the subcutaneous rat model of prostate cancer, CMT-3 was most effective when fed to rats by gavage beginning several days prior to cell injection.

Several *in vivo* models of aggressive prostate cancer described above have demonstrated the efficacy of CMT-3 against tumor incidence, tumor growth, and tumor metastasis to soft or skeletal tissue. In both subcutaneous and intravenous rat models of prostate cancer, treatment with CMT-3 by gavage did not have any adverse effects on the animals indicating its safe nature. The enhanced efficacy of CMT-3 upon pre-dosing and oral bioavailability, with minimal adverse reactions within a tolerable dose, suggests that CMT-3 could be used as an adjuvant to hormone ablation or radiation therapy in prostate cancer.

Phase I clinical trial of CMT-3:

Besides prostate cancer, CMTs have also been shown to exhibit *in vitro* and *in vivo* anti-tumor invasion and metastasis potential in many aggressive types of tumor, including breast cancer and melanoma (Meng et al., 2000; Seftor et al., 1998). Because of its interesting mechanism of action and potent preclinical activity, COL-3 or CMT-3

was entered into phase I testing (Rudek et al., 2001; Lokeshwar et al., 2002). A study conducted by the Investigational Drug Branch, Cancer Therapy Evaluation Program at the National Cancer Institute evaluated maximum tolerated dose and dose-limiting toxicities of CMT-3 in patients with refractory solid tumors (Rudek et al., 2001).

In this phase I clinical trial of CMT-3, patients with advanced refractory metastatic cancer were given a daily dose of CMT-3. Eight patients had stable disease at the first 2-month follow-up and continued on-study for more than 61 days. One patient with hemangioendothelioma experienced disease stabilization for more than 26 months. This patient had not received any prior cytotoxic chemotherapy, suggesting that MMP inhibitors are more effective if given early in the course of treatment. Of seven patients with tumors of nonepithelial origin, three (43%) showed some degree of clinical benefit from COL-3. These patients had disease stabilization for more than 6 months and included three women with hemangioendothelioma, metastatic Sertoli-Leydig cell tumor of the ovary and fibrosarcoma metastatic to the lung. Those patients that demonstrated disease stabilization, were also shown to have a significant reduction in plasma MMP-2 levels. MMP-2 levels decreased with increasing cumulative dose of COL-3 in many of the patients with drug-induced toxicity to a greater degree than the reduction seen in patients with stable disease. The reason for this association and the mechanism by which COL-3 inhibits the production of MMP-2 is not clear. It is also not clear whether MMP-2 production was from vascular endothelial cells, tumor cells, or both. The major dose-limiting toxicity of CMT-3 was photosensitivity. Drug-induced phototoxicity was observed in 40-70% of the patients receiving CMT-3 at a dose greater than or equal to 70 mg/m^2/day. Based on the results of this study a daily dose of 36 mg/m^2 was

recommended for a phase II clinical trial. However, a dose of 70 mg/m^2/day may be considered if diligent sun precautions are used.

Conclusions

CMTs could be an effective therapy for prostate cancer. They have been shown to inhibit cell proliferation and Matrigel invasion of several prostate cancer cell lines, as well as, cause a decrease in matrix metalloproteinase (MMP) production and activity *in vitro*. A decrease in the incidence of metastasis was observed in several different rat tumor models of prostate cancer where animals received a daily dose of CMT-3. Results obtained from many *in vitro* and *in vivo* cancer studies using CMT-3 support the concept that the ability of CMTs to inhibit MMPs is an effective approach to reducing tumor growth and metastasis. Most important is the ability of CMTs to inhibit the production and activity of MMP-2 because increased expression of MMP-2 is of significant interest in prostate cancer progression. Combined with their cytotoxic property and little systemic toxicity, CMTs may have great potential as anticancer drugs. Therefore, the screening of additional CMTs and future clinical trials may be necessary to identify compounds which show greater efficacy in the treatment of prostate cancer.

Literature cited

Chambers, A.F., and Matrisian, L.M.: Changing views of the role of matix metalloproteinases in metastasis. Journal of the National Cancer Institute 89:1260-1270, 1997.

Chang, K., Rani, A.S., Chang, K.: Plasminogen activator activity is decreased in rat gingival during diabetes. Journal of Periodontal Research 67:743-747, 1996.

Chu, W.: Matrix metalloproteinases in tissue remodeling, regeneration and prostate cancer. Masters of Science Thesis, Michigan State University, East Lansing, MI, USA, pp.55-70, 1998.

Fidler, I.J.: The biology of human cancer metastasis. Acta Oncologica 30:668-675, 1991.

Fridman, R., Toth, M., Pena, D., and Mobashery, S.: Activation of progelatinase B (MMP-9) by gelatinase A (MMP-2). Cancer Research 55:2548-2555, 1995.

Golub, L.M., Ramamurthy, N.S., and McNamara, T.F.: Tetracyclines inhibit connective tissue breakdown: new therapeutic implications for an old family of drugs. Critical Reviews in Oral Biology and Medicine 2:297-322, 1991.

Golub, L.M., Lee, H.M., Lehrer, G., Nemiroff, A., McNamara, T.F., Kaplan, R. and Ramamurthy, N.S.: Minocycline reduces gingival collagenolytic activity during diabetes: preliminary observations and a proposed new mechanism of action. Journal of Periodontal Research 18:516-526, 1987.

Isaacs, J.T., Isaacs, W.B., Feitz, W.F. and Scheres, J.: Establishment and characterization of seven Dunning rat prostatic cancer cell lines and their use in developing methods for predicting metastatic abilities of prostatic cancers. Prostate 9:261 -281, 1986.

Kapusnik-Uner, J.E., Sande, M.A., and Chambers, H.F.: Tetracyclines, chloramphenicol, erythromycin, and miscellaneous antibacterial agents. In: Goodman & Gilman's The Pharmacological Basis of Therapeutics, Wonsiewicz, M.J. and McCurdy, P. (eds.), New York, The McGraw-Hill Companies, Inc., 9th Edition:1123-1130, 1995.

Lee, H.M., Hall, J.E., Sorsa, T., Simon, S. and Golub.L.M.: Doxycycline inhibits PMN -mediated tissue breakdown in culture. Journal of Dental Research (special issue) 71:245, 1992.

Lemasters, J.J., Nieminen, A.L., Quian, T., Trost, L.C., Elmore, S.P., Nishimura, ., Crowe, R.A., Cascio, W.E., Bradham, C.A., Brenner, D.A., and Herman, B.: The mitochondrial permeability transition in cell death: a common mechanism in necrosis, apoptosis and autophagy. Biochimica et Biophysica Acta 1366:177 -196, 1998.

Liotta, L.A., Kleinerman, J., Catanzaro, P., and Rynbrandt, D.: Degradation of basement membrane by murine tumor cells. Jounal of the National Cancer Institute 58:1427-1431, 1977.

Liotta, L.A. and Stetler-Stevenson, W.G.: Priniciples of molecular cell biology of cancer: cancer metastasis. In: Cancer: principles and practive of oncology. DeVita, V.T., Hellman, S., and Rosenberg, S.A. (eds.), Philidelphia, Lippincott, 134-149, 1993.

Liotta, L.A., Tryggvason, K., Garbisa, S., Hart, I., Foltz, C.M., Shafie, S.: Metastatic potential correlates with enzymatic degradation of basement membrane collagen. Nature 284:67-68, 1980.

Lokeshwar, B.L., Selzer, M.G., Zhu, B., Block, N.L. and Golub, L.M.: Inhibition of cell proliferation, invasion, tumor growth and metastasis by an oral non-antimicrobial tetracycline analog (COL-3) in a metastatic prostate cancer model. International Journal of Cancer 98:297-309, 2002.

Lokeshwar, B.L.: MMP inhibition in prostate cancer. Annals New York Academy of Sciences 878:271-289, 1999.

Lokeshwar, B.L., Houston-Clark, H.L., Selzer, M.G., Block, N.L., and Golub, L.M.: Potential application of a chemically modified non-antimicrobial tetracycline (CMT-3) against metastatic prostate cancer. Advances in Dental Research 12:97 -102, 1998.

Lokeshwar, B.L., Selzer, M.G., Block, N.L., and Gunja-Smith, Z.: Secretion of matrix metalloproteinases and their inhibitors (tissue inhibitor of metalloproteinases) by human prostate in explant cultures: reduced tissue inhibitor of metalloproteinase secretion by malignant tissues. Cancer Research 53:4493-4498, 1993.

Meng, Q., Xu, J., Goldberg, I.D., Rosen, E., Greenwald, R., and Fan, S.: Influence of chemically modified tetracyclines on proliferation, invasion, and migration properties of MDA-MB-468 human breast cancer cells. Clinical & Experimental Metastasis 18:139-146, 2000.

Newling, D.W.: The management of hormaone refractory prostate cancer. European Journal of Urology 29:69-74, 1996.

Rudek, M.A., Figg, W.B., Dyer, V., Dahut, W., Turner, M.L., Steinberg, S.M., Liewehr, D.J., Kohler, D.R., Pluda, J.M., and Reed, E.: Phase I clinical trial of oral COL-3, a matrix metalloproteinase inhibitor, in patients with refractory metastatic cancer. Journal of Clinical Oncology 19:584-592, 2001.

Seftor, R.E.B., Seftor, E.A., De Larco, J.E., Kleiner, D.E., Leferson, J., Stetler-Stevenson, W.G., McNamara, T.F., Golub, L.M., and Hendrix, M.J.C.: Chemically modified tetracyclines inhibit human melanoma cell invasion and metastasis. Clinical & Experimental Metastasis 16:217-225, 1998.

Selzer, M.G., Zhu, B., Block, N.L., and Lokeshwar, B.L.: CMT-3, a chemically modified tetracycline, inhibits bony metastases and delays the development of paraplegia in a rat model of prostate cancer. Annals New York Academy of Sciences 878:678-682, 1999.

Stearns, M. and Stearns, M.E.: Evidence for increased activated metalloproteinase 2 (MMP-2a) expression associated with human prostate cancer progression. Oncology Research 8:69-75, 1996.

Webber, M.M., and Waghray, A.: Urokinase-mediated extracellular matrix degradation by human prostatic carcinoma cells and its inhibition by retinoic acid. Clinical Cancer Research 1:755-761, 1995.

Webber, M.M., Waghray, A., Bello, D., and Rhim, J.S., Mini review: proteases and invasion in human prostate epithelial cell lines: implications in prostate cancer prevention and intervention. Radiation Oncology Investigations 3:358-362, 1996.

Wojtowicz-Praga, S.M., Dickson, R.B., and Hawkins, M.J.: Matrix metalloproteinase inhibitors. Investigational New Drugs 15:61-75, 1997.

Yu, L.P., Smith, G.N., Hasty, K.A. and Brandt, K.D.: Doxycycline inhibits type XI collagenolytic activity of extracts from human osteoarthritic cartilage and of gelatinase. Journal of Rheumatology 18:1450-1452, 1992.

PART 2

ORIGINAL RESEARCH

CHAPTER SIX

EVALUATION OF THE EFFICACY OF CHEMICALLY MODIFIED TETRACYCLINES (CMTs) AS AGENTS FOR THE TREATMENT OF PROSTATE CANCER: A PILOT STUDY USING CMT 2215

Abstract

Chemically modified tetracyclines (CMTs) may be effective chemotherapeutic agents for prostate cancer. Results obtained from *in vitro* and *in vivo* studies, in addition to a phase I clinical trial, suggest a potential use for CMTs as an oral, nontoxic drug to treat metastatic prostate cancer and other cancers. Additional screening of CMTs may lead to the identification of compounds which show greater efficacy in the treatment of prostate cancer. Thus, in this chapter, I examine the ability of CMT 2215, to inhibit the growth of two human prostate epithelial cell lines, RWPE2-W99 and CTPE, *in vivo*. RWPE2-W99 forms slow growing tumors when injected into nude mice and mimics the behavior of the majority of primary human prostate cancers, while CTPE forms rapidly growing, aggressive tumors, and represents the more aggressive, late stage of tumor progression. Treatment of RWPE2-W99 cells grown in monolayer cultures with 50 μg/ml 2215 caused ~65% growth inhibition. *In vivo*, I assessed the ability of CMT 2215 to inhibit growth and reduce the size and number of tumors produced after subcutaneous injection of RWPE2-W99 or CTPE cells in immune-suppressed mice. Using the slow growing RWPE2-W99 cells, treatment with CMT 2215 (0.675 mg/ml) caused a decrease in tumor volume, but CMT 2215 (2.25 mg/ml) appeared to have no effect on tumor growth in the aggressive CTPE cells. Based on the results of these *in vitro* and *in vivo* studies, I selected the RWPE2-W99 model for additional studies using other CMTs.

Keywords

Chemically modified tetracycline, CTPE, gavage, prostate cancer, RWPE2-W99, subcutaneous, tumor

Introduction

Chemically modified tetracyclines (CMTs) have been shown to inhibit cell proliferation and Matrigel invasion of several prostate cancer cell lines, as well as, cause a decrease in matrix metalloproteinase production and activity *in vitro* (Lokeshwar, 1999; Lokeshwar et al., 2002). In male Copenhagen rats, given subcutaneous injection of MAT LyLu cells, treatment with CMT-3 by gavage inhibited tumor incidence and reduced the tumor growth rate (Lokeshwar et al., 1999). In Copenhagen rats given an intravenous injection of MAT LyLu cells, treatment with CMT-3 decreased the frequency of tumor metastasis to soft or skeletal tissue and also resulted in an increase in survival (Lokeshwar, 1999; Selzer et al., 1999). Other CMTs are now being extensively investigated because of their increased efficacy as compared to their natural derivatives.

In this study CMT 2215 was tested for its effects on the growth of the tumorigenic RWPE2-W99 and highly aggressive CTPE human prostate cancer cell lines (Achanzar et al., 2004; Achanzar et al., 2001; Bello et al., 1997; Webber et al., 1997a). These two cell lines are related because they share a common origin. The following describes the process by which the RWPE2-W99 cell line was developed. Human prostate epithelial cells were derived from the peripheral zone of a normal human prostate and immortalized with a single copy of human papilloma virus-18 (HPV-18) DNA to give rise to the RWPE-1 cell line (Bello et al., 1997; Webber et al., 1997a). RWPE-1 cells were then

transformed by *v*-Ki-*ras*, giving rise to the RWPE-2 cell line (Bello et al., 1997; Webber et al., 1997a). The transformed RWPE-2 cells are tumorigenic and can grow in soft agar in an anchorage-independent manner. In order to select cells that showed high Ki-*ras* expression, RWPE-2 cells were grown in agar and colonies were screened for Ki-*ras* expression. One of these colonies was expanded and it gave rise to the RWPE2-W99 cell line. I used this cell line for *in vitro* studies and for *in vivo* studies to assess the efficacy of CMT 2215 to inhibit tumor growth when RWPE2-W99 cells were grown as a xenograft in nude mice. RWPE2-W99 cells represent an early stage of prostate cancer progression. In addition, I used the CTPE cell line, which represents a more aggressive, rapidly growing tumor. The CTPE cell line was derived from RWPE-1 cells by chronic exposure to cadmium, a carcinogen (Achanzar et al., 2001).

Both RWPE2-W99 and CTPE cell lines are tumorigenic and CTPE cells have also been shown to be invasive and metastatic following subcutaneous injection in nude mice (Achanzar et al., 2004; Achanzar et al., 2001; Bello et al., 1997; Webber et al., 1997a and b). Since both cell lines are related and mimic different stages of human prostate cancer progression, they are useful for testing agents for the prevention and treatment of prostate cancer. Such agents include chemically modified tetracyclines (CMTs).

The objectives of this study were to determine the ability of CMT 2215 to inhibit cell growth *in vitro* and tumor growth *in vivo* of these two human prostate cancer cell lines. This study was conducted to develop a xenograft model for assessing the efficacy of CMTs for the treatment of prostate cancer. In order to determine dose levels that might be used for *in vivo* studies, the effects of the test agent on the growth of RWPE2-W99 cells were first tested in cell culture.

Materials & Methods

In vitro studies

Cell culture:

Both RWPE2-W99 and CTPE cells were grown in complete keratinocyte serum-free medium (KSFM) containing 50 μg/ml bovine pituitary extract (BPE), 5 ng/ml epidermal growth factor (EGF) and 1X antibiotic/antimycotic solution. Cultures were maintained at 37^0C in a humidified atmosphere containing 5% CO_2 and subcultured weekly.

Dose response using a microplate assay:

RWPE2-W99 cells were plated, six replicate wells per treatment, in complete keratinocyte serum-free medium (K-SFM) containing 50 μg/ml bovine pituitary extract (BPE) and 5 ng/ml epidermal growth factor (EGF), 10,000 cells/well in 96-well plates and allowed to attach for 48 h at which time medium was changed to medium containing varying concentrations of the test agent. The test agent, CMT 2215, was dissolved in DMSO. The final concentration of the DMSO vehicle in the culture medium was 0.1%. Treatment groups consisted of untreated control, vehicle-treated control, and CMT 2215 at doubling dilutions from 0.39 μg/ml to 50 μg/ml. Cells received fresh CMT treatment every 48 h for 5 days, receiving a total of three treatments. At the end of the 5-day treatment, plates were processed using the MTT [3-(4,5-dimethyl thiazol-2-yl)-2,5-diphenyl tetrazolium bromide) assay described previously (Webber et al., 2001). Results represent the average of two experiments.

In vivo studies

Mice:

Eight week old, albino male mice, *nu/nu* strain (NSWNU-M, homozygotes) (Taconic farms, Inc., Germantown, NY), were used in this study. This strain of mice is the standard athymic model for the National Cancer Institute (NCI) studies as well as many pharmaceutical and institutional oncology screening programs. Mice were socialized for four days after arrival from Taconic. The mice were provided with autoclaved tap water to drink and fed a complete, irradiated diet (Teklad 7904, manufactured by Harlan, Madison, WI). To ensure the health of the mice, their physical condition and food and water intake were examined daily. For enrichment purposes the mice were given nestlettes once a week.

Animal maintenance:

The mice were maintained at the University Laboratory Animal Resources (ULAR) facility in a clean room dedicated for this experiment (Figure 6.1). The room was maintained at 72^0 -74^0 F and on a twelve-hour light-twelve hour dark schedule. The mice were housed individually in autoclaved cages on paper chip bedding in a laminar flow rack. The Clinical Center is one of several buildings on campus that houses animals (Figure 6.1a). The entrance to the ULAR facility of the Clinical Center Building (Figure 6.1b), animal room (Figure 6.1c) and laminar flow cage rack (Figure 6.1d) in which the mouse cages are separated by rows for the four groups of mice, are shown. Investigators and caretakers were required to wear the following upon entrance to the room: Bonnet,

mask, booties, sterile gloves, and sterile gown. All procedures involving mice were performed in a laminar flow hood. The drug (CMT 2215) was administered to mice by gavage feeding. Gavage feeding was done in the laminar flow hood under yellow light to protect the CMT. A laminar flow hood (Figure 6.1e), where cell injections, daily feeding by gavage (Figure 6.1f) using a sterile feeding tube, weighing, and cage changes take place is also shown. This study was conducted with the approval of the All University Committee on Animal Use and Care (AUCAUC) and all guidelines were followed.

Figure 6.1 The facility, experimental design and equipment used for *in vivo* studies. 6.1a. Clinical Center Building; 6.1b. University Laboratory Animal Resources (ULAR) facility; 6.1c. room for housing immune-deficient mice (nude mice); 6.1d. laminar flow mouse cage rack. The cages were arranged in rows for the four groups of mice; row 1 = RWPE2-W99 controls; row 2 = RWPE2-W99 treated; row 3 = CTPE controls; row 4 = CTPE treated. Mice were housed, one mouse per cage, in autoclaved cages, and provided with autoclaved drinking water and irradiated food. 6.1e. laminar flow hood where gavage feeding was performed; 6.1f. Gavage feeding procedure. The control mice were fed 300 µl of a 5% sucrose solution in water by gavage. The treated mice were similarly fed with 0.675 mg or 2.25 mg of 2215/mouse in 300 µl of a 5% sucrose solution starting 3 days prior to cell injection. Gavage feeding was performed daily for a total of 10 weeks.

Sucrose solution: vehicle for CMT 2215:

The control mice were fed 300 µl of a 5% sucrose solution in water by gavage. A 5% sucrose (Sigma, Cat. No. S-5016) solution was prepared in de-ionized water and autoclaved. Aliquots of 1.5 ml/tube were prepared for gavage feeding of control mice and stored in a -20^0 C freezer. Gavage feeding was performed daily for a total of 10 weeks. This solution was used as the vehicle for CMT 2215.

Drug stock solutions:

CMT 2215 was provided by Innapharma Inc./Tetragenex Pharmaceuticals, Inc., Park Ridge, NJ (from ACROS Organics, NJ), stored at 4^{0}to 6^0 C, and protected from the light. A low-dose and a high-dose stock solution of CMT 2215 was prepared. The low-dose stock solution (6.75 mg/ml) was prepared in sterile 5% sucrose and further diluted to obtain a 2.25 mg/ml (0.675 mg/ 300 µl) solution and filter-sterilized using a 0.22 µm pore size filter. The high-dose stock solution of CMT 2215 (7.5 mg/ml or 2.25 mg/ 300 µl) was also prepared in sterile 5% sucrose solution and filter-sterilized using a 0.22 µm pore size filter. Aliquots of both low-dose and high-dose CMT 2215 of 1.5 ml/ brown Eppendorf tube were prepared and stored in a -20^0 C freezer, in boxes to protect from light, until needed. The treated mice were fed 300 µl of a 5% sucrose solution, containing 0.675 mg or 2.25 mg of 2215/mouse by gavage, starting 3 days prior to cell injection.

Cells for injections:

A sterile cell suspension of RWPE2-W99 (Bello et al., 1997; Webber et al., 1997a) or CTPE cells was prepared in basal keratinocyte serum-free growth medium and mixed with an equal volume of Matrigel (Webber et al., 2001) to obtain 4 million cells/ml. All steps with Matrigel were performed on ice. The cell suspension was kept on ice and taken to the animal facility. A 1.0 cc syringe with a 23 gauge needle (or 25 gauge for CTPE) was used to inject 250 µl of the cell suspension containing one million cells, per inoculation site. Before injection the mice were swabbed with alcohol at the injection site. Cells were injected subcutaneously and bilaterally on the dorso-lateral side. The mice were kept on a heating pad during the procedure to maintain body temperature.

Experimental groups:

The study involved four groups of mice.

Group 1: RWPE2-W99 controls:

Four mice were gavage fed (Figure 1f) with 300 µl of 5% sucrose solution in water daily for three days prior to being injected with RWPE2-W99 cells. After cell injection, daily gavage feeding with sucrose solution continued for 10 weeks. A fresh vial of sucrose was used each day.

Group 2: RWPE2-W99 CMT #2215 low dose treated mice:

Four mice were gavage fed, each receiving 300 µl of 5% sucrose solution in water containing CMT 2215 daily for three days prior to being injected with RWPE2-W99 cells. Group 2 mice, with average body weight of ~27 g, received 0.675 mg of

CMT 2215/mouse. After cell injection, daily gavage feeding with CMT 2215 in sucrose solution continued for 10 weeks. A fresh vial of CMT solution was used each day. Each day's supply was thawed just before use and the vials were kept in cardboard boxes to prevent light exposure.

Group 3: CTPE controls:

Three mice were gavage fed with 300 µl of 5% sucrose solution in water daily for three days prior to being injected with CTPE cells. After cell injection, daily gavage feeding with sucrose solution continued for 10 weeks. A fresh vial of sucrose was used each day. (Note: Groups 3 and 4 only had 3 mice each because two mice became dehydrated and expired prior to start of this experiment.)

Group 4: CTPE CMT 2215 high dose treated mice:

Three mice were gavage fed with 300 µl of 5% sucrose solution in water containing CMT 2215 daily for three days prior to being injected with CTPE cells. Group 4 mice, with average body weight of ~30 g, received 2.25 mg of CMT 2215/mouse. After cell injection, daily gavage feeding with CMT 2215 in sucrose solution continued for 10 weeks. A fresh vial of CMT solution was used each day. Each day's supply was thawed just before use and the vials were kept in cardboard boxes to prevent light exposure.

Animal weights:

Animals were weighed at the start of the experiment and then weekly until the end of the experiment, and the weights were recorded. Mice were given a physical examination daily, and their food and water intake were also monitored daily. The average weight of mice on day zero was ~27 g for treatment groups 1 and 2 and ~30 g for treatment groups 3 and 4.

Tumor size and histology:

When tumors became palpable, their size was measured periodically in two dimensions (length and width), using digital calipers, and all measurements were recorded. Tumor volume (TV) was calculated using the formula: $TV = a \, X \, b^2/2$ where a is the longest dimension and b is the width (Nemeth et al., 1999). Upon termination of the experiment at 10 weeks, mice were sacrificed using CO_2, and photographed for tumor size. Tumors were dissected, fixed in 10% buffered formalin and processed for histology. Tumor sections were cut at 5μm thickness. In addition, abdominal wall, liver and lungs were examined for visible tumor metastasis. Lungs, liver and other areas showing invasion were also fixed for histology.

Results:

In vitro studies

Effect of CMT 2215 on anchorage–dependent growth

In order to examine the effects of CMT 2215, concentrations from 0.39 to 50 μg/ml were tested. Two independent experiments, using six replicate wells/treatment,

were conducted. Results shown in Figure 6.2 represent the average of these two experiments. From these data, it is evident that RWPE2-W99 cells show a dose-dependent inhibition of growth at concentrations higher than 1.56 µg/ml for CMT 2215. Approximately 65% growth inhibition was observed at 50 µg/ml. The ID_{50} for 2215 was ~35.74 µg/ml when cells were plated at 10,000 cells/well.

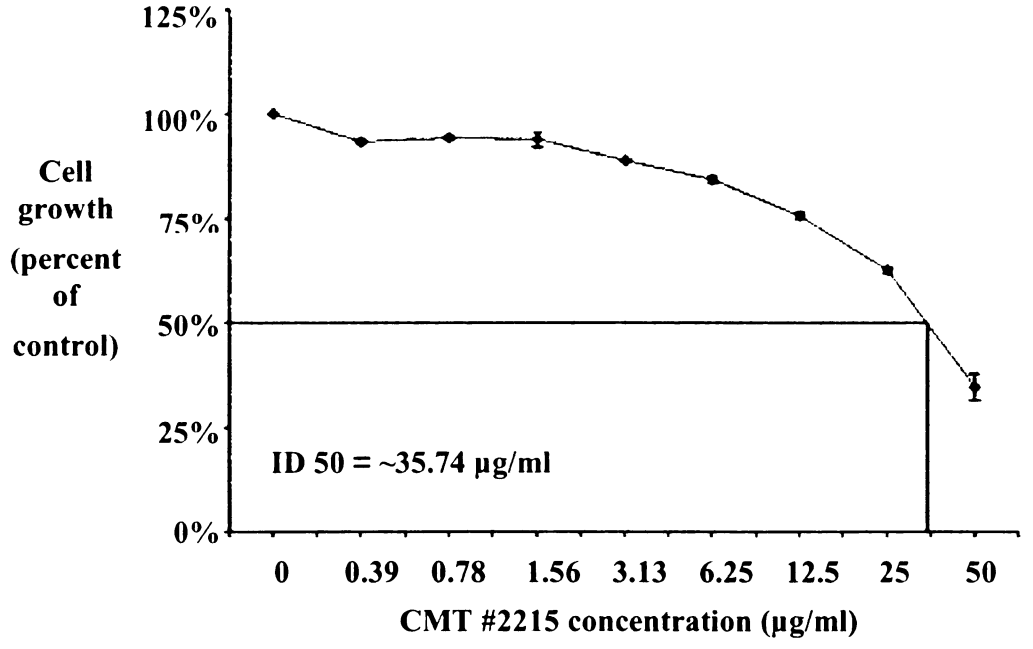

Figure 6.2 The effects of CMT 2215 on anchorage-dependent growth of RWPE2-W99 cells. Cells were plated in 96-well plates at a density of 10,000 cells per well and treated for 5 days. Results are plotted as percent of DMSO-treated control, ±SEM.

In vivo studies

Weight:

Mice with RWPE2-W99 cell xenografts

Animals were weighed weekly. Figure 6.3 shows the average weight of control and CMT 2215-treated mice, injected with RWPE2-W99 cells. The treated mice received CMT 2215 at 0.675 mg/mouse by gavage, daily. Results show that there was no difference in the average weight of mice between the control and treated groups over a 10 week period.

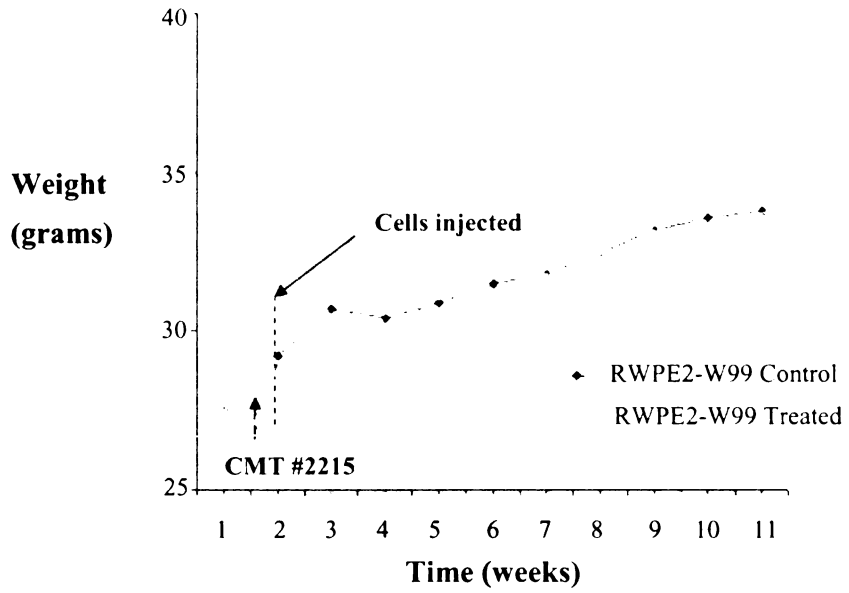

Figure 6.3 Average weight of control and treated mice injected with RWPE2-W99 cells. In the control group, four mice were given vehicle alone (5% sucrose solution in water) by gavage daily for 10 weeks. Four mice in the treated group were given 0.675 mg of CMT 2215/mouse daily by gavage for 10 weeks. The days on which gavage feeding was started, and cells injected, are shown.

Mice with CTPE cell xenografts

Figure 6.4 shows the average weight of control and CMT 2215-treated mice injected with CTPE cells. The treated mice received CMT 2215 at 2.25 mg/mouse by gavage, daily. Results show that the treated mice have a slightly lower average weight as compared to control mice and the shape of the curves at 10 weeks suggests a divergence in weight.

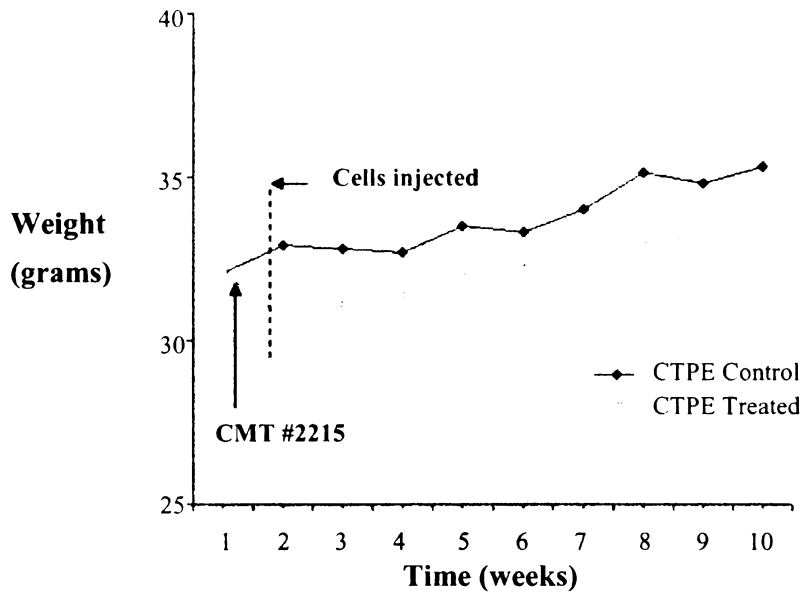

Figure 6.4 Average weight of control and treated mice injected with CTPE cells. In the control group, three mice were given vehicle alone (5% sucrose solution in water) by gavage daily for 10 weeks. Three mice in the treated group were given 2.25 mg of CMT 2215/mouse daily by gavage for 10 weeks. The days on which gavage feeding was started, and cells injected, are shown.

Tumor development:

RWPE2-W99 cells

Figure 6.5a shows tumors in mice injected with RWPE2-W99 cells. Mice in Figure 6.5a are controls that were given a 5% sucrose solution. Mice treated with CMT 2215 were given a daily dose of 0.675 mg/mouse by gavage. Tumor measurements show an average tumor volume of 3.2 cc for the RWPE2-W99 controls and 1.8 cc for the CMT 2215- treated mice that received a daily dose of 0.675 mg/mouse. These preliminary results suggest that using the slow growing RWPE2-W99 model, treatment with CMT 2215 caused a decrease in tumor volume. The average tumor size from treated animals was approximately half the average size of tumors from the controls.

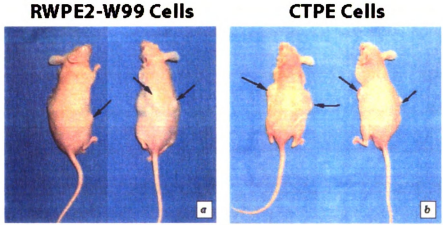

Figure 6.5 Nude mice (strain NCRNU-M male, homozygotes, ~8 weeks old from Taconic farms, Germantown, NY) were bilaterally injected subcutaneously with 250 µl of a cell suspension in Matrigel (cells:Matrigel volume 1:1) containing 1 million cells. Figure 6.5a shows mice given injections of RWPE2-W99 cells. Figure 6.5b shows mice given injections of CTPE cells. Mice were sacrificed 10 weeks later. These mice were fed 300 µl of a 5% sucrose solution by gavage starting 3 days prior to cell injection. Gavage feeding was performed daily for 10 weeks. Arrows point to tumors.

CTPE cells

Figure 6.5b shows tumors in mice injected with CTPE cells. Mice in Figure 6.5b are controls that were given a 5% sucrose solution. Mice treated with CMT 2215 were given a daily dose of 2.25 mg/mouse by gavage. Tumor measurements show an average tumor volume of 6.6 cc for the CTPE controls and 8 cc for the CMT 2215-treated mice. These preliminary results suggest that using the fast growing and invasive CTPE model, treatment with CMT 2215 did not show an effect on average tumor volume. It should be noted that in the CTPE experiment, only three mice per group were used.

Histology:

Histology of the RWPE2-W99 tumors in control mice

The RWPE2-W99 tumors are slow growing. It is possible that for this reason, the test agent may have shown a greater effect on tumor volume than on the fast growing CTPE tumors. Figure 6.6 shows RWPE2-W99 tumors in control mice. Figure 6.6a shows a subcutaneous tumor. Under the skin, the tumor margin appears to be well defined. Figure 6.6b shows the interface between the adipose tissue and the tumor with clear margins, and does not show invasion at this site. It is possible that if the animals are maintained for longer than 10 weeks, one may see invasion and metastasis. Figure 6.6c shows tumor histology at a higher magnification. Figure 6.6d shows skeletal muscle cells amongst tumor cells.

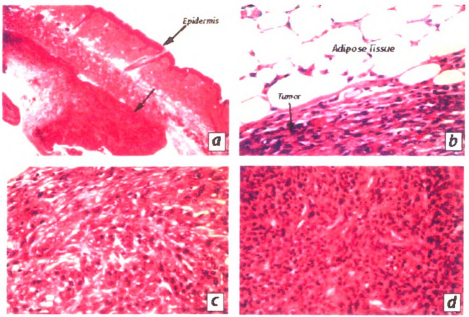

Figure 6.6 Histology of the RWPE2-W99 tumors in control mice: Figure 6.6a shows a subcutaneous tumor (arrow). Under the skin, the tumor margin appears to be well defined and separate from the skin. Figure 6.6b shows tumor:adipose tissue interface with clear margins, and the tumor does not show invasion at this site. It is possible that if the animals are maintained for longer than 10 weeks, one may see invasion and metastasis. Figure 6.6c shows tumor histology at a higher magnification. Figure 6.6d shows skeletal muscle cells amongst tumor cells. H & E stain.

Histology of the RWPE2-W99 tumors in CMT-treated mice

Figure 6.7 shows RWPE2-W99 tumors in CMT 2215-treated mice. Figure 6.7a shows an area of the tumor that appears similar to the control tumor. Figure 6.7b shows a representative area with many vacuolated cells. Figure 6.7c shows squamous metaplasia. There are also areas that show large lymphocytic infiltration (Figure 6.7d). Many areas showed what appeared to be apoptotic cells (Figure 6.7e). Such changes were not seen as frequently in the control tumors.

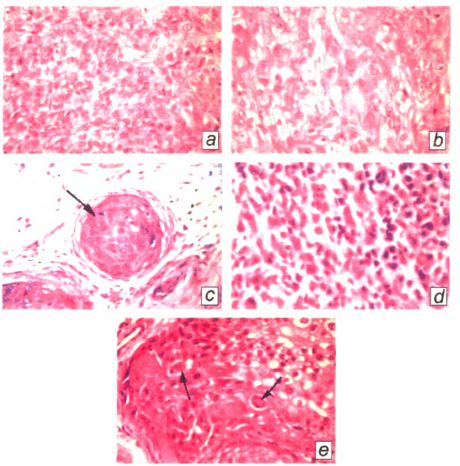

Figure 6.7 Histology of the RWPE2-W99 tumors in CMT-treated mice. Figure 6.7a shows an area of the tumor that does not appear to show any difference from the control tumor. Figure 6.7b shows a representative area with many vacuolated cells. Figure 6.7c shows (arrow) squamous metaplasia. There are also areas that show large lymphocytic infiltration (dark staining nuclei) (Figure 6.7d). Many areas showed what appear to be apoptotic cells (arrows) (Figure 6.7e). Such changes were not seen as frequently in the control tumors. H & E stain.

Histology of the CTPE tumors in control mice

The CTPE tumors are rapidly growing, invasive tumors and invasion can be seen at the 10 week experimental period (Figure 6.8). Figures 6.8a shows a subcutaneous tumor showing invasion into the sub-epidermal layer. The tumor does not have clear cut

margins as can be seen in Figure 6.8b. Figures 6.8c and 6.8d show that the tumor cells are intermingled with skeletal muscle (Figure 6.8c) and fat cells (Figure 6.8d). The tumor cell population is very heterogeneous with considerable variation in cell size (Figure 6.8e).

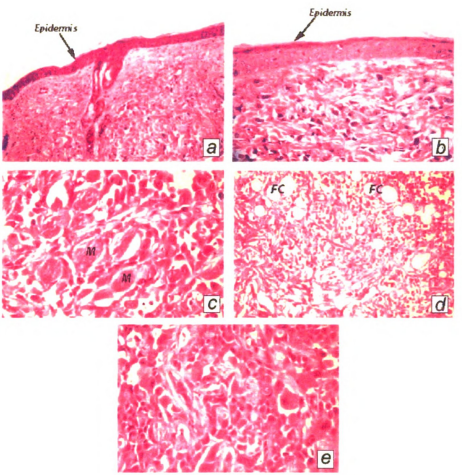

Figure 6.8 Histology of CTPE tumors in control mice. The CTPE tumors are rapidly growing, invasive tumors and invasion was observed at the 10 week experimental period. Figures 6.8a shows a subcutaneous tumor with invasion into the sub-epidermal layer. The tumor has infiltrated into the dermis and does not have clear cut margins as can be seen in Figure 6.8b. Figures 6.8c and 6.8d show that the tumor cells are intermingled with skeletal muscle (M) (Figure 6.8c) and fat cells (FC) (Figure 6.8d). The tumor cell population is very heterogeneous with considerable variation in cell size (Figure 6.8e). H & E stain.

Histology of the CTPE tumors in CMT-treated mice

Figure 6.9 shows some features seen in CMT-treated CTPE tumors. A tumor with undifferentiated characteristics, shown in Figure 6.9a, suggests the aggressive nature of CTPE tumors. Invasion into skeletal muscle is seen in Figure 6.9b. Cells, which appear to be undergoing apoptosis, are seen in Figures 6.9c and 6.9d. Such cells were not seen as frequently in the control CTPE tumors. Areas showing lymphocytic infiltration were seen in several tumors (Figure 6.9e). The appearance of apoptotic cells in tumors from treated mice is an observation that needs to be further examined and may have some significance when assessing the effects of the CMT.

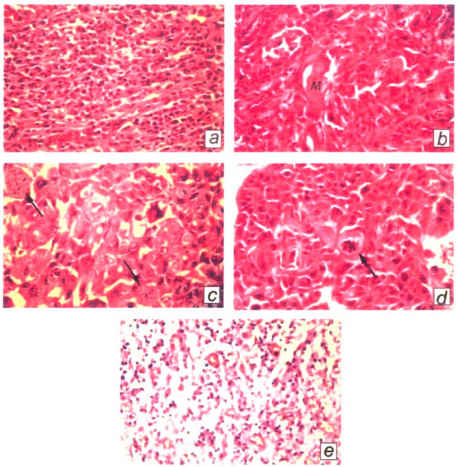

Figure 6.9 Histology of CTPE tumors in CMT-treated mice. This figure shows some features observed in CMT-treated CTPE tumors. A tumor with undifferentiated characteristics shown in Figure 6.9a suggests the aggressive nature of CTPE tumors. Invasion into skeletal muscle (M) is seen in Figure 6.9b. Cells which appear to be undergoing apoptosis are shown (arrows) in Figures 6.9c and 6.9d. Such cells were not seen as frequently in the control CTPE tumors. Areas with lymphocytic infiltration were observed in several tumors (Figure 6.9e). H & E stain.

Histology of CTPE tumor metastasis to the lung

One control mouse (1/3) showed metastasis to the lung (Figure 6.10). Figure 6.10a shows a normal area of the lung. Figure 6.10b and 6.10c are low magnification pictures of the lung showing metastatic tumors. Figure 6.10d is a higher magnification

picture of the lung showing lung tissue:tumor interface. The lung tissue has the alveoli represented by clear spaces against which the tumor tissue has a solid appearance. One treated mouse (1/3) also showed tumor adhering to the lung.

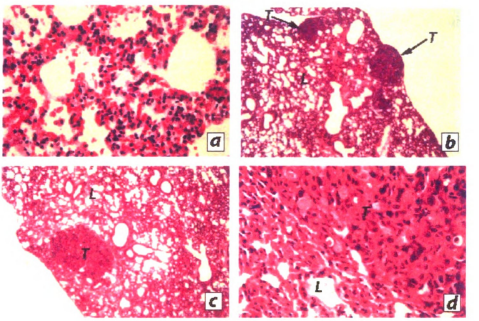

Figure 6.10 Histology of the normal lung and of CTPE tumor metastasis to the lung. Figure 6.10a shows a normal area of the lung. One of the control mice (1/3) showed metastasis to the lung. Figures 6.10b and 6.10c are low magnification picture of the lung (L) showing metastatic tumors (T). Figure 6.10d is a higher magnification picture of the lung (L) showing lung tissue:tumor (T) interface. The lung tissue has the alveoli represented by clear spaces against which the tumor tissue has a solid appearance. H & E stain.

Discussion

This study was conducted primarily to develop methods for conducting *in vivo* experiments using CMTs. The treatment groups are very small, hence, the results are suggestive, and should be considered as such. Eight mice were given subcutaneous

injections of RWPE2-W99 cells and six were given subcutaneous injections of CTPE cells. Half of the mice given subcutaneous injections for each cell line were treated with CMT 2215 and the other half were treated with 5% sucrose daily by gavage for 10 weeks.

The preliminary results suggest that in the slow growing RWPE2-W99 model, treatment with CMT 2215 (2.25 mg/ml) caused a decrease in tumor volume. The average tumor size from treated animals was approximately half the average size of tumors from the controls. Metastasis was not observed in any of the mice given subcutaneous injections of RWPE2-W99 cells. In contrast to RWPE2-W99, tumors produced in control mice by CTPE cells following subcutaneous injection were ~2-fold larger. Despite the fact that mice with CTPE tumors were given a high-dose (7.5 mg/ml) of CMT 2215, tumor measurements show an average tumor volume of 6.6 cc for the CTPE controls and 8.0 cc for the CMT 2215-treated mice. Thus, using the fast growing and invasive CTPE model, treatment with CMT 2215 did not show a growth inhibitory effect on average tumor volume. Although CMT 2215 appeared to have no effect on the tumor growth of CTPE cells, the tumors collected from both groups of CMT-treated mice had many sections showing what appeared to be apoptotic cells. Such changes were not seen as frequently in the control tumors. Induction of apoptosis could be one of the mechanisms by which CMTs inhibit tumor growth.

The RWPE2-W99 tumors are slow growing. It is possible that for this reason, the test agent may have shown a greater effect on tumor growth than on the fast growing CTPE tumors. On the other hand, studies have confirmed the highly invasive and metastatic behavior of CTPE cells *in vivo* (Achanzar et al., 2001). As a more appropriate model of human prostate cancer, the RWPE2-W99 cell line, which is slow growing, was

selected to conduct a second study in nude mice to test the effects of two other chemically modified tetracyclines, CMT 2137 and CMT 2147 (see Chapter 7).

Acknowledgements

Chemically modified tetracycline 2215 was provided by Tetragenex Pharmaceuticals, Inc., Park Ridge, NJ. Suppport for this project by Tetragenex is acknowledged.

Literature cited

Achanzar, W.E., Lamar, P.C., Tokar, E.J., Rivette, A.S., Bello-DeOcampo, D., Prozialeck, W.C., Webber, M.M. and Waalkes, M.P.: Human prostate cell lines mimic heterogeneity of cadherin expression in human prostate cancer. UroOncology 4:15-25, 2004.

Achanzar, W.E., Diwan, B.A., Liu, J., Quader, S.T., Webber, M.M. and Waalkes, M.P.: Cadmium-induced malignant transformation of human prostate epithelial cells. Cancer Research 61:455-458, 2001.

Bello, D., Webber, M.M., Kleinman, H.K., Wartinger, D.D., and Rhim, J.S.: Androgen responsive adult human prostatic epithelial cell lines immortalized by human papillomavirus 18. Carcinogenesis 18:1215-1223, 1997.

Nemeth, J.A., Harb, J.F., Barroso, Jr., U., He, Z., Grignon, D.J. and Cher, M.L.: Severe combined immunodeficient-hu model of human prostate cancer metastasis. Cancer Research 59:1987-1993, 1999.

Webber, M.M., Bello, D., Kleinman, H.K., and Hoffman, M.P.: Acinar differentiation in non-malignant immortalized human prostatic cells and its loss by malignant cells. Carcinogenesis 18:1225-1231, 1997a.

Webber, M.M., Bello, D., and Quader, S.: Immortalized and tumorigenic adult human prostatic epithelial cell lines. Characteristics and applications. Part 2. Tumorigenic cell lines. The Prostate 30:58-64, 1997b.

Webber, M.M., Quader, S., Kleinman, H.K., Bello-DeOcampo, D., Storto, P.D., Bice, G., de Mendonca-Calaca, W., and Williams, D.E.: An *in vitro/in vivo* model of human cell lines for prostate carcinogenesis and tumor progression. The Prostate 47:1-13, 2001.

CHAPTER SEVEN

THE EFFECTS OF CMT 2137 AND 2147 ON TUMOR GROWTH USING THE TUMORIGENIC RWPE2-W99 HUMAN PROSTATE CELL LINE

Abstract

Chemically modified tetracyclines (CMTs) may be effective chemotherapeutic agents for prostate cancer. Results obtained from *in vitro* and *in vivo* studies, in addition to a phase I clinical trial, suggest a potential use of CMTs as an oral, nontoxic drug to treat metastatic prostate cancer and other cancers. Additional screening of CMTs may lead to the identification of compounds which show greater efficacy in the treatment of prostate cancer. Thus, in this chapter, I examine the ability of two new CMTs, CMT 2137 and 2147, to inhibit the growth of a human prostate epithelial cell line, RWPE2-W99 both *in vitro*, and as a xenograft *in vivo*. Treatment of RWPE2-W99 cells grown in monolayer cultures with 2137 (50 μg/ml) caused ~25% growth inhibition, while treatment with 2147 (50 μg/ml) caused ~60% growth inhibition. *In vivo*, the ability of CMT 2137 and 2147, to reduce the size and number of tumors produced after subcutaneous injection of RWPE2-W99 cells in immune-suppressed mice, was examined. The mice treated with the test agents had a higher percentage of tumors in the small category (11-110 mm^3) as compared to the control mice. Based on the results of these *in vitro* and *in vivo* studies, both CMT 2137 and 2147 demonstrate potential as anticancer drugs and warrant further study.

Keywords

Chemically modified tetracycline, gavage, prostate cancer, subcutaneous, tumor

Introduction

Chemically modified tetracyclines (CMTs) have been shown to inhibit cell proliferation and Matrigel invasion of several prostate cancer cell lines, as well as, cause a decrease in matrix metalloproteinase production and activity *in vitro* (Lokeshwar, 1999; Lokeshwar et al., 2002). In male Copenhagen rats, given subcutaneous injection of MAT LyLu cells, treatment with CMT-3 by gavage inhibited tumor incidence and reduced the tumor growth rate (Lokeshwar et al., 1999). In Copenhagen rats given an intravenous injection of MAT LyLu cells, treatment with CMT-3 decreased the frequency of tumor metastasis to soft or skeletal tissue and also resulted in an increase in survival (Lokeshwar, 1999; Selzer et al., 1999). Other CMTs are now being extensively investigated because of their increased efficacy as compared to their natural derivatives.

Based on the pilot study with CMT 2215 (see chapter 6), a protocol was developed to conduct a study in nude mice to test the effects of two other chemically modified tetracyclines, CMT 2137 and CMT 2147. These two CMTs were first tested for their effects on the growth of RWPE2-W99 cells *in vitro* and were shown to inhibit cell proliferation. The tumorigenic human prostate epithelial cell line RWPE2-W99 (Bello et al., 1997; Webber et al., 1997a) was used to examine the potential of CMTs *in vitro* and *in vivo*. Using RWPE2-W99 cells to produce tumors in immune-deficient mice is a relevant model because it mimics the majority of human prostate cancers which are slow growing (Webber et al., 1997b; Webber et al., 2001).

The following describes the process by which the RWPE2-W99 cell line was developed. Human prostate epithelial cells were derived from the peripheral zone of a normal human prostate and immortalized with a single copy of human papilloma virus-18

(HPV-18) DNA to give rise to the RWPE-1 cell line (Bello et al., 1997; Webber et al., 1997a). RWPE-1 cells were then transformed by *v*-Ki-*ras*, giving rise to the RWPE-2 cell line (Bello et al., 1997; Webber et al., 1997a). The transformed RWPE-2 cells are tumorigenic and can grow in soft agar in an anchorage-independent manner. In order to select cells that showed high Ki-*ras* expression, RWPE-2 cells were grown in agar and colonies were screened for Ki-*ras* expression. One of these colonies was expanded and gave rise to the RWPE2-W99 cell line. Using the RWPE2-W99 cell line, the objectives of this study were to determine the ability of CMT 2137 and 2147 to inhibit cell growth *in vitro* and tumor growth *in vivo* using RWPE2-W99 cells which form slow growing tumors when injected into immune-suppressed mice.

Materials & Methods:

In vitro studies

Cell culture general:

RWPE2-W99 cells were grown in complete keratinocyte serum-free medium (KSFM) containing 50 μg/ml bovine pituitary extract (BPE), 5 ng/ml epidermal growth factor (EGF) and 1X antibiotic/antimycotic solution. Cultures were maintained at 37^0C in a humidified atmosphere containing 5% CO_2 and subcultured weekly.

Dose response using a microplate assay:

RWPE2-W99 cells were plated, six wells per treatment, in complete keratinocyte serum-free medium (K-SFM) containing 50 μg/ml bovine pituitary extract (BPE) and 5 ng/ml epidermal growth factor (EGF), at 10,000 cells/well in 96-well plates and

allowed to attach for 48 h at which time medium was changed to medium containing varying concentrations of the test agent. The test agents, CMT 2137 and 2147 were dissolved in DMSO. The final concentration of the DMSO vehicle in the culture medium was 0.1%. Treatment groups consisted of untreated control, vehicle-treated control, CMT 2137 or CMT 2147 at doubling dilutions from 0.39 μg/ml to 50 μg/ml. Cells received fresh CMT treatment every 48 h for 5 days, receiving a total of three treatments. At the end of the 5-day treatment, plates were processed using the MTT [3-(4,5-dimethyl thiazol-2-yl)-2,5-diphenyl tetrazolium bromide) assay as described previously (Webber et al., 2001). Two or three replicate experiments were conducted for each test agent.

In vivo studies

Mice:

Eight week old, albino male mice, ***nu/nu*** strain (NSWNU-M, homozygotes) (Taconic farms, Inc., Germantown, NY), were used in this study. This strain of mice is the standard athymic model for the National Cancer Institute (NCI) studies as well as many pharmaceutical and institutional oncology screening programs. Mice were socialized for five days after arrival from Taconic. The mice were provided with autoclaved tap water to drink and fed a complete, irradiated diet (Teklad 7904, manufactured by Harlan, Madison, WI). For enrichment purposes the mice were given nestlettes once a week. To ensure the health of the mice, their physical condition and food and water intake were examined daily.

Animal maintenance:

The mice were maintained at the University Laboratory Animal Resources (ULAR) facility in a clean room dedicated for this experiment. The room was maintained at 72^0 -74^0 F and on a twelve-hour light-twelve hour dark schedule. The mice were housed individually in autoclaved cages on paper chip bedding in a laminar flow rack. The animal room and laminar flow cage rack, where the mouse cages are color-coded for the three groups of mice, are shown in Figure 7.1.

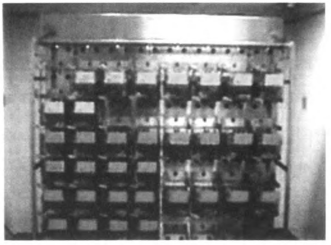

Figure 7.1 Laminar flow mouse cage rack. The cages were color-coded for the three groups of mice; yellow = controls; blue = 2137; red: 2147. Mice were housed, one mouse per cage, in autoclaved cages, and provided with autoclaved drinking water and irradiated food. The control mice were fed 300 µl of a 5% sucrose solution in water by gavage. The treated mice were similarly fed with 1.2 mg of 2137 or 2147/mouse in 300 µl of a 5% sucrose solution starting 3 days prior to cell injection. Gavage feeding was performed daily for a total of 11 weeks.

Investigators and caretakers were required to wear the following upon entrance to the room: bonnet, mask, booties, sterile gloves, and sterile gown. All procedures involving mice were performed in a laminar flow hood. The drug was administered to mice by gavage feeding. Gavage feeding was done in the laminar flow hood under yellow light to protect the CMTs. Cell injections, daily feeding by gavage using a sterile feeding tube weighing, and cage changes took place in a laminar flow hood. This study was conducted with the approval of the All University Committee on Animal Use and Care (AUCAUC) and all guidelines were followed.

Sucrose solution:

The control mice were fed 300 µl of a 5% sucrose solution in water by gavage. A 5% sucrose (Sigma, Cat. No. S-5016) solution was prepared in de-ionized water and autoclaved. Aliquots of 2.5 ml/tube were prepared for gavage feeding of mice and stored in a -20^0 C freezer. Gavage feeding was performed daily for a total of 11 weeks. This 5% sucrose solution was also used as the vehicle for CMTs 2137 and 2147.

Drug stock solutions:

Chemically modified tetracycline: CMTs 2137 (Lot No. 14-77-1) and 2147 (Lot No. 14-95-2) were provided by Innapharma Inc/Tetragenex Pharmaceuticals, Inc., Park Ridge, NJ (from RSA Corporation). Test reagents were stored at 4^0 to 6^0 C, and protected from light. The treated mice were fed 300 µl of a 5% sucrose solution by gavage starting 3 days prior to cell injection with 1.2 mg of 2137 or 2147/mouse. Stock solutions containing 4 mg/ml of 2137 or 2147 were prepared in sterile 5% sucrose and

filter-sterilized using a 0.22 μm pore size filter. Aliquots of 2.5 ml in sterile brown glass vials were prepared and stored in a -20^0 C freezer, in boxes to protect from light, until needed. Gavage feeding was performed daily for a total of 11 weeks.

Cells for injections:

A sterile cell suspension of RWPE2-W99 cells was prepared in keratinocyte serum-free basal medium (Bello et al., 1997; Webber et al., 1997a) and mixed with an equal volume of Matrigel (Webber et al., 2001) to obtain four million cells/ml. All steps with Matrigel were performed on ice. The cell suspension was kept on ice and taken to the animal facility. A 1.0 cc syringe with a 25 gauge needle was used to inject 250 μl of the cell suspension containing one million cells per inoculation site. Before the cells were injected, the mice were placed under methoxyflurane anesthesia and swabbed with alcohol at the injection site. The cells were injected subcutaneously and bilaterally on the dorso-lateral side. The mice were kept on a heating pad during the procedure to maintain body temperature.

Experimental groups:

The study involved three groups of mice. Mice were randomly selected and placed in three groups.

Group 1: RWPE2-W99 controls:

Starting on day zero, ten mice were gavage fed with 300 μl of 5% sucrose solution in water, daily for three days, prior to being injected with RWPE2-W99 cells. After cell

injection, daily gavage feeding with sucrose solution continued for a total of 11 weeks. Fresh vials of sucrose were used each day.

Group 2: RWPE2-W99 CMT 2137:

Twelve mice were gavage fed, each mouse receiving 300 µl of 5% sucrose solution in water containing 1.2 mg of CMT 2137, daily for three days prior to being injected with RWPE2-W99 cells. Daily gavage feeding, at the same dose, continued after cell injection, for a total of 11 weeks from day zero. Fresh vials of the test agent solution were used each day. Each day's supply was thawed just before use and the vials were kept in cardboard boxes to prevent light exposure.

Group 3: RWPE2-W99 CMT 2147:

Twelve mice were gavage fed, each mouse receiving 300 µl of 5% sucrose solution in water containing 1.2 mg of CMT 2147 daily for three days prior to being injected with RWPE2-W99 cells. Daily gavage feeding, at the same dose, continued after cell injection, for a total of 11 weeks from day zero. Fresh vials of the test agent solution were used each day. Each day's supply was thawed just before use and the vials were kept in cardboard boxes to prevent light exposure.

Animal weights:

Animals were weighed at the start of the experiment and then weekly until the end of the experiment, and the weights were recorded. Mice were given a physical

examination daily, and their food and water intake were also checked daily. The average weight of mice on day zero was 28.2 g.

Tumor size and histology:

When tumors became palpable, their size was measured periodically in two dimensions (length and width), using digital calipers, and all measurements were recorded. Tumors were measured and photographed at the termination of the experiment at 11 weeks. Tumor volume (TV) was calculated using the formula: $TV = a X b^2/2$ where *a* is the longest dimension and *b* is the width (Nemeth et al., 1999). Tumors were dissected, fixed in 10% buffered formalin and processed for histology. Tumor sections were cut at 5μm thickness. In addition, abdominal wall, liver and lungs were examined for visible tumor metastasis.

Results

In vitro studies

Anchorage–dependent growth

In order to examine the effects of CMT 2137 and 2147, concentrations from 0.39 to 50 μg/ml were tested using the RWPE2-W99 cell line. Two or three independent experiments, using six replicate wells/treatment, were conducted. Results shown in Figure 7.2 represent the average of three experiments. From these data, it is evident that RWPE2-W99 cells show a dose-dependent inhibition of growth at concentrations higher than 25 and 3.13 μg/ml for CMT 2137 and 2147, respectively. Approximately 25% inhibition was observed at 50 μg/ml for CMT 2137 and 60% growth inhibition at

50 µg/ml for CMT 2147. The ID_{50} for 2147 was ~31.26 µg/ml when cells were plated at 10,000 cells/well.

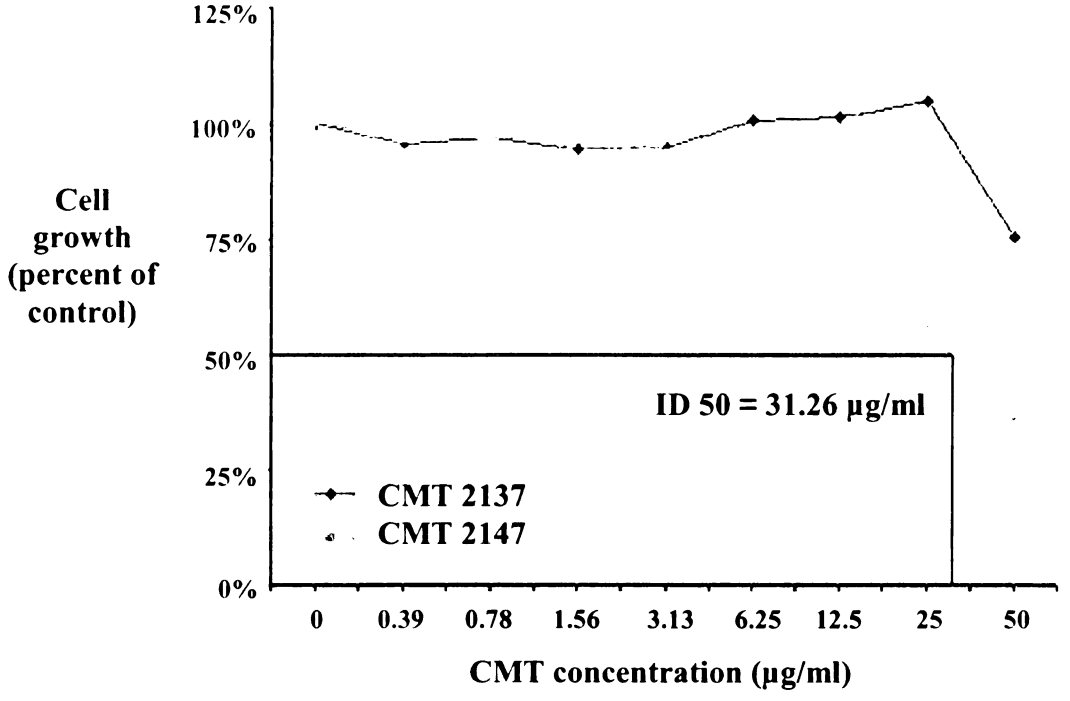

Figure 7.2 The effects of CMT 2137 or CMT 2147 on anchorage dependent growth of RWPE2-W99 cells. Cells were plated in 96-well plates at a density of 10,000 cells per well and treated for 5 days. Results are plotted as percent of DMSO-treated control, ±SEM.

In vivo studies
Animal weight:

Animals were weighed weekly. Figure 7.3 shows the average weight of control mice and those treated with CMT 2137 or 2147. The treated mice received 1.2 mg of the test agent daily for 11 weeks. Results show that there was no apparent difference in the average weight of mice between the control and treated groups up to about 9 weeks. At 11

weeks, the control mice weighed 32.3 g, the 2137-treated mice weighed 32.7g, while the 2147-treated mice weighed 31.6g.

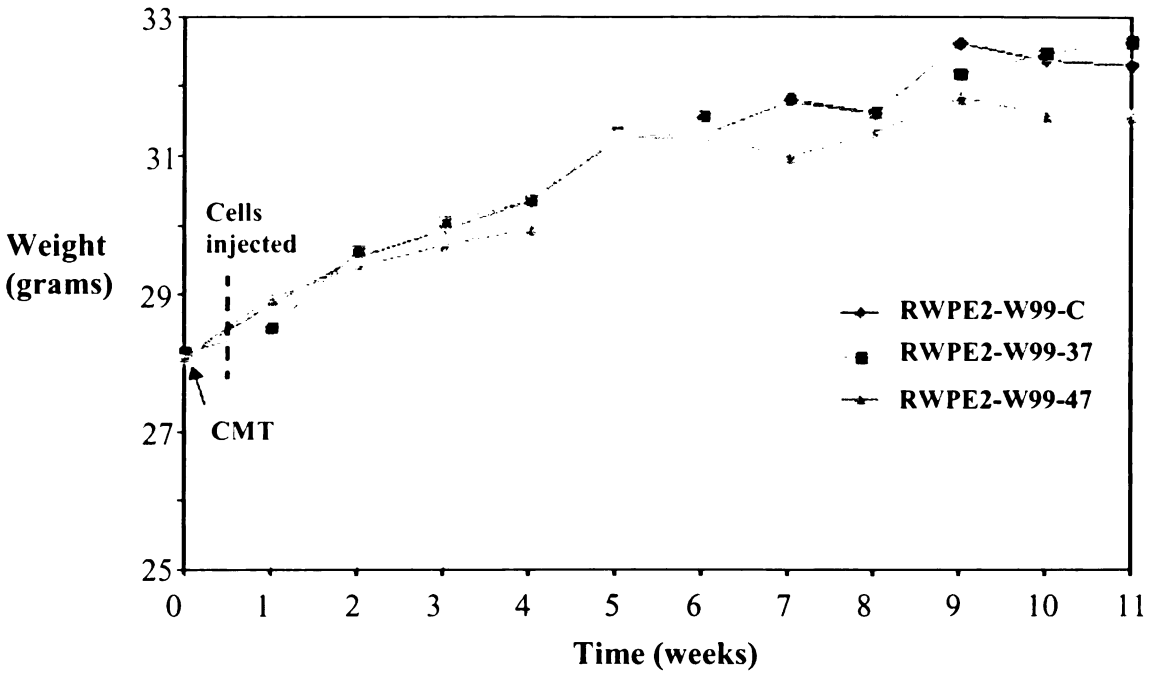

Figure 7.3 Average weight of mice injected with RWPE2-W99 cells. This graph shows weight gain, over time, in the control mice given vehicle alone (5% sucrose solution in water) by gavage daily for 11 weeks, and in the mice gavage-fed with 1.2 mg/mouse of 2137 or 2147 in 5% sucrose solution. Mice were weighed at time zero and then weekly for 11 weeks. Beginning at time zero, mice were gavage-fed for three days prior to the injection of RWPE2-W99 human prostate tumorigenic cell line. The day on which gavage feeding was started (labeled as CMT), and the day when the cells were injected, are shown. RWPE2-W99-C = control; RWPE2-W99-37 = mice on 2137; RWPE2-W99-47 = mice on 2147.

Tumor volume:

Tumors were measured at the time of sacrifice. Tumor measurement results are shown in Tables 7.1, 7.2 and 7.3 and Figure 7.4. Table 7.1 shows the relationship between tumor volume and percent of tumors having the indicated size. Tumor volumes

were divided into four groups. There is considerable variation in tumor size within each group. The size interval in the first group (11-110 mm^3) is smaller than the other groups. This was done to enable recording of the smallest tumors. While only 8% of the tumors in control mice were in the smallest tumor volume category (11-110 mm^3), 34% and 21% of the tumors in mice treated with 2137 or 2147, respectively, were in the smallest tumor volume category (Figure 7.4). Furthermore, while 25% of the tumors in the control mice were in the largest tumor volume category, none or only 5% (one tumor) of the tumors were in the largest category in 2137 or 2147 treated mice, respectively. These data are summarized in Table 7.2. If the tumors of the two small categories are combined, 66% of the control tumors fall within this group, while 77% and 84% of the tumors fall in this group for 2137 or 2147 treated mice, respectively. Similarly, when the two large categories are combined, 34% of control, 23% of 2137 and 16% of 2147-treated mice, fall into the large tumor volume category. In Table 7.3, tumors have been grouped, according to volume into nine groups which again show that the mice treated with the test agent have no or very few tumors in the largest categories while 25% of the tumors in the control mice are in the largest categories. Representative tumors of varying sizes from control and treated mice are shown in Figure 7.5. These results suggest that the two test agents caused a decrease in tumor size.

Table 7.1 This table shows the relationship between tumor volume, following injection of RWPE2-W99 cells, and percentage of tumors having the indicated size. Tumor volumes have been divided into four groups. The average tumor volume, range, and percent of tumors having the indicated size in each group are shown for control mice, and mice treated with 2137 or 2147.

Tumor Volume (mm^3)	Control			2137			2147		
	Average	Range	% of tumors	Average	Range	% of tumors	Average	Range	% of tumors
11-110	24	24	8%	41	12-73	34%	82	72-92	21%
111-510	196	116-298	58%	262	125-489	43%	242	127-451	63%
511-910	519	519	9%	728	663-825	23%	691	628-754	11%
>911	1214	1118-1272	25%	0	0	0%	1462	1462	5%

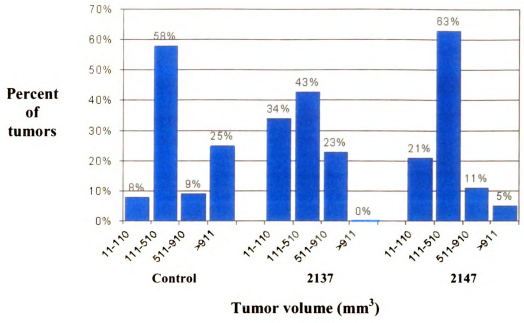

Figure 7.4 Relationship between tumor volume, following injection of RWPE2-W99 cells, and percentage of tumors having the indicated tumor size. This is a graphic representation of the data shown in Table 7.1. Tumor volumes have been divided into four groups. The effects of treatment with 2137 or 2147 are evident in this bar graph. Results indicate that overall, the treatment groups have a larger percentage of small tumors as compared to the control.

Table 7.2 This table is a summary of Table 7.1., comparing tumor volumes of RWPE2-W99 cells in control mice and mice treated with 2137 or 2147. Data are shown as percent of tumors in each group having the indicated tumor volume.

Tumor volume (mm^3)	**% of tumors having the indicated size**		
	Control	**2137**	**2147**
11-110	8	34	21
111-510	58	43	63
511-910	9	23	11
>911	25	0	5

Table 7.3 In this table tumor volumes resulting from injection of RWPE2-W99 cells have been divided into nine groups which are arranged from the smallest to the largest. Data are shown as percent of tumors in each group having the indicated tumor volume.

Tumor Volume (mm^3)	**% of mice with tumors with the indicated size**		
	Control	**2137**	**2147**
11-60	8	24	0
61-110	0	10	21
111-310	58	33	58
311-510	0	10	5
511-710	9	9	6
711-910	0	14	5
911-1110	0	0	0
1111-1310	25	0	0
1311-1510	0	0	5

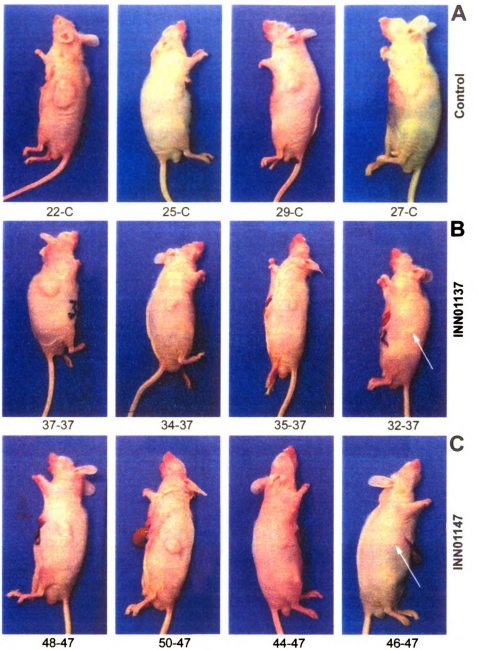

Figure 7.5 Nude mice (NSWNU-M *nu/nu* strain) were bilaterally injected with 250 µl of a cell suspension in Matrigel (cell: Matrigel volume, 1:1) containing one million RWPE2-W99 cells. Mice were sacrificed 11 weeks later. This figures shows (from left to right) four representative mice with tumors from each of the three groups. A. Control mice (22-C, 25-C, 29-C, and 27-C); B. 2137-treated mice (37-37, 34-37, 35-37, and 32-37); C. 2147-treated mice (48-47, 50-47, 44-47, and 46-47); arrows point to small tumors.

Histology:

A histological examination of the tumors shows that RWPE2-W99 tumors are of an undifferentiated type (Figure 7.6). RWPE2-W99 produces slow growing tumors which, after 11 weeks, did not show marked signs of invasion into the surrounding tissue at this time. The tumors show clear boundaries between the tumor and the adjacent connective tissue, fat or muscle. There were no obvious signs of visible metastatic tumors. However, it is possible that if the mice were maintained for a longer period, signs of invasion and metastasis may become apparent.

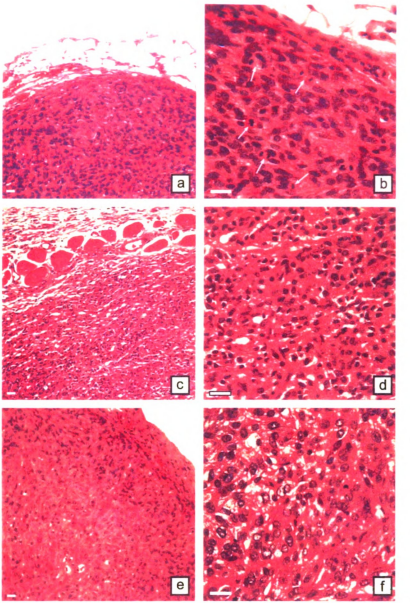

Figure 7.6 H & E-stained sections showing tumor histology. Figures 7.6a and 7.6b: Histology of the RWPE2-W99 tumors in control mice at low (Figure 7.6a) and high magnification (Figure 7.6b). The tumor appears to be an undifferentiated tumor with clear margins at the interface with connective and adipose tissue. In Figure 7.6b, many mitotic figures can be seen (arrows). Figures 7.6c and 7.6d show a tumor from a mouse treated with 2137. Examination of the tumor at higher magnification (Figure 7.6d) shows little evidence of cells in mitosis, in contrast to the control tumors. Figures 7.6e and 7.6f show a tumor from a mouse treated with 2147. Examination of the tumor at higher magnification (Figure 7.6f) again shows little evidence of cells in mitosis, in contrast to the control tumors. Bar = 10 μm.

A preliminary examination of the histological slides suggests that while the control tumors have an abundance of mitotic figures (Figure 7.6b), mitotic figures were seen less frequently in tumors from treated mice. Further evaluation would be required to substantiate this observation. However, this observation appears to be consistent with the smaller tumor size in treated mice.

Discussion:

Because mortality from some common cancers, such as, lung, breast and prostate, using chemotherapy, has not significantly decreased, it is necessary and sensible to explore other strategies to treat cancer (Sporn and Suh, 2000; Quader et al., 2001). The main cause of death among prostate cancer patients is metastasis and bone is one of the most frequent sites to support metastatic tumors. Members of the tetracycline family of antibiotics have potential treatment value for bone metastasis; they inhibit cancer cell proliferation and they are also potent MMP inhibitors (Duivenvoorden et al., 2002). In rats given intravenous cell injection of the Dunning MAT LyLu tumor cells, daily treatment by gavage with CMT-3 resulted in both an increase in survival and a decrease in skeletal and soft tissue metastasis (Selzer et al., 1999). Members of the tetracycline family not only offer potential for the treatment of metastatic cancer, but also primary tumor growth. In a MAT LyLu model of prostate cancer, treatment of rats with CMT-3 by gavage decreased tumor incidence and growth (Lokeshwar, 1999). The growth inhibitory nature of CMTs, has been demonstrated against BPH-1, LNCaP, DU145, PC-3, TSU-Pr1 and MAT LyLu cell lines (Lokeshwar et al., 1998; Lokeshwar, 1999). *In*

vitro, CMTs have also been shown to induce dose- and time-dependent apoptosis in several tumor cell lines (Lokeshwar et al., 1998; Lokeshwar, 1999).

The mode of action of CMTs is often related to their capacity to bind the critical Zn^{2+} ions in the active centers of the MMP molecules, thus inhibiting MMP activity (Golub et al., 1992; Sorsa et al., 1998). CMT-3 has been shown to reduce invasive activity of tumor cells by specifically inhibiting MMPs without significantly inhibiting their natural inhibitors (Lokeshwar et al., 2002). Matrix metalloproteinases have been repeatedly implicated in tumor cell invasion and metastasis. However, recent evidence suggests that MMPs also play an important role in the establishment and growth of the primary tumor (Chambers and Matrisian, 1997). This is supported by experiments using other MMP inhibitors to block MMP activity. These matrix metalloproteinase inhibitors caused significant inhibition of primary tumor growth both at the subcutaneous and orthotopic site in animal models (Conway et al., 1996; Lokeshwar, 1999; Wang et al., 1994). Similarly in this study, treatment of mice bearing subcutaneous tumors with a CMT, an MMP inhibitor, caused a decrease in tumor size.

Consistent with the ability of CMT 2137 and 2147 to inhibit anchorage-dependent growth of RWPE2-W99 *in vitro*, they were also shown to cause a decrease in tumor size *in vivo*. The mice treated with the test agents had a higher percentage of tumors in the small category (11-510 mm^3) and a lower percentage of tumors in the large category (>500 mm^3) as compared to the control mice. It is interesting to note that, in addition to the smaller tumor size in treated mice, tumor sections from the control mice showed a large number of mitotic figures. Mitoses appeared to be less frequent in tumor sections

from mice treated with the test agents. The observed cellular effects and the mechanism by which the test agents exert their effects on tumor growth need to be further explored.

MMPs have been shown to play an important role in supporting the growth of primary tumors, thus, if CMTs have a negative effect on MMP production, as do other members of the tetracycline family, then this could explain the small tumor size and decreased mitoses observed in mice treated with CMT 2137 and 2147. Although, CMT 2147 appears to be more effective at inhibiting the growth of RWPE2-W99 in cell cultures than CMT 2137, both CMT 2137 and 2147 were shown to inhibit tumor growth *in vivo*. Therefore, CMT 2137 and 2147 demonstrate potential as anticancer drugs and warrant further screening.

Acknowledgements

Chemically modified tetracyclines, CMT 2137 and 2147, were provided by Tetragenex Pharmaceuticals, Inc., Park Ridge, NJ. Suppport for this project by Tetragenex is acknowledged.

Literature cited

Bello, D., Webber, M.M., Kleinman, H.K., Wartinger, D.D., and Rhim, J.S.: Androgen responsive adult human prostatic epithelial cell lines immortalized by human papillomavirus 18. Carcinogenesis 18:1215-1223, 1997.

Chambers, A.F. and Matrisian, L.M.: Changing views of the role of matrix metalloproteinases in metastasis (review). Journal of the National Cancer Institute 89:1260-1270, 1997.

Conway, J.G., Trexler, S.J., Wakefield, J.A., Marron, B.E., Emerson, D.L., Bickett, D.M., Deaton, D.N., Garrison, D., Elder, M., McElroy, A., Willmott, N., Dockerty, A.J.P. and McGeehan, G.M.: Effect of matrix metalloproteinase inhibitors on tumor growth and spontaneous metastasis. Clinical & Experimental Metastasis 14:115-124, 1996.

Duivenvoorden, W.C.M., Popovic, S.V., Lhotak, S., Seidlitz, Hirte, H.W., Tozer, R.G. and Singh, G.: Doxycycline decreases tumor burden in a bone metastasis model of human breast cancer. Cancer Research 62:1588-1591, 2002.

Golub, L.M., Suomalainen, K. and Sorsa, T.: Host modulation by tetracyclines and their chemically-modified non-antimicrobial derivatives. Current Opinions in Dentistry 2:80-90, 1992.

Lokeshwar, B.L., Houston-Clark, H.L., Selzer, M.G., Block, N.L., and Golub, L.M.: Potential application of a chemically modified non-antimicrobial tetracycline (CMT-3) against metastatic prostate cancer. Advances in Dental Research 12:97 -102, 1998.

Lokeshwar, B.L.: MMP inhibition in prostate cancer. Annals New York Academy of Sciences 878:271-289, 1999.

Lokeshwar, B.L., Selzer, M.G., Zhu, B., Block, N.L. and Golub, L.M.: Inhibition of cell proliferation, invasion, tumor growth and metastasis by an oral non-antimicrobial tetracycline analog (COL-3) in a metastatic prostate cancer model. International Journalof Cancer 98:297-309, 2002.

Nemeth, J.A., Harb, J.F., Barroso, Jr., U., He, Z., Grignon, D.J. and Cher, M.L.: Severe combined immunodeficient-hu model of human prostate cancer metastasis. Cancer Research 59:1987-1993, 1999.

Quader, S.T.A., Bello-DeOcampo, D., Williams, D.E., Kleinman, H.K., Webber, M.M.: Evaluation of the chemopreventative potential of retinoids using a novel in vitro human prostate carcinogenesis model. Mutation Research 496:153-161, 2001.

Selzer, M.G., Zhu, B., Block, N.L., and Lokeshwar, B.L.: CMT-3, a chemically modified tetracycline, inhibits bony metastases and delays the development of paraplegia in a rat model of prostate cancer. Annals New York Academy of Sciences 878:678-682, 1999.

Sorsa, T., Ding, Y., Salo, T., Lauhio, A., Teronen, O., Ingman, T., Ohtani, H., Andoh, N., Takeha, S. and Konttinen, Y.T.: Effects of tetracyclines on neutrophil, gingival and salivary collagenases. Annals New York Academy of Science 732:112-131, 1994.

Sorsa, T., Ramamurthy, N.S., Vernillo, A.T., Zhang, X., Konttinen, Y.T., Rifkin, B.R., and Golub, L.M.: Functional sites of chemically-modified tetracyclines: inhibition of the oxidative activation of human neutrophil and chicken osteoclast promatrix metalloproteinase. Journal of Rheumatology 25:975-982, 1998.

Sporn, M.B. and Suh, N.: Chemoprevention of cancer. Carcinogenesis 21:525-530, 2000.

Wang, X., Fu, X., Brown, P.D., Crimmin, M.J. and Hoffman, R.M.: Matrix metalloproteinase inhibitor BB-94 (Batimastat) inhibits human colon tumor growth and spread in a patient like orthotopic model in nude mice. Cancer Research 54:4726-4728, 1994.

Webber, M.M., Bello, D., Kleinman, H.K., and Hoffman, M.P.: Acinar differentiation in non-malignant immortalized human prostatic cells and its loss by malignant cells. Carcinogenesis 18:1225-1231, 1997a.

Webber, M.M., Bello, D., and Quader, S.: Immortalized and tumorigenic adult human prostatic epithelial cell lines. Characteristics and applications. Part 2. Tumorigenic cell lines. The Prostate 30:58-64, 1997b.

Webber, M.M., Quader, S., Kleinman, H.K., Bello-DeOcampo, D., Storto, P.D., Bice, G., de Mendonca-Calaca, W., and Williams, D.E.: An *in vitro/in vivo* model of human cell lines for prostate carcinogenesis and tumor progression. The Prostate 47:1-13, 2001.

CHAPTER EIGHT

SELECTION OF CELL LINES WITH ENHANCED INVASIVE PHENOTYPE FROM XENOGRAFTS OF THE HUMAN PROSTATE CANCER CELL LINE WPE1-NB26

Abstract

Prostate cancer is the second leading cause of death from cancer in American men and metastasis is the main cause of death in prostate cancer patients. In order to better understand the disease and to accelerate development of new therapies, *in vivo* models that reflect different disease stages are needed. A family of cell lines, that mimic multiple steps in cancer development and progression, have been developed in our laboratory. The parent, non-tumorigenic, RWPE-1 cell line was derived by immortalization with human papillomavirus-18 (HPV-18) (Bello et al., 1997; Webber et al., 1997a). Several tumorigenic cell lines, the MNU cell lines, were derived from RWPE-1 by transformation with *N*-methyl-*N*-nitrosourea (MNU) (Webber et al., 1997c). In a tumor progression model, WPE1-NB26 is the most malignant MNU-transformed cell line and it forms metastases in the lungs of nude mice after intravenous injection. Two new cell lines, WPE1-NB26-64 and WPE1-NB26-65, showing more malignant characteristics than the parent WPE1-NB26 cell line, were derived from tumors that resulted from subcutaneous injection of WPE1-NB26 cells into nude mice. The WPE1-NB26-64 and WPE1-NB26-65 cell lines show an increase in anchorage-dependent growth and invasive ability as compared to the parent WPE1-NB26 cells. While the parent WPE1-NB26 cells express barely detectable levels, the new cell lines produce increased levels of matrix metalloproteinase (MMP) MMP-2 and detectable levels of MMP-9. By immunostaining, all three cell lines were positive for cytokeratins Ck5/14 and Ck18. These cell lines, having the same lineage, represent another step in the multi-step process of tumor progression and provide novel and useful cell models for

studies on tumor progression and for drug development for the treatment of prostate cancer.

Keywords

Cell line, metastasis, matrix metalloproteinase, *N*-methyl-*N*-nitrosourea, prostate cancer

Introduction

Prostate cancer is the most common cancer (excluding skin cancer) in men in the United States of America (American Cancer Society, 2004). Prostate cancers show heterogeneity in their composition and diversity in behavior, thus, xenograft models of prostate cancer that reflect different disease stages of prostate cancer are necessary. Xenograft models permit one to directly compare the histopathology and molecular biology of the patient-derived specimen and the resulting xenograft tumor. Xenografts have been widely used in cancer studies and some of their applications include: i) validation and testing the utility of therapeutic agents for clinical trials ii) determination of the influence of the microenvironment on gene expression, growth, and behavior of tumor cells within the prostate and other organ sites and iii) studies on the importance of hormonal status and of androgen-independence in tumor progression and metastasis. The majority of commonly used human prostate cancer cell lines have been derived from biopsies of metastatic prostate cancer and thus, are more appropriate for studies on advanced disease and progression to metastasis (Webber et al., 1996a; Webber et al., 1997b). Therefore, human prostate cancer cell lines that represent early events in carcinogenesis, tumor progression and metastasis, have been developed in our laboratory.

Included in this family of cell lines is the parental, non-tumorigenic, RWPE-1 cell line which serves as a control *in vitro* or as a standardized model *in vivo* when studying prostate carcinogenesis and cancer progression (Bello et al., 1997; Webber et al., 1997a; Webber et al., 1997c).

RWPE-1 cells were isolated from the peripheral zone of the normal prostate of a 54 year-old Caucasian man undergoing radical cystoprostatectomy for bladder cancer and immortalized with a single copy of the human papilloma virus-18 (HPV-18) DNA (Bello et al., 1997; Webber et al., 1997a). The RWPE-1 cells, although immortalized, have retained properties exhibited by normal prostate epithelial cells *in vivo*, such as, the ability to undergo acinar morphogenesis in 3-dimensional (3D) Matrigel cultures and *in vivo* upon subcutaneous cell injection in athymic mice. Furthermore, they have the ability to produce PSA upon exposure to androgen (Bello et al., 1997; Webber et al., 1997a; Bello-DeOcampo et al., 2001a; Bello-DeOcampo et al., 2001b). A family of cell lines, the MNU cell lines, was generated from RWPE-1 cells (Figure 8.1) (Webber et al., 1997c).

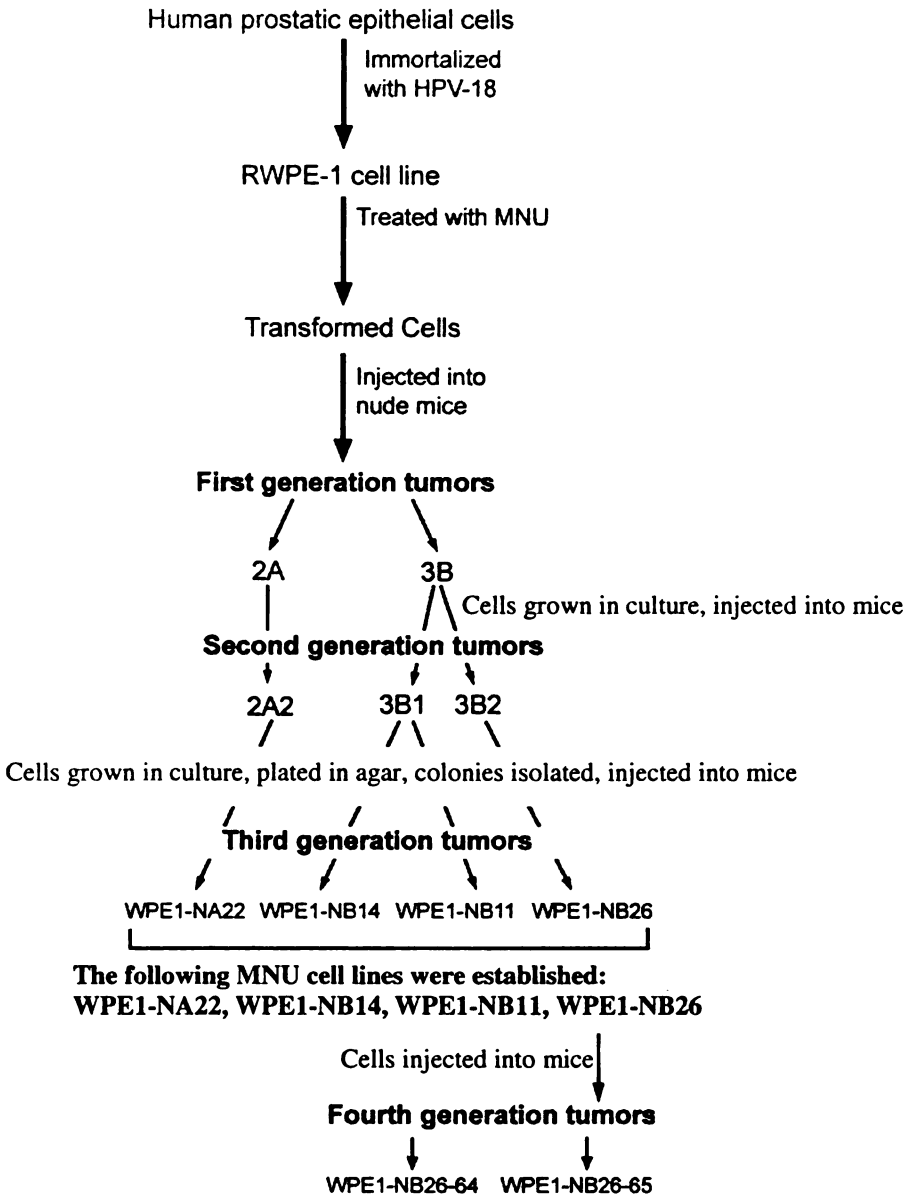

Figure 8.1. Derivation of MNU-transformed human prostate epithelial cell lines from RWPE-1, a non-tumorigenic human prostatic epithelial cell line, and the subsequent derivation of WPE1-NB26-64 and WPE1-NB26-65 cell lines. The 2A tumor was derived from treatment with MNU at 50 μg/ml and 3B at 100 μg/ml (Modified from Webber et al., 1997c).

RWPE-1 cells were treated with MNU, a chemical carcinogen, at 50 or 100 μg/ml. Carcinogen-exposed cells were injected subcutaneously in nude mice and tumors were removed 10 weeks after cell injection. Cells from these tumors were grown in culture to give rise to 2A (50 μg/ml MNU) and 3B (100 μg/ml MNU) cells. These cells were again injected subcutaneously into nude mice and tumors were collected and plated in culture to expand the cell population. Cells were then plated in soft agar. Individual colonies were isolated and expanded and gave rise to the MNU cell lines, which all share a common lineage. These cell lines include: WPE1-NA22, WPE1-NB14, WPE1-NB11, and WPE1-NB26 (Figure 8.1). The RWPE-1 and the MNU cell lines are unique because they show progression of characteristics from non-tumorigenic, to low, and then to a high level of malignancy which mimic different stages of carcinogenesis and progression as they occur in the human prostate. On the basis of their *in vitro* and *in vivo* characteristics the MNU cell lines rank in the following order of increasing malignancy: WPE1-NA22 showing the lowest invasion and tumorigenicity, the WPE1-NB14 and WPE1-NB11 showing intermediate, and WPE1-NB26 the greatest invasion and tumorigenicity (Webber et al., 1997c).

In the present study we show that intravenous injection of WPE1-NB26 cells into nude mice results in the production of distant metastases. We were also successful in isolating two new cell lines from tumors resulting from subcutaneous injection of WPE1-NB26 cells. These two new cell lines designated, WPE1-NB26-64 and WPE1-NB26-65, may be more tumorigenic and metastatic than the parental WPE1-NB26 cell line based on the results presented here. The most significant differences between the parental and tumor-derived cell lines are the increased growth and expression of

MMPs in tumor-derived cell lines. The three cell lines, WPE1-NB26, WPE1-NB26-64, and WPE1-NB26-65, described here, provide a model system for studying prostate carcinogenesis, matrix metalloproteinase expression and tumor progression, including metastasis. These cell lines may also be used for testing agents for the treatment of localized and metastatic prostate cancer.

Materials & Methods

Materials:

Keratinocyte serum-free medium (KSFM) with supplements of bovine pituitary extract (BPE) and epidermal growth factor (EGF) (Gibco/In Vitrogen, Grand Island, NY); antibiotic/antimycotic mixture (Gibco/In Vitrogen, Grand Island, NY); Dulbecco's phosphate buffered formalin (DPBS) (Mallinckrodt Baker, Inc., Phillipsburg, NJ), Matrigel (Collaborative Biomedical Products, Bedford, MA); donor calf serum (DCS) (Intergen, Purchase, NY); trypsin/EDTA (Gibco/In Vitrogen, Grand Island, NY); bovine serum albumin (BSA) (Pierce, Rockford, IL); Falcon T-75 flasks (Becton Dickinson Labware, Franklin Lakes, NJ); Falcon T-25 flasks (Becton Dickinson Labware, Franklin Lakes, NJ); 96-well flat bottom plates (Becton Dickinson Labware, Franklin Lakes, NJ), 4-chamber slides (Becton-Dickinson Labware, Franklin Lakes, NJ); MoAb to cytokeratin 5/14 (Cat. #M0630, Dako, Carpinteria, CA); MoAb to cytokeratin 18 (Cat. #C8541, Sigma, St. Louis, MO); MoAb to AR (Cat. #sc-7305, Santa Cruz Biotechnology, Santa Cruz, CA), MoAb to PSA (Cat. #M0750, Dako, Carpinteria, CA); 3-[4,5-dimethyl thaizol-2-yl]-2,5-diphenyl tetrazolium bromide (MTT) (Sigma, St. Louis, MO); Vectastain Elite ABC peroxidase kit (Vector Labs, Burlingame, CA); 3,3'-

diaminobenzidine (DAB) substrate kit (Vector Labs, Burlingame, CA); Glacial acetic acid (EM SCIENCE, Gibbstown, NJ); Nucleopore filters (8.0 μm pore size, 13 mm diameter, Fisher Scientific, Chicago, IL); Boyden chambers (Neuro Probe, Inc., Cabin John, MD); HEMA-3 kit (Fisher Scientific); Coomassie brilliant blue R-250 (Gibco/In Vitrogen, Grand Island, NY); Laemmli sample buffer (BIO-RAD, Hercules, CA); Mini-protean II apparatus (BIO-RAD, Hercules, CA); triton-X (BIO-RAD, Hercules, CA); Bis-Acrylamide (BIO-RAD, Hercules, CA)

Methods

Cells and cell culture:

The WPE1-NB26 cell line was derived from RWPE-1 cells by exposure to *N*-methyl-*N*-nitrosourea (MNU). The WPE1-NB26-64 and WPE1-NB26-65 cell lines were selected from WPE1-NB26 cells that formed subcutaneous tumors following cell injection in athymic mice. The cells were grown in complete keratinocyte serum-free medium (KSFM) containing 50 μg/ml bovine pituitary extract (BPE), 5 ng/ml epidermal growth factor (EGF) and 1X antibiotic/antimycotic solution. Cultures were maintained at 37^0C in a humidified atmosphere containing 5% CO_2 and subcultured weekly.

Growth in nude mice by subcutaneous injection:

Cells were tested for tumorigenicity by subcutaneously injecting a cell suspension of two million WPE1-NB26 cells in 250 μl of basal KSFM (without BPE or EGF) containing an equal volume of Matrigel. Cells were injected bilaterally on the dorso-lateral sides of three male, athymic (NSWNU-M) (Taconic Inc., Germantown, NY) *nu/nu*

mice. When tumors became palpable, their size was measured periodically in two dimensions (length and width), using digital calipers, and all measurements were recorded. Tumors were measured and photographed at the termination of the experiment at 14 weeks. Tumor volume (TV) was calculated using the formula: $TV = a X b^2/2$ where *a* is the longest dimension and *b* is the width as described by Nemeth et al., (1999). Tumor tissue was removed aseptically from the site of injection and divided into two; one part was processed for cell culture and the other fixed in 10% phosphate-buffered formalin and processed for histology.

Growth in nude mice by intravenous injection:

Cells were tested for their metastatic ability by intravenously injecting a cell suspension of one million WPE1-NB26 cells in 100 µl of phosphate-buffered saline. Cells were injected intravenously using the tail vein of six male, athymic (NSWNU-M) (Taconic Inc., Germantown, NY) *nu/nu* mice under anesthesia. Lung and liver tissue was removed from the animals at the time of sacrifice, fixed in 10% phosphate-buffered formalin, and processed for histology. This study was conducted with the approval of the All University Committee on Animal Use and Care (AUCAUC) and all guidelines were followed.

Selection of WPE1-NB26-64 and WPE1-NB26-65 cell lines:

WPE1-NB26 cells were injected subcutaneously on the left and right dorso-lateral sides of nude mice, and the resultant tumors were harvested by aseptic technique. Tumors were removed 14 weeks after cell injection from two nude mice, #64 and #65,

one tumor each and divided into two pieces. One half was fixed in 10% phosphate-buffered formalin for histology and the other half was rinsed with distilled H_20 containing 2X antibiotic/antimycotic solution. Tumor tissue for *in vitro* culture was minced into 1 mm size pieces and digested in full strength trypsin/EDTA to facilitate release of cells. The tumor tissue was placed in the incubator for 2 hours and the tissue suspension was triturated every 30 min. Trypsin/EDTA was neutralized with 2% donor calf serum (DCS) and removed after centrifugation. The pellet was resuspended in complete KSFM and plated in 60 mm plates. Epithelial cell cultures were expanded and designated as WPE1-NB-26-64 and WPE1-NB-26-65 cell lines.

Cell morphology *in vitro:*

Cells plated and grown in 4-well chamber slides were rinsed twice with D-PBS and then fixed with 10% phosphate-buffered formalin for five min. Chamber slides were then rinsed in distilled water, and stained with hematoxylin for 1.5 min, and rinsed in 1% Glacial Acetic water to remove excess stain. Following a rinse in tap water, the slides were rinsed with 70% and 95% ethanol prior to staining with Eosin (2 min). Slides were dehydrated in two changes of 100% ethanol, xylol (1:1, 100% ethanol: xylene), and xylene and mounted in Permount.

Immunostaining for cytokeratin expression:

Protein expression was detected by a modified avidin-biotin immunoperoxidase Vector protocol, using monoclonal antibodies. The antibody dilutions were made in normal horse serum. The primary antibody dilution used for detection of Ck18

expression was 1:500 and for Ck5/14, 1:100. The following sequential steps were conducted at room temperature and cells were rinsed twice with PBS between steps after application of the primary antibody: cells were blocked with normal horse serum for 1 h; incubated with the appropriate specific antibody for 1 h, followed by biotinylated secondary antibody (1:200) for 30 min; treated with 3% H_2O_2 for 3 min to quench endogenous peroxidase activity; incubated with the avidin-biotin complex for 30 min; developed with DAB and dehydrated and mounted on alcohol washed slides. Negative controls included incubation with PBS in place of the primary antibody.

Immunostaining for PSA and AR expression:

Cells grown in chamber slides for immunostaining were pretreated in KSFM medium containing 5 nM mibolerone, a non-metabolizable androgen, for 4 days, beginning 48 h after plating. Absolute ethanol was used as the vehicle for mibolerone. Controls consisted of ethanol-treated cultures. Cells on 4-well chamber slides were processed as described above. The primary antibody dilutions, incubation temperature and times were: PSA, 1:50, 4^0C, 24 h; AR, 1:100, room temperature, 2 h. Negative controls included incubation with PBS in place of the primary antibody.

Anchorage-dependent growth in monolayer:

Cells were plated in 96-well plates at densities of 625, 1250, 2500, 5000, and 10000 cells/well in 200 µl of KSFM, using 12 wells per cell density, and allowed to attach for 48 h at which time medium was changed. Cells were allowed to grow for five days with medium change every 48 h. Plates were stained with MTT as previously

described (Webber et al., 1997c). Absorbance was measured at 540 nm with a Titertek microplate reader. Results represent the average of three experiments.

Invasion assay:

The invasive ability of WPE1-NB26, WPE1-NB26-64 and WPE1-NB26-65 cell lines was examined using Matrigel coated filters in the Boyden chamber assay (Webber et al., 1997c). The day prior to running the assay, cells were plated at a density of four million cells in two T-75 flasks. Nucleopore filters were coated with 25 μg Matrigel in 50 μl of distilled water and left to dry overnight at room temperature under sterile conditions. Cells were lifted 24 h after plating, by incubation with 1 μM EDTA (~9 min). Cells were dislodged by tapping, suspended in KSFM medium containing 0.1% BSA, and recovered by centrifugation. NIH/3T3 cell conditioned medium (212 μl) served as the chemo-attractant in the bottom of the Boyden chamber. A cell suspension, containing 200,000 cells in 200 μl medium, was added to the top chamber of five replicate chambers, allowed to remain for 15 min, then overlayed with 650 μl of the medium containing 0.1% BSA. The invasion assay was carried out for 48 hrs at 37^0C. The filters were then fixed and stained with HEMA-3 kit. After the non-migrated cells on the Matrigel-coated side of the filter were wiped off, the stain was extracted with 0.1 N HCl and absorbance was measured at 620 nm using a Titertek microplate reader. Percent absorbance for the tumor-derived cell lines were calculated and compared with the parental WPE1-NB26 cell line. The results shown represent the average of two experiments.

Collection of conditioned medium for MMP activity:

WPE1-NB26, WPE1-NB26-64, and WPE1-NB26-65 cells were plated in complete KSFM at one million cells/60 mm culture plate and placed in the incubator. After 48 h, the medium was removed and cells were washed once with D-PBS. The medium was replaced with basal KSFM (without BPE or EGF). The conditioned medium was collected 48 h later and centrifuged to remove cell debris. The supernatant was mixed with 2.0% Triton X-100 to obtain a final concentration of 0.01% and analyzed by SDS-PAGE zymography to detect MMP-2 and MMP-9 activity.

SDS-PAGE zymography:

Analysis of the levels of MMPs released into serum-free medium by WPE1-NB26, WPE1-NB26-64, and WPE1-NB26-65 cells was performed using SDS-PAGE zymography. Conditioned media were collected by plating cells in complete KSFM at a density of one million cells/60 mm plate. After 48 h, the medium was slowly removed and each plate was washed once with 3 ml of D-PBS. Next, 2.2 ml basal KSFM (no BPE or EGF) was added to each dish. After 48 h, the conditioned media were removed from each dish, added individually to sterile 15 ml centrifuge tubes and centrifuged at 2500 rpm for 5 minutes to remove cell debris. The supernatant was transferred to new sterile 15 ml centrifuge tubes. To each tube 2.0% Triton-X 100 was added at a final concentration of 0.01%, the media were gently vortexed to mix, and aliquoted into sterile 200 µl Eppendorf tubes. The protein content of each sample was determined using the Lowry High protein assay. Samples of conditioned media were stored at -80^{0}C until needed.

To determine the MMP-2 and MMP-9 activity of these cell lines, 0.75 mm thick 10% acrylamide gels, containing 0.1% gelatin were prepared for SDS-PAGE zymography. The gels were allowed to polymerize overnight at 4^0C. Conditioned media containing 8 μg of protein in 4 μl of Laemmli Sample Buffer were loaded into each well. Using a Bio-Rad Mini Protean II apparatus, the gels were electrophoresed (4^0C) at 150 volts in approximately 800 ml of 1X running buffer (24 g Tris base, 115.2 g Glycine Bio-Rad), pH 8.3. After electrophoresis for 1.5 h, the gels were soaked in 2.5% Triton X-100 on a shaker for one hour, changing the solution after 30 minutes, to eliminate SDS. The gels were then rinsed with distilled water and placed in Tris-HCl soaking buffer (50 mM Tris-HCl, 200 mM NaCl, 5 mM $CaCl_2$, 0.02% Brij-35, Bio-RAD), pH 7.5, to renature protease activity. After 24 h incubation in soaking buffer at 37^0C, the gels were rinsed in distilled water in preparation for staining. The gels were stained for 20 minutes with 0.25% Coomassie Brilliant Blue R-250 stain and then de-stained after which clear bands of digested gelatin were visible against a blue background. The gels were briefly rinsed in distilled water and scanned. The area of each band was measured densitometrically to determine MMP-2 and MMP-9 activity.

Statistical analysis:

All of the results in this study were obtained from at least two independent experiments. Results are expressed as averages with standard error of the mean (SEM). Differences between the means were considered significant if $P<0.05$. The results obtained from the *in vitro* anchorage-dependent growth and Boyden chamber invasion assays of each cell line were compared using one-way analysis of variance (ANOVA)

and Tukey-Kramer multiple comparison tests. GraphPad InStat 3 was used for these analyses.

Results

Histology of xenografts in nude mice:

Tissue samples were collected 14 weeks after subcutaneous injection of cells into nude mice and prepared for histology. WPE1-NB26 cells formed large tumors in all mice injected subcutaneously (Figure 8.2A). The average volume of the tumors from which WPE1-NB26-64 and WPE1-NB26-65 cells were derived, were approximately 280.0 and 460.0 mm^3, respectively. Figure 8.2B shows the histology of the two tumors.

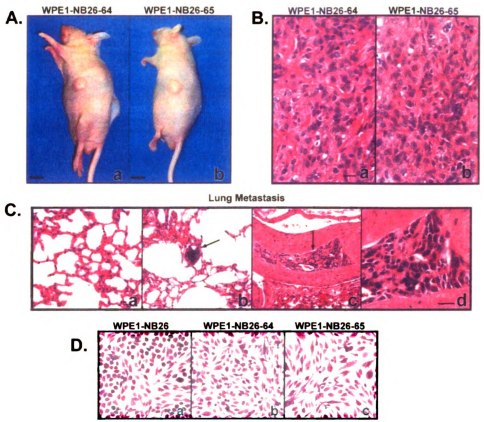

Figure 8.2. 8.2A. Nude mice (NSWNU-M) were bilaterally injected with 250 µl of a cell suspension in Matrigel (cell: Matrigel volume, 1:1) containing two million WPE1-NB26 cells. Mice were sacrificed 14 weeks later. This figure shows two mice with tumors from which the WPE1-NB26-64 and WPE1-NB26-65 cell lines were derived. Bar = 1 cm. 8.2B. Histological sections of the (a) WPE1-NB26-64 and (b) WPE1-NB26-65 tumors. H & E, Bar = 20 microns. 8.2C. Histological sections of mouse lung tissue: (a) Normal area of mouse lung tissue, (b) Necrotic WPE1-NB26 prostate tumor cells in a blood vessel (arrow) of mouse lung at 20 weeks after intravenous cell injection, (c) WPE1-NB26 cells (arrow) surrounded by hyperplastic, fibrous connective tissue in the lung of a mouse at 20 weeks after intravenous cell injection, (d) shows a higher magnification of the metastasis in (c). H & E, Bar = 20 microns. 8.2D. Morphology of (a) WPE1-NB26, (b) WPE1-NB26-64, (c) WPE1-NB26-65 cells. H & E, Bar = 20 microns.

Histology of metastases in nude mice:

Tissue samples were collected 140 days after intravenous injection of WPE1-NB26 cells in nude mice. Histopathology of the lungs of nude mice showed 2/5 (40%) mice injected intravenously with one million WPE1-NB26 cells, established metastatic tumors. Figure 8.2C shows histology of a normal area of the lung (Figure 8.2C,a), necrotic tumor cells in a blood vessel in the lung (Figure 8.2C,b), and of metastatic tumors in lung tissue of mice (Figure 8.2C,c-d) given intravenous cell injection of WPE1-NB26 cells. The metastatic tumor shown in 8.2c and 8.2d is surrounded by fibrous tissue formed in reaction to the presence of tumor cells.

Cell morphology *in vitro:*

Stepwise changes in cell morphology have been observed in the MNU family of cell lines, from typical epithelial cells of the WPE1-NA22 cell line showing low tumorigenicity, to a more elongated morphology of the WPE1-NB26 cell line showing high tumorigenicity, with the other cell lines having an intermediate morphology (Webber et al., 1997c). Similarly, both tumor-derived cell lines, WPE1-NB26-64 and WPE1-NB26-65, show a more elongated and spindle-shaped morphology compared to WPE1-NB26 cells (Figure 8.2D).

Immunostaining for cytokeratin expression:

The expression of Ck18 and Ck5/14, two epithelial cell markers, was examined by immunocytochemistry. Results show that WPE1-NB26, WPE1-NB26-64, and

WPE1-NB26-65 cells all express Ck18 and Ck5/14 (Figure 8.3), which confirms their common epithelial origin.

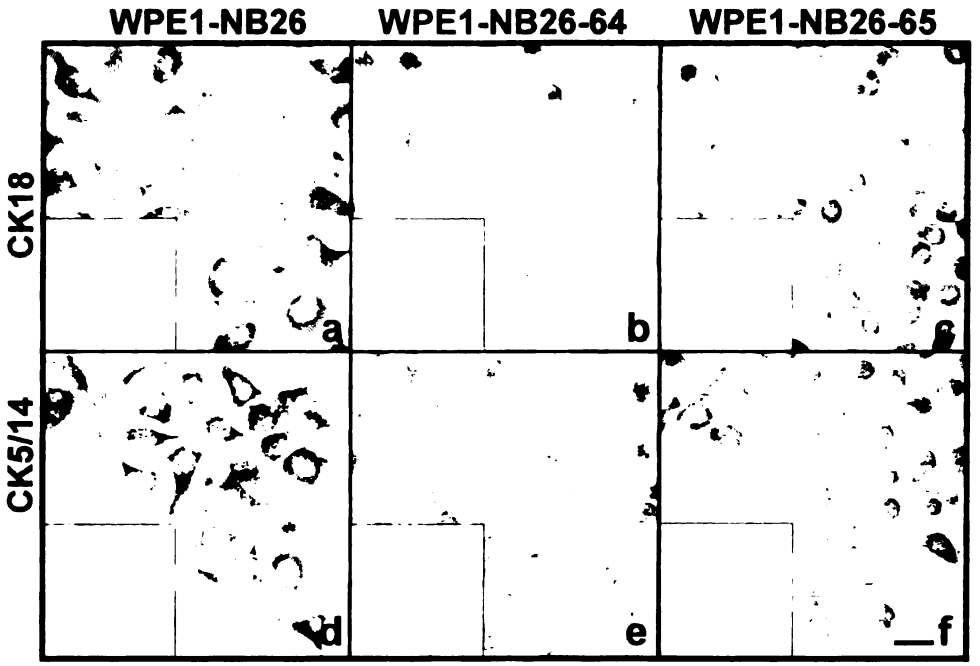

Figure 8.3. Characterization of WPE1-NB26, WPE1-NB26-64, and WPE1-NB26-65 cells on the basis of cellular proteins. Proteins were detected by immunoperoxidase staining. (a-c) positive staining for cytokeratin 18, the inset in each is a control lacking primary antibody; (d-f) positive staining for cytokeratin 5/14, the inset in each is a control lacking primary antibody. Bar = 20 microns.

Expression of prostatic epithelial cell markers in cells:

The expression of AR and PSA, two prostatic epithelial cell markers, was examined by immunocytochemistry. Results show nuclear staining for AR (Figure 8.4A), as well as, cytoplasmic expression of PSA (Figure 8.4B) in WPE1-NB26,

WPE1-NB26-64, and WPE1-NB26-65 cells. An increase in AR and PSA expression was induced in all three cell lines after treatment with 5nM mibolerone for six days.

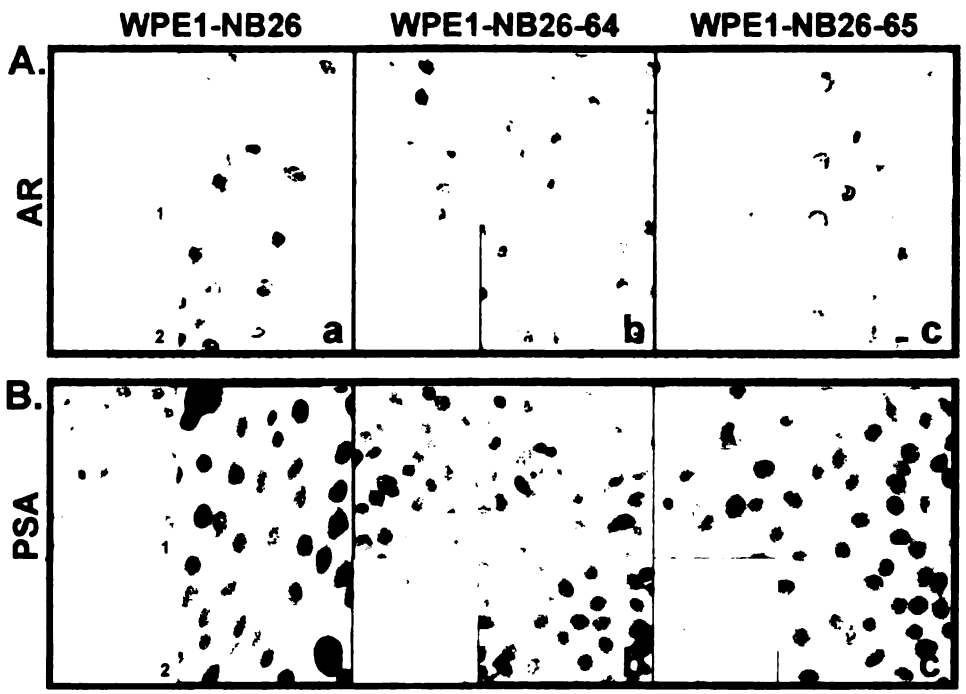

Figure 8.4. Immunostaining for androgen receptor (Figure 8.4A) and PSA (Figure 8.4B) demonstrates androgen responsiveness and prostatic epithelial origin of WPE1-NB26, WPE1-NB26-64, and WPE1-NB26-65 cell lines. Cells were treated with 5 nM mibolerone for 6 days. Positive nuclear staining for AR is shown in 8.4A,a,b,c for all three cell lines. Panel a1 shows only weak nuclear staining in untreated control. Panel a2 and other insets are negative controls lacking primary antibody. Positive cytoplasmic staining for PSA is shown in 8.4B,a,b,c for all three cell lines. Panel a1 shows very weak staining in untreated control. Panel a2 and other insets are negative controls lacking primary antibody. Bar = 20 microns.

Anchorage-dependent growth in monolayer:

Anchorage-dependent growth of the tumor-derived cell lines, WPE1-NB26-64 and WPE1-NB26-65 in monolayer culture is shown in Figure 8.5A and is compared with that of the parental WPE1-NB26 cell line. Both tumor derived cell lines,

WPE1-NB26-64 and WPE1-NB26-65, grow more rapidly than the parental WPE1-NB26 cell line. The difference in the growth of WPE1-NB26-64 and WPE1-NB26-65 cells, in comparison to WPE1-NB26 cells, is very significant at each cell density ($p<0.001$).

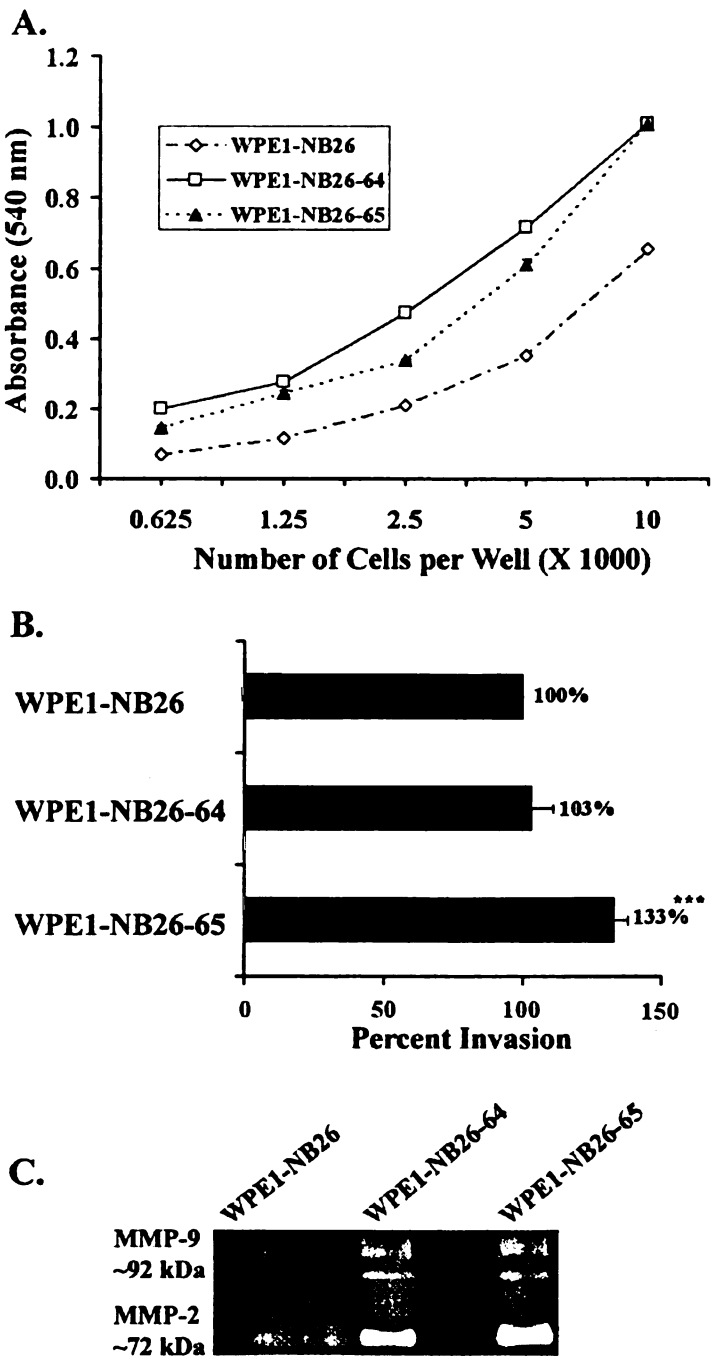

Figure 8.5. 8.5A. A comparison of the anchorage-dependent growth of WPE1-NB26, WPE1-NB26-64, and WPE1-NB26-65 cell lines. Cells were plated at densities of 625, 1250, 2500, 5000 and 10,000 cells per well in 96-well plates in complete KSFM. Plates were stained with MTT five days after plating. Absorbance values were measured at 540 nm and plotted ± SEM. Results represent the average of 3 experiments. The growth of both WPE1-NB26-64 and WPE1-NB26-65 cell lines are significantly greater ($p<0.001$) in comparison to the WPE1-NB26 cell line at each cell density using ANOVA. 8.5B. The invasive ability of WPE1-NB26-64 and WPE1-NB26-65 cell lines

was compared with that of WPE1-NB26 cells by a modified Boyden chamber *in vitro* invasion assay. Cells were plated at 200,000 cells/ chamber on a Matrigel-coated filter and allowed to invade for 48 h. ± SEM. The difference in the invasive ability of WPE1-NB26-65 as compared to WPE1-NB26 is very significant using ANOVA ($p<0.001$). 8.5C. Zymographic analysis of MMP expression in culture medium of WPE1-NB26, WPE1-NB26-64, and WPE1-NB26-65 cells. Samples of conditioned medium containing 8 μg protein each, were electrophoresed using 10% polyacrylamide gels. Lane 1, WPE1-NB26 cells; Lane 2, WPE1-NB26-64 cells; Lane 3, WPE1-NB26-65 cells. The gel is a representative of 3 independent experiments.

Comparison of invasive ability:

The invasive ability of WPE1-NB26-64 and WPE1-NB26-65 was compared with that of the parent WPE1-NB26 cell line where invasion was set at 100% (Figure 8.5B). Both tumor-derived cell lines showed different invasive ability, with WPE1-NB26-64 showing 103% and WPE1-NB26-64 showing 133% invasion as compared to control. The invasive ability of the WPE1-NB26-65 cell line is considered very significant ($p< 0.001$) in comparison to the WPE1-NB26 cell line and also in comparison to WPE1-NB26-64 ($p<0.001$). On the basis of these results, the three cell lines can be placed in the following order of increasing invasive ability: WPE1-NB26< WPE1-NB26-64< WPE1-NB26-65, with WPE1-NB26 being the least invasive. This order is in agreement with their secreted MMP activity.

Matrix metalloproteinase (MMP) expression:

The activity of MMPs secreted into the conditioned medium by WPE1-NB26, WPE1-NB26-64, and WPE1-NB26-65 cell lines was examined by zymography. As shown in Figure 8.5C, the parent WPE1-NB26 cells show only trace levels of MMP-2 and MMP-9 activity. In comparison to the parental WPE1-NB26 cell line, the tumor-

derived cell lines produce increased levels of both MMP-2 and MMP-9. Densitometric analysis of the bands showed that WPE1-NB26-65 showed ~40% more MMP-2 activity than the WPE1-NB26-64 cell line.

Discussion

The tumor derived cell lines, WPE1-NB26-64 and WPE1-NB26-65, described here, are new members of the MNU family and represent stages of prostate cancer progression more advanced than the parental WPE1-NB26 cell line. Carcinogenesis and tumor progression have been described variously as multistep processes or as a continuum. The RWPE-1 cell line and the MNU family of cell lines, previously described, mimic different stages of carcinogenesis and progression as they occur in the human prostate (Bello et al., 1997; Webber et al., 1997a; Webber et al., 1997c). This unique family of cell lines shows progression of characteristics from non-tumorigenic, to low, and then to a high level of malignancy. The WPE1-NB26 cell line was the most malignant member of the MNU-transformed family but now the WPE1-NB26-64 and WPE1-NB26-65 cell lines represent the most malignant members of the MNU family based on their *in vivo* and *in vitro* characteristics (Figure 8.6).

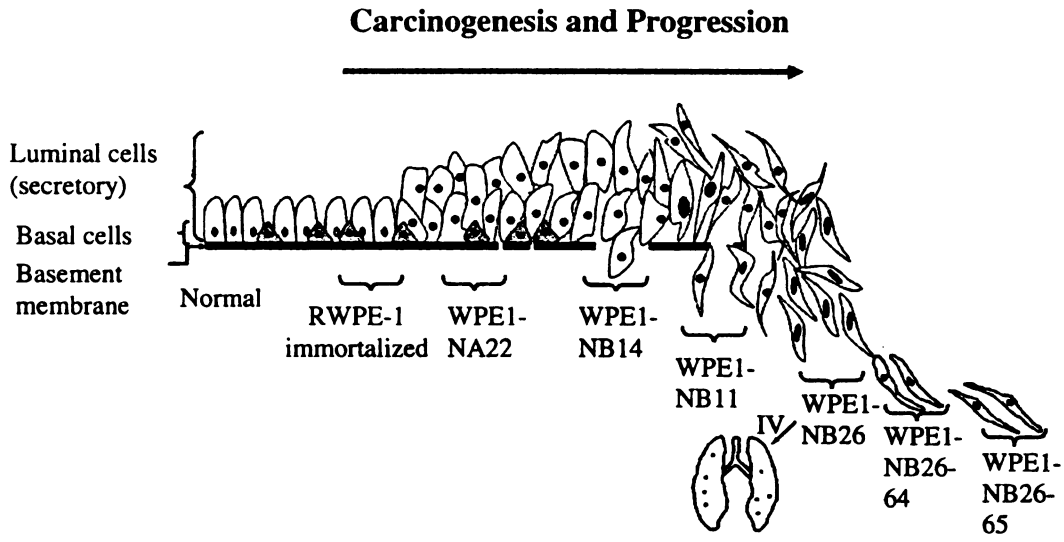

Figure 8.6. A schematic diagram showing steps in the multi-step process of carcinogenesis and tumor progression in the prostate and the points represented by RWPE-1, the MNU cell lines, and the WPE1-NB26 tumor-derived cell lines, WPE1-NB26-64 and WPE1-NB26-65. The ability of WPE1-NB26 cells to form lung metastases after intravenous injection is also shown (Modified from Webber et al., 1997c).

The addition of these two tumor-derived cell lines to the MNU family expands the continuum of related progression models for prostate cancer studies. All of the cell lines, WPE1-NB26, WPE1-NB26-64, and WPE1-NB26-65, express Ck18 and Ck5/14, which confirms their epithelial origin. These cell lines also respond to androgen by upregulation of the AR and PSA expression, thus, confirming their prostatic origin. Amongst the MNU cell lines, WPE1-NB26 shows the highest growth rate (Webber et al., 1997c). However, the tumor-derived, WPE1-NB26-64 and WPE1-NB26-65 cell lines, have an even higher growth rate than the parental WPE1-NB26 cell line. The growth of WPE1-NB26 *in vivo,* at the subcutaneous site, has apparently resulted in the selection of cells that have a higher growth rate than the parent cell line.

Recent evidence suggests that MMPs play an important role in the establishment and growth of the primary tumor (Chambers and Matrisian, 1997). This is supported by experiments using MMP inhibitors to block MMP activity. MMP inhibitors caused statistically significant inhibition of primary tumor growth in mice bearing subcutaneous tumors of PC-3 human prostate cancer or MAT LyLu rodent prostate cancer cells (Conway et al., 1996). In another study, a regression or disappearance of palpable tumor was also observed in animals treated with an MMP inhibitor following subcutaneous injection of MAT LyLu cells (Lokeshwar, 1999). In an orthotopic transplant model of human colon cancer in nude mice, administration of BB-94 (batimastat), a synthetic MMP inhibitor, caused a reduction in the median weight of the primary tumor (Wang et al., 1994). Batimastat has also been shown to inhibit the growth of subcutaneous mouse melanoma (B16-BL6) tumors and human ovarian tumors implanted in the intraperitoneal cavity of nude mice (Davies et al., 1993; Chirivi et al., 1994). Matrix metalloproteinases promote tumor progression and angiogenesis by regulating cell attachment, cell proliferation, migration and growth, either directly or via the release of growth factors sequestered in the extracellular matrix (ECM) (Stetler-Stevenson and Yu, 2001). It is interesting to note that both tumor-derived cell lines show a more elongated and spindle-shaped morphology in comparison to the parent WPE1-NB26 cells, possibly due to cell:matrix interactions (Figure 2D).

While the present study focuses on the association of MMPs with invasion and metastasis by prostate cancer cells, it is important to briefly examine the role of other proteases in the proteolytic cascade. Invasion and metastasis are complex processes where degradation of the basement membrane (BM) by proteases, accompanied by

invasion, is a critical step in the metastatic cascade. A correlation between metastatic potential and increase in protease expression has been demonstrated (Webber and Waghray, 1995). In the prostate, some important proteases include serine proteases and matrix metalloproteinases. Prostate epithelial cells have the intrinsic ability to secrete two serine proteases, urokinase-type plasminogen activator (uPA) and PSA. In normal prostatic epithelium, the secretory luminal cells are polarized, where the cells are attached to the BM at their basal end while secretion of proteins takes place at the apical, luminal end of glandular epithelial cells (Webber et al., 1995). However, disorganization of epithelial cell arrangement occurs in high grade PIN (HGPIN) and in cancer. This apparently leads to a loss of polarized secretion, so that cells begin to secrete proteases at their basal end, causing localized proteolysis which culminates in invasion and metastasis (Webber and Waghray, 1995; Webber et al., 1995). Our laboratory has shown that both uPA and PSA have the ability to degrade the BM and ECM proteins (Webber and Waghray, 1995; Webber et al., 1995). In addition to uPA and PSA, another important component of the proteolytic cascade involves MMPs. MMPs are transiently produced during normal tissue remodeling. However, it is well established that a persistent increase in MMP activity occurs during cancer development (Webber et al., 1996b).

The increased invasiveness observed in tumor-derived cell lines compared to the parental WPE1-NB26 cell line may also, in part, be related to MMP expression. Of all three cell lines, WPE1-NB26-65 cells were significantly more invasive. While the parent, WPE1-NB26 cells express low or undetectable levels of MMP-2 and MMP-9, both tumor-derived cell lines express increased levels of MMP-2 and MMP-9 (Figure 8.5C). WPE1-NB26-65 cells, which were collected from the mouse with the larger

tumor, produce the highest level of MMP-2. Comparing the two tumor-derived cell lines, WPE1-NB26-65 showed ~40% more MMP-2 activity than the WPE1-NB26-64 cell line. The difference in invasive ability and expression of MMP-2 in the tumor-derived cell lines suggests that the parental WPE1-NB26 cell line consists of a heterogeneous cell population and subcutaneous injection resulted in the selection of WPE1-NB26 cells that express increased levels of MMPs. Results also show that following intravenous cell injection in nude mice, WPE1-NB26 cells were capable of establishing metastatic tumors in the lungs.

Matrix metalloproteinases have been repeatedly implicated in metastasis. Several studies have demonstrated a positive correlation between MMP expression, invasive behavior, and metastatic potential in animal models (Stetler-Stevenson and Yu, 2001). Thus, they are not only important in tumor establishment and growth, but in the development of metastases, which makes them appropriate targets for anti-metastasis therapies. MMPs have been associated with matrix degradation, invasion, intravasation, extravasation, and local migration, all of which are steps involved in the metastatic process (Fidler, 1991; Liotta and Stetler-Stevenson, 1993). Specifically, an increased expression of the gelatinases, MMP-2 and MMP-9, whose substrate is type IV collagen, has been shown to be associated with malignant progression of prostate and other cancers (Liotta et al., 1977; Liotta et al., 1980; Webber et al., 1996b). Overexpression of MMP-9 in rat embryo fibroblasts results in increased metastatic potential following injection into nude mice and inhibition of this enzyme decreases lung colonization (Bernhard et al., 1994; Hua and Muschel, 1996). Other studies have shown that only those sublines of prostate cancer cells that produce high levels of MMPs are capable of distant metastasis

when tumors are generated by orthotopic cell injection (Stephenson et al., 1992). Of significant interest is the increased expression of MMP-2 in prostate cancer progression (Lokeshwar et al., 1993; Stearns and Stearns, 1996). Analysis of conditioned medium by gelatin zymography and enzyme assays show that both benign and neoplastic prostate tissues secrete MMP-9 and MMP-2 (Lokeshwar et al., 1993). However, conditioned medium from malignant prostate explants contained a higher proportion of MMP-2. Expression of MMP-2 has been shown in many types of human tumors including: prostate, breast, ovary, and colon, and this expression was usually limited to the malignant epithelial cells (Stetler-Stevenson et al., 1993). Increased expression of both MMP-2 and MMP-9 have also been associated with the Gleason score of human prostate tumors (Stearns and Stearns, 1996; Kuniyasu et al., 2000). Thus, MMP expression levels may be useful as indicators of the progression or grade of prostate cancer.

In conclusion, both tumor-derived cell lines, WPE1-NB26-64 and WPE1-NB26-65, express increased levels of MMPs in comparison to the parental WPE1-NB26 cell line. WPE1-NB26-65 also produces more MMP-2 than the other tumor-derived cell line, WPE1-NB26-64. Therefore, the tumor-derived cell lines, WPE1-NB26-64 and WPE1-NB26-65, would be particularly useful for prostate cancer studies involving MMP expression, and especially for comparison with the related MNU family of cell lines, which express low or undetectable levels of MMPs and mimic varying degrees of tumor progression. These cell lines can also be used to screen for single agents and combinations of agents for cancer treatment.

Literature cited

American Cancer Society: Cancer Facts and Figures 2004, Atlanta, GA, pp.16-17, 2004.

Bello-DeOcampo, D., Kleinman, H.K., DeOcampo, N.D. and Webber, M.M.: Laminin 1 and $\alpha_6\beta_1$ integrin regulate acinar morphogenesis of normal and malignant human prostate epithelial cells. Prostate 46:142-153, 2001a.

Bello-DeOcampo, D., Kleinman, H.K. and Webber, M.M.: The role of $\alpha 6\beta 1$ integrin and EGF in normal and malignant acinar morphogenesis of human prostatic epithelial cells. Mutation Research 480-481, 209-217, 2001b.

Bello, D., Webber, M., Kleinman, H.K., Wartinger, D.D. and Rhim, J.S.: Androgen responsive adult human prostatic epithelial cell lines immortalized by human papillomavirus 18. Carcinogenesis 6:1215-1223, 1997.

Bernhard, E.J., Gruber, S.B. and Muschel, R.J.: Direct evidence linking expression of matrix metalloproteinase 9 (92-kDa gelatinase/collagenase) to the metastatic phenotype in transformed rat embryo cells. Proceedings of the National Academy of Science USA 91:4293-4297, 1994.

Chambers, A.F. and Matrisian, L.M.: Changing views of the role of matrix metalloproteinases in metastasis (review). Journal of the National Cancer Institute 89:1260-1270, 1997.

Chirivi, R., Garofalo, A., Crimmin, M.J., Bawden, L., Stoppacciaro, A., Brown, P.D. and Giavazzi, R.: Inhibition of the metastatic spread and growth of B16-BL6 murine melanoma by a synthetic matrix metalloproteinase inhibitor. International Journal of Cancer 58:460-464, 1994.

Conway, J.G., Trexler, S.J., Wakefield, J.A., Marron, B.E., Emerson, D.L., Bickett, D.M., Deaton, D.N., Garrison, D., Elder, M., McElroy, A., Willmott, N., Dockerty, A.J.P. and McGeehan, G.M.: Effect of matrix metalloproteinase inhibitors on tumor growth and spontaneous metastasis. Clinical & Experimental Metastasis 14:115-124, 1996.

Davies, B., Brown, P.D., East, N., Crimmin, M.J. and Balkwill, F.R.: A synthetic matrix metalloproteinase inhibitor decreases tumor burden and prolongs survival of mice bearing ovarian carcinoma xenografts. Cancer Research 53:2087-2091, 1993.

Fidler, I.J.: The biology of human cancer metastasis. Acta Oncologica 30, 668-675, 1991.

Hua, J. and Muschel, R.: Inhibition of matrix metalloproteinase 9 expression by a ribozyme blocks metastasis in a rat sarcoma model system. Cancer Research 56:5279-5284, 1996.

Kuniyasu, H., Troncoso, P., Johnston, D., Bucana, C.D., Tahara, El, Fidler, I.J., and Pettaway, C.A.: Relative expression of type IV collagenase, E-cadherin, and vascular endothelial growth factor/vascular permeability factor in prostatectomy specimens distinguishes organ-confined from pathologically advanced prostate cancers. Clinical Cancer Research 6:2295-2308, 2000.

Liotta L and Stetler-Stevenson W. Priniciples of molecular cell biology of cancer: cancer metastasis. In: Cancer VT and SR (eds.): principles and practice of oncology. Philidelphia: Lippincott, pp.134-149, 1993.

Liotta, L.A., Kleinerman, J., Catanzaro, P. and Rynbrandt, D.: Degradation of basement membrane by murine tumor cells. Journal of the National Cancer Institute 58:1427-1431, 1977.

Liotta, L.A., Tryggvason, K., Garbisa, S., Hart, I., Foltz, C.M., Shafie, S.: Metastatic potential correlates with enzymatic degradation of basement membrane collagen. Nature 284:67-68, 1980.

Lokeshwar, B.L.: MMP inhibition in prostate cancer. Annals of the New York Academy of Science 878:271-289, 1999.

Lokeshwar, B.L., Selzer, M.G., Block, N.L. and Gunja-Smith, Z.: Secretion of matrix metalloproteinases and their inhibitors (tissue inhibitor of metalloproteinases) by human prostate in explant cultures: reduced tissue inhibitor of metalloproteinase secretion by malignant tissues. Cancer Research 53:4493-4498. 1993.

Nemeth, J.A., Harb, J.F., Barroso, Jr., U., Zhanquan, H., Grignon, D.J. and Cher, M.L.: Severe combined immunodeficient-hu model of human prostate cancer metastasis to human bone. Cancer Research 59:1987-1993, 1999.

Stearns, M. and Stearns, M.E.: Evidence for increased activated metalloproteinase 2 (MMP-2a) expression associated with human prostate cancer progression. Oncology Research 8:69-75, 1996.

Stephenson, R.A., Dinney, C.P., Gohji, K., Ordonez, N.G., Killion, J.J. and Fidler, I.J.: Metastatic model for human prostate cancer using orthotopic implantation in nude mice. Journal of the National Cancer Institute 84:951-957, 1992.

Stetler-Stevenson, W.G., Aznavoorian, S., and Liotta, L.A.: Tumor cell interactions with the extracellular matrix during invasion and metastasis. Annual Reviews in Cell Biology 9:541-573, 1993.

Stetler-Stevenson, W.G. and Yu, S.E.: Proteases in invasion: matrix metalloproteinases. Seminars in Cancer Biology 11:143-152, 2001.

Wang, X., Fu, X., Brown, P.D., Crimmin, M.J. and Hoffman, R.M.: Matrix metalloproteinase inhibitor BB-94 (batimastat) inhibits human colon tumor growth and spread in a patient-like orthotopic model in nude mice. Cancer Research 54:4726-4728, 1994.

Webber, M., Bello, D., Kleinman, H.K. and Hoffman, M.P. :Acinar differentiation by non-malignant immortalized human prostatic epithelial cells and its loss by malignant cells. Carcinogenesis 18:1225-1231, 1997a.

Webber, M., Bello, D. and Quader, S.: Immortalized and tumorigenic adult human prostatic epithelial cell lines: characteristics and applications. part 1. cell markers and immortalized non-tumorigenic cell lines. Prostate 29:386-94, 1996a.

Webber, M., Bello, D. and Quader, S.: Immortalized and tumorigenic adult human prostatic epithelial cell lines: characteristics and applications. part 2. tumorigenic cell lines. Prostate 30:58-64, 1997b.

Webber, M., Quader, S., Kleinman, H.K., Bello-DeOcampo, D., Storto, P.D., Bice, G., DeMendonca-Calaca, W. and Williams, D.E.: Human cell lines as an in vitro/in vivo model for prostate carcinogenesis and progression. Prostate 47:1-13, 1997c.

Webber, M., Waghray, A., Bello, D. and Rhim, J.S.: Mini review: proteases and invasion in human prostate epithelial cell lines: Implications in prostate cancer prevention and intervention. Radiation Oncology Investigations 3:358-362, 1996b.

Webber, M.M. and Waghray, A.: Urokinase-mediated extracellular matrix degradation by human prostatic carcinoma cells and its inhibition by retinoic acid. Clinical Cancer Research 1:755-761, 1995.

Webber, M.M., Waghray, A. and Bello, D.: Prostate-specific antigen, a serine protease, facilitates human prostate cancer cell invasion. Clinical Cancer Research 1:1089 -1094, 1995.